Titre: Title:	Development of an Automated In-Line Resin Metering and Mixing System for Composites in the Automotive Industry
Auteur: Author:	Philippe Murray
Date:	2019
Type:	Mémoire ou thèse / Dissertation or Thesis
Référence: Citation:	Murray, P. (2019). Development of an Automated In-Line Resin Metering and Mixing System for Composites in the Automotive Industry [Mémoire de maîtrise, Polytechnique Montréal]. PolyPublie. https://publications.polymtl.ca/3802/

URL de PolyPublie: PolyPublie URL:	https://publications.polymtl.ca/3802/
Directeurs de recherche: Advisors:	Louis Laberge Lebel, & Robin Dubé
Programme: Program:	Génie aérospatial

UNIVERSITÉ DE MONTRÉAL

DEVELOPMENT OF AN AUTOMATED IN-LINE RESIN METERING AND MIXING SYSTEM FOR COMPOSITES IN THE AUTOMOTIVE INDUSTRY

PHILIPPE MURRAY

DÉPARTEMENT DE GÉNIE MÉCANIQUE

ÉCOLE POLYTECHNIQUE MONTRÉAL

MÉMOIRE PRÉSENTÉ EN VUE DE L'OBTENTION

DU DIPLÔME DE MAÎTRISE ÈS SCIENCES APPLIQUÉES

(GÉNIE AÉROSPATIAL)

FÉVRIER 2019

UNIVERSITÉ DE MONTRÉAL

ÉCOLE POLYTECHNIQUE MONTRÉAL

Ce mémoire intitulé :

DEVELOPMENT OF AN AUTOMATED IN-LINE RESIN METERING AND MIXING SYSTEM FOR COMPOSITES IN THE AUTOMOTIVE INDUSTRY

présenté par : MURRAY Philippe

en vue de l'obtention du diplôme de : Maîtrise ès sciences appliquées

a été dûment accepté par le jury d'examen constitué de :

M. VADEAN Aurelian, Doctorat, président

M. LABERGE-LEBEL Louis, Ph. D., membre et directeur de recherche

M. DUBÉ Robin, M. Sc. A., membre et codirecteur de recherche

M. JONCAS Simon, Ph. D., membre

DEDICATION

To Mom and Dad,

who encouraged me to go on every adventure,

especially this one.

ACKNOWLEDGMENTS

The work presented in this thesis was performed at Centre technologique en aérospatiale, École nationale d'aérotechnique and Cegep Édouard-Montpetit with the financial support of Magna Exteriors Inc. and the Natural Sciences and Engineering Research Council.

The completion of this undertaking would not have been possible without the assistance and knowledge of many people. Their contributions are greatly appreciated and sincerely acknowledged. However, I would like to express my deep appreciation to the following:

Mr. Robin Dubé, P.Eng. M.A.Sc., for this project opportunity, his technical assistance throughout the project and his expertise on system design.

Pr. Louis Laberge-Lebel, P. Eng. Ph.D., for his academic rigour and help on how to be a better researcher.

Mr. Bruno Croteau-Labouly, P. Eng. M.A.Sc., for teaching me his project management knowledge and for his good and funny attitude in the workplace.

Daniel Gareau, M.A.Sc. and Carl Ouellet, M.A.Sc. for their help and review on FTIR analysis and polymer chemistry.

To all relatives, friends and others who in one way or another shared their support, financially or morally, thank you.

RÉSUMÉ

L'utilisation de composites structuraux pour les applications automobiles est considérée comme un moyen d'atteindre les nouvelles réglementations à venir en matière d'émission de CO_2 des véhicules et les initiatives d'allégement. Le composé de moulage en feuille (SMC) de résine vinyle ester et de fibre de carbone utilisé avec le moulage par compression à chaud est actuellement l'une des solutions les plus performantes pour atteindre les cadences de production élevées requises par l'industrie. Les résines à polymérisation rapide utilisées contiennent une large gamme de charges et d'additifs permettant de réduire le coût de la matière et d'améliorer diverses propriétés. Les entreprises automobiles souhaitant rester compétitives doivent disposer d'une machine permettant le dosage et le mélange de cette résine, ainsi que de ses multiples additifs et charges, pour une distribution en continu à la chaîne de production. Magna International, un des principaux fournisseurs automobiles au monde, est actuellement en phase de validation d'un nouveau sous-châssis SMC et a demandé au Centre technologique en aérospatiale (CTA) de développer un nouveau prototype de système de dosage et de mélange de la résine en ligne. Le projet a été rendu possible grâce à la combinaison d'un étudiant à la maîtrise de l'École polytechnique de Montréal à travers une subvention Mitacs et d'une subvention RDA niveau 3 du CRSNG. Les objectifs du projet étaient de démontrer les performances de l'utilisation d'un mélangeur statique pour obtenir un échantillon de résine homogène, de développer et de fabriquer un nouveau système de dosage et de mélange de résine à deux composants et de valider la performance et les capacités du système. Les systèmes de dosage et de mélange à deux composants présentement disponibles ne sont pas adaptés pour traiter des fluides abrasifs et opérer dans des zones dangereuses de Classe 1 Division 1. En ce qui concerne le mélange, les mélangeurs statiques semblent offrir des performances suffisantes pour mélanger un système de résine à deux composants, mais leur performance est difficile à prédire à l'aide de modèles et de simulations. La performance d'un mélangeur statique de type Kenics a été évaluée par spectroscopie infrarouge à transformée de Fourier à réflexion totale atténuée (ATR-FTIR). Les résultats des travaux ont démontré que l'utilisation d'un mélangeur statique permet de mélanger les composants avec 98% d'homogénéité. Le nouveau système de mélange a été conçu, fabriqué et testé au CTA avant d'être installé et intégré à la ligne expérimentale de production de préimprégné SMC de Magna International. Il offre une large plage de ratio de mélange de 0,8:1 à 320:1 et un débit allant jusqu'à 2500 ml/min à un ratio de mélange nominal de 20,5:1. Le dosage de la machine repose sur un ensemble innovant de pompes à plongeur

multiplex. Il présente une précision de ratio de mélange de ± 1% et une homogénéité de mélange de 98,5% (CoV de 1,5%). Le système est automatisé et ajuste sa cadence de mélange et distribution automatiquement via une boucle de rétroaction de contrôle PID avec la ligne de production.

Mots clés: système de mélange en ligne, FTIR, mélange statique, composites, durcissement rapide, industrie automobile

ABSTRACT

The use of structural composites for automotive applications is seen as a means of reaching the upcoming new regulations regarding CO_2 emission of vehicles and light-weighting initiatives. Carbon fibre vinyl ester Sheet Moulding Compound (SMC) used with hot compression moulding is currently one of the leading solutions to achieve high-volume production cadences required by the industry. The fast-cured resins used contain a wide range of fillers and additives to lower the material costs and improve various properties. Automotive companies wishing to remain competitive must have a machine that allows the dosing and mixing of this resin, along with its multiple additives and fillers, for delivery to the production line continuously. Magna International, a world-leading tier one automotive supplier, is currently in the validation phase of a new SMC front car subframe and mandated Centre technologique en aérospatiale (CTA) to develop a new prototype in-line resin metering and mixing system. The project was made possible with the combination of a master's student from Polytechnique Montréal through a Mitacs grant and an NSERC ARD level 3 grant. The objectives of the project were to demonstrate the performance of using a static mixer to obtain a homogeneous sample, develop and manufacture a new two-component resin metering and mixing system and validate its performance and capabilities. Commercially available two-component metering and mixing system are not capable of processing abrasive fluids while operating in Class 1 Division 1 classified locations. With respect to mixing, static mixers seem to offer adequate performance to mix two-component resin system but their performance is hard to predict with models and simulations. The performance of a Kenics static mixer was evaluated using attenuated total reflection Fourier transform infrared spectroscopy (ATR-FTIR). The use of a static mixer allows the resin and thickening agent to be mixed to 98 % homogeneity. The new system was designed, manufactured and tested at CTA before being installed and integrated to Magna International SMC prepreg development line. It offers a wide range of mixing ratio of 0,8:1 to 320:1 and flow rate of up to 2500 ml/min at a nominal mixing ratio of 20,5:1. The machine's metering relies on an innovative multiplex assembly of plunger pumps. It has a mixing ratio precision of ± 1 % and a mixing homogeneity of 98,5 % (CoV of 1,5 %). The system is automated and adjusts its production rate automatically through a PID control feedback loop.

Keywords: in-line mixing system, FTIR, static mixing, composites, fast-cure, automotive industry

TABLE OF CONTENTS

DEDICATION iii

ACKNOWLEDGMENTS iv

RÉSUMÉ v

ABSTRACT vii

TABLE OF CONTENTS viii

LIST OF TABLES xii

LIST OF FIGURES xiv

LIST OF APPENDICES xviii

CHAPTER 1 INTRODUCTION 1

CHAPTER 2 LITERATURE REVIEW 4

2.1 Composite materials in the automotive industry 4

2.2 Manufacturing processes 5

2.3 Applications of composites in the automotive industry 8

2.4 Thermoset resins, the importance of mix homogeneity and characterization methods 10

2.4.1 Mixing homogeneity 13

2.5 Mixing technologies for in-line mixing systems 20

2.5.1 Static mixing 20

2.5.2 Dynamic mixing 26

2.5.3 Impingement mixing 28

2.6 Pumping technologies for in-line mixing systems 30

2.6.1 Positive displacement pumps 31

2.6.2 Importance of flow rate linearity 35

2.7 Resin metering and mixing systems 36

2.7.1 Hazardous classified locations 37
2.7.2 Resin abrasiveness 39
2.7.3 Two-component metering and mixing systems 39
2.7.4 Summary of current systems limitations 43
2.8 Summary and knowledge gaps 43
2.9 Project objectives 44
CHAPTER 3 DEMONSTRATION OF THE PERFORMANCE OF A STATIC MIXER TO OBTAIN AN HOMOGENEOUS RESIN SAMPLE 45
3.1 Materials 45
3.2 Equipment 46
3.3 Procedure 49
3.3.1 FTIR spectroscopy as a technique to evaluate the homogeneity of a resin sample ... 49
3.3.2 Performance of a static mixer to obtain a homogeneous resin sample 52
3.3.3 Qualitative evaluation of the impact of mixing ratio variation on mix homogeneity 53
3.4 Results and analysis 54
3.4.1 FTIR spectroscopy as a technique to evaluate the homogeneity of a resin sample ... 54
3.4.2 Performance of a static mixer to obtain a homogeneous resin sample 62
3.4.3 Qualitative evaluation of the impact of mixing ratio variation on mix homogeneity 64
3.5 Conclusions 66
CHAPTER 4 DEVELOPMENT AND MANUFACTURING OF A PROTOTYPE IN-LINE METERING AND MIXING SYSTEM 68
4.1 Requirements 68
4.1.1 Process requirements 68
4.1.2 System requirements 69
4.1.3 Additional requirements 70

4.2 Preliminary design 73
4.2.1 Resin preparation 75
4.2.2 Metering system 76
4.2.3 Mixing and delivery 77
4.2.4 Equipment technology choice 77
4.3 Detailed design 80
4.3.1 Computer-assisted design (CAD) 81
4.3.2 Automation and control logic 85
4.3.3 HMI 87
4.3.4 System technical and performance data 89
4.4 Manufacturing 90
4.4.1 Metering system 90
4.4.2 Mixing and delivery system 91
4.4.3 Control panel 92
CHAPTER 5 VALIDATION OF THE SYSTEM'S PERFORMANCE 95
5.1 Flowmeter precision validation 95
5.2 Control logic 98
5.2.1 Overpressure safety 98
5.2.2 Doctor box level control 99
5.3 Flow rate linearity 101
5.4 Cleaning 105
5.5 Mix homogeneity 106
5.6 System performance summary 107
5.7 Commissioning 109

CHAPTER 6 CONCLUSION AND RECOMMENDATIONS 111

6.1 Future work and recommendations 112

BIBLIOGRAPHY 114

LIST OF TABLES

Table 1 – Price and tensile strength comparison of polyester, vinyl ester and epoxy resins 11

Table 2 – Common additives and fillers and their effect on resin properties 13

Table 3 - Advantages and disadvantages of mix homogeneity characterization methods.....19

Table 4 – Popular types of static mixers 21

Table 5 - Mixing performance analysis of static mixers.....23

Table 6 – Pressure drop and interfacial stretch of different static mixers.....25

Table 7 - Comparison of static, dynamic and impingement mixers.....30

Table 8 - Project relevant flammable gas and vapour classification definitions in Canada.....38

Table 9 - Reviewed metering and mixing system technical data 41

Table 10 – Parts A and B technical information 46

Table 11 - Beer-Lambert law sample composition 50

Table 12 – Raw, time compensated and normalized isocyanate absorbance peak height and CoV of hand mixed samples.....61

Table 13 – Raw, time compensated and normalized isocyanate absorbance peak height and CoV of samples mixed using the Kenics static mixer 63

Table 14 – Isocyanate absorbance peak height coefficient of variation 65

Table 15 - Mixing ratio precision requirements.....68

Table 16 – System's operating range 69

Table 17 - Resin system properties 69

Table 18 - In-line metering and mixing system component identification 75

Table 19 - Pressure drop calculations from the outlet of the metering pump to the outlet of the static mixer.....81

Table 20 - Programmable logic controller (PLC) inputs and outputs list 85

Table 21 - System alarms and warnings.....89

Table 22 - Developed system theoretical technical and performance data 89

Table 23 - Stack light colour code definition.....94

Table 24 - Flow rate linearity and dampening efficiency at 100 psig.....103

Table 25 - Coefficient of variation of samples mixed with the system.....107

Table 26 - System's performance, capabilities and features.....108

Table 27 - Chemical compatibility of various chemicals of interest with metals, plastics and elastomers.....121

LIST OF FIGURES

Figure 1 - SMC material manufacturing process and hot compression moulding [13] 6

Figure 2 – Use of structural composites in the automotive industry: (a) BMW i3's cabin made using HP-RTM [27] and (b) BMW's 7-series hybrid-construction Carbon-Core [26] 9

Figure 3 – SMC use in the automotive industry: (a) SMC carbon fibre subframe and (b) inner door panel, JEC Show 2018 9

Figure 4 - SMC front subframe by Magneti Mirelli [29].....10

Figure 5 - Typical SMC resin formulations additive and filler content [17] 12

Figure 6 – FTIR transmittance spectra of polyvinyl acetate (left) and methyl isocyanate (right) [65] 15

Figure 7 - FTIR calibration graph for aspirin dissolved in chloroform [63].....16

Figure 8 - Visual evaluation of the homogeneity of a two-component product mix through a static mixer [70].....18

Figure 9 - SMX mixer geometrical configuration (n, N_P, N_X, θ) = (3, 5, 9, 90°) 22

Figure 10 - Mixing profiles and layers as a function of the number of mixing elements [73] 24

Figure 11 – Actual interfaces produced (Scheme 2) per mixing element.....25

Figure 12 – In-line dynamic mixer by Silverson [81].....27

Figure 13 – Static-Dynamic mixing heads: (a) Static-Dynamic by DOPAG [82] and (b) LC 5/3 by Tartler [83] 28

Figure 14 –Impingement mixer: (a) Schematic of a typical impingement mixing head and (b) Simulation of impingement mixing for a two-component fluid [85].....29

Figure 15 – Rotary positive displacement pumps: (a) gear, (b) lobe, (c) progressive cavity and (d) peristaltic 32

Figure 16 – Reciprocating positive displacement pumps: (a) double diaphragm pump, (b) piston (left) and plunger (right) pump.....34

Figure 17 - Pulsation dampening on a 1" air operated double diaphragm positive displacement pump 36

Figure 18 - Electrical area classification around an open container in a ventilated area 38

Figure 19 – Commercially available two-component metering and mixing system: (a) Mahr MarMax, (b) Tartler Nodopur, (c) Cannon B-System, (d) Meter Mix PAR200 and (e) DOPAG Compomix 40

Figure 20 - Kenics RL 180 static mixer 47

Figure 21 – Pumps used during testing: (a) Resin injection piston, (b) laboratory scale syringe pump, and (c) peristaltic pump 48

Figure 22 - Perkin Elmer UATR Two 49

Figure 23 – (a) FTIR sample positions and (b) mixing jar 50

Figure 24 - V-shaped sample collector: (a) Puller and (b) output of the static mixer into the V-shaped container 52

Figure 25 - Sampling positions within the V-shaped container to validate the performance of the static mixer 53

Figure 26 - Sampling positions within the V-shaped container using the static mixer and the peristaltic pump 53

Figure 27 - Overlay FTIR spectra of parts A and B 54

Figure 28 - Beer-Lambert law isocyanate absorbance peak height versus mix concentration 56

Figure 29 - FTIR spectra of samples mixed by hand for 2 minutes, data collected 1 hour after mixing 57

Figure 30 – Overlay FTIR spectra of hand mixed sample with parts A and B of the resin 58

Figure 31 – FTIR spectra evolution of a mixed sample over 48h 59

Figure 32 - Amplitude of the isocyanate absorbance peak at one and two hours after mixing 60

Figure 33 - FTIR spectra of samples mixed with the static mixer, data collected 1h after mixing 62

Figure 34 - Overlay of isocyanate absorbance peak height and pulsed flow rate model 65

Figure 35 – 1" Sanitary Stainless Steel Ball Valves: (a) amateur brewery application [101] and (b) industrial food and pharmaceutical applications [102] 71

Figure 36 - Use of an intrinsic safety barrier for instrumentation located in a hazardous location The safety barrier, installed in the control panel, falls outside the hazardous location [103] 72

Figure 37 - In-line metering and mixing system process and instrumentation diagram: resin preparation, metering system and mixing and delivery areas 74

Figure 38 - Working principal of a plunger pump - Image courtesy of TKM LLC..... 78

Figure 39 - Sanitary tri-clamp piping connection with PTFE gasket: (a) assembled [104] and (b) disassembled [105] 80

Figure 40 - Resin preparation 3D CAD 82

Figure 41 - Metering system 3D CAD 83

Figure 42 - Mixing and delivery 3D CAD 84

Figure 43 - HMI Screens: (a) Home, (b) Status, (c) Calibration, (d) Manual Mode, (e) Data Logging and (f) Alarms 88

Figure 44 – Metering system assembly 91

Figure 45 - Mixing and delivery system mock-up 92

Figure 46 – Control panel..... 93

Figure 47 - Coriolis flowmeter precision validation: (a) Experimental data with error bars for the individual measurements and (b) Average of experimental data with error bars representing the standard deviation for each flowrate 96

Figure 48 - Gear flowmeter precision validation: (a) Experimental data with error bars for the individual measurements and (b) Average of experimental data with error bars representing the standard deviation for each flowrate 97

Figure 49 - Validation of doctor boxes level control logic 100

Figure 50 - Flow rate dampening of part A of the metering system at 100 psig..... 102

Figure 51 - Mixing ratio evolution after system start-up at nominal speed (39 Hz)..... 104

Figure 52 - Part B (top) and Part A (bottom) acetone samples colour evolution following three clean-in-place flush procedures 105

Figure 53 - SMX mixer used in the final system 106

Figure 54 – System resin outlet to doctor box one at the partner's facility: (a) Level sensor and system output and (b) system in operation with the prepreg line 109

Figure 55 - SMC prepreg material manufactured using the new in-line metering and mixing system at the partner's facility 110

Figure 56 - Doctor box individual control logic 122

Figure 57 - PID cases for metering system output control 123

LIST OF APPENDICES

Appendix A – Chemical compatibility.....121

Appendix B – Doctor box level control logic 122

CHAPTER 1 INTRODUCTION

To address climate change, Canada set an aim to reduce its greenhouse gas emissions by 30% by 2030 compared to current predictions [1]. Of the current emissions, the transportation industry is responsible for almost a quarter [2]. In fact, the Passenger Automobile and Light Truck Greenhouse Gas Emission Regulations, from the Canadian Environmental Protection Act, forces car manufacturers to find new solutions to reduce the fuel consumption of their vehicles [3]. Throughout its complete lifecycle, a vehicle's useful life accounts for up to 80% of its total environmental footprint and among this impact, the vehicle's mass has the most direct effect [4]. Recently, this industry has turned to the use of composite materials for structural applications. The use of such materials is mainly aimed at reducing weight when compared to traditional metallic materials. Consequently, these advanced materials provide a significant reduction in the emission of greenhouse gases throughout the useful life of the part and as a result, predictions suggest that more than one-third of global production of carbon-reinforced composites will be made by the automotive industry by 2021 [5]. To compensate for this higher demand, the development of rapid and low-cost manufacturing methods for composite materials is essential.

The high-performance composite materials used for load-bearing applications are generally formed of a high-temperature thermosetting matrix reinforced with high strength fibres. A common example is the combination of a vinyl ester resin matrix with a carbon fibre reinforcement [6]. Sheet Molding Compound (SMC) is a composite material that is best suited to manufacture large parts at high production volumes [7]. In fact, Magna International (Magna) and Ford Motor Co. are currently in the validation phase of a carbon fibre reinforced polymer front subframe manufactured using this material [8]. SMC is composed of a fast cure resin, short fibres reinforcement, fillers and a pre-mixed catalyst (hardener). This mixture, ready for hot compression moulding, is in the form of sheets and can be stacked at various thicknesses and put into a mould. To improve the applicability of these materials, additives (or fillers) are mixed with the resin. The type and amount of additives can influence several properties of the resin like reducing gas permeability, improve solvent resistance, increase mechanical and thermal properties and improve flame retardancy. With these multiple additives, automotive companies wishing to remain competitive must have a machine that allows the mixture of this resin with its multiple additives and allow the delivery to the production line continuously. Resin mixing systems play an important

role in the fabrication of composite parts and can range from the simple open top container with manual batch mixing, to the fully automated in-line resin mixing system that allows for continuously mixed resin dispensing. Ultimately, no matter the system used for the mixing process, resin homogeneity must be very high for manufacturers to get consistency in their products' properties.

The use of composites for structural parts in the automotive industry is now of interest for mass market production cars. Many companies are in search of a resin mixing system that is versatile and robust enough to allow for the development and optimization of these new materials. Systems readily available do not offer enough versatility to adapt to new resin formulations. Resin properties are adjusted by modifying the manufacturing process parameters, mixing ratio of the various chemical components and adding additives to the resin. Unfortunately, these changes often alter the physical characteristics of the resin, requiring a versatile mixing system that performs well with a wide range of fluid viscosities and chemical compatibility. Currently available metering and mixing systems do not allow to process abrasive fluids in a Class 1 Division 1 hazardous location, limiting the manufacturers' room for development and improvement. Likewise, the systems generally work in batches, making it difficult to manufacture the material continuously, a major drawback when high production output is the required.

To address these issues, Magna Exteriors Inc. (Magna), a division of Magna International Inc., worked jointly with the Centre technologique en aérospatiale (CTA) and Polytechnique Montréal on a research project. The objective was to develop a new and tailored in-line resin metering and mixing system to address the commercially available systems' problems. The project team has great knowledge on system design, resin chemistry, composite manufacturing processes and project management, four important assets to the success of such an undertaking.

This thesis presents the results of the project and is divided into five (5) chapters. The first chapter goes over background information on composites in the automotive industry, mixers, pumps and resin mixing systems to put the reader in context. The second chapter demonstrates the performance of using a static mixer to obtain a homogeneous resin sample. Then, chapter three presents the development and assembly of the new automated in-line metering and mixing system. The fourth chapter is on the validation of the new system's performance. Finally, the last chapter

draws conclusions and traces the path for future research work along with various recommendations.

CHAPTER 2 LITERATURE REVIEW

2.1 Composite materials in the automotive industry

Composite materials, or simply composites, are mostly known for their excellent mechanical properties. They are an assembly of two or more immiscible components with different properties that, when combined, create a material with usually better mechanical properties and lower weight than traditional metals. These high-performance materials, already used extensively for trim parts of niche vehicles[1] in the automotive industry, have made little to no appearance in high production volume cars as of now, especially for structural parts [9], [10].

There is no proper definition for what a high production volume car is. Sales number vary greatly depending on the country, year and car model. Looking at the statistics of various popular cars of today's industry, high-volume production vehicles sell somewhere in the mid to high hundreds of thousands of units per year. For example, Ford Motor Co. sells about 200,000 Focus and 900,000 F-series per year in the U.S. alone [11]. In a production perspective, considering a high-volume vehicle to sell on average 300,000 units per year with three 8 hour shifts per day, this means that original equipment manufacturers (OEMs) target part cycle times of 1 to 2 minutes. The manufacturing cost of composites is the main challenge the industry must overcome to implement these new materials to the production lines. Automakers must find ways to simplify and automate the production cycle to bring the cost down for structural composite materials to compete with traditional metals [10].

Composites are made of a matrix and a reinforcement. The fundamental role of the reinforcement is to carry the mechanical loads and to increase the mechanical properties of the matrix. In the automotive industry, fibre reinforcements are mostly made of glass or carbon in the form of chopped fibres, filament yarns and fabric.

On a mechanical level, the matrix is made of a polymer, multiple additives and a catalyst that binds the reinforcement and transfer the load between the fibres as well as protect them from the environment. On a physical level, the matrix gives the component shape and has an impact on the

[1] A niche vehicle is sold in low-volumes.

quality of the surface finish. Matrices come in three main categories: polymer, ceramic or metallic. The use of polymer matrices is most common because of their lower processing temperature when compared to ceramic or metallic matrices and therefore allow for simpler tooling. Polymeric matrices are then subdivided into two categories: thermosets and thermoplastics.

A thermoset resin is a polymer that, through polymerization, exhibits a modification of its molecular chain called crosslinking. This chemical change results in a three-dimensional network of bonds. Advantages of thermoset matrices over thermoplastics include low processing temperatures and viscosity, liquid state at room temperature and excellent mechanical resistance. However, they cannot be recycled due to the chemical reaction they exhibit during cure. On the other hand, thermoplastics can be melted and reshaped if heated above a certain temperature. In addition, they have the advantage of having high impact resistance but have a characteristic high processing viscosities and show low heat resistance when compared to thermosets [12].

2.2 Manufacturing processes

Depending on a part's geometry, application and production volume, different composite manufacturing processes are employed. In most high production volume parts, hot compression moulding using sheet moulding compound (SMC) is used. SMC combines short chopped fibres pre-impregnated with thermoset resins to produce a material in which only the concentration of the strengthening fibres is controlled but not their exact dimensions or orientation [6]. Figure 1 shows a typical SMC line from material manufacturing to hot compression moulding of the part.

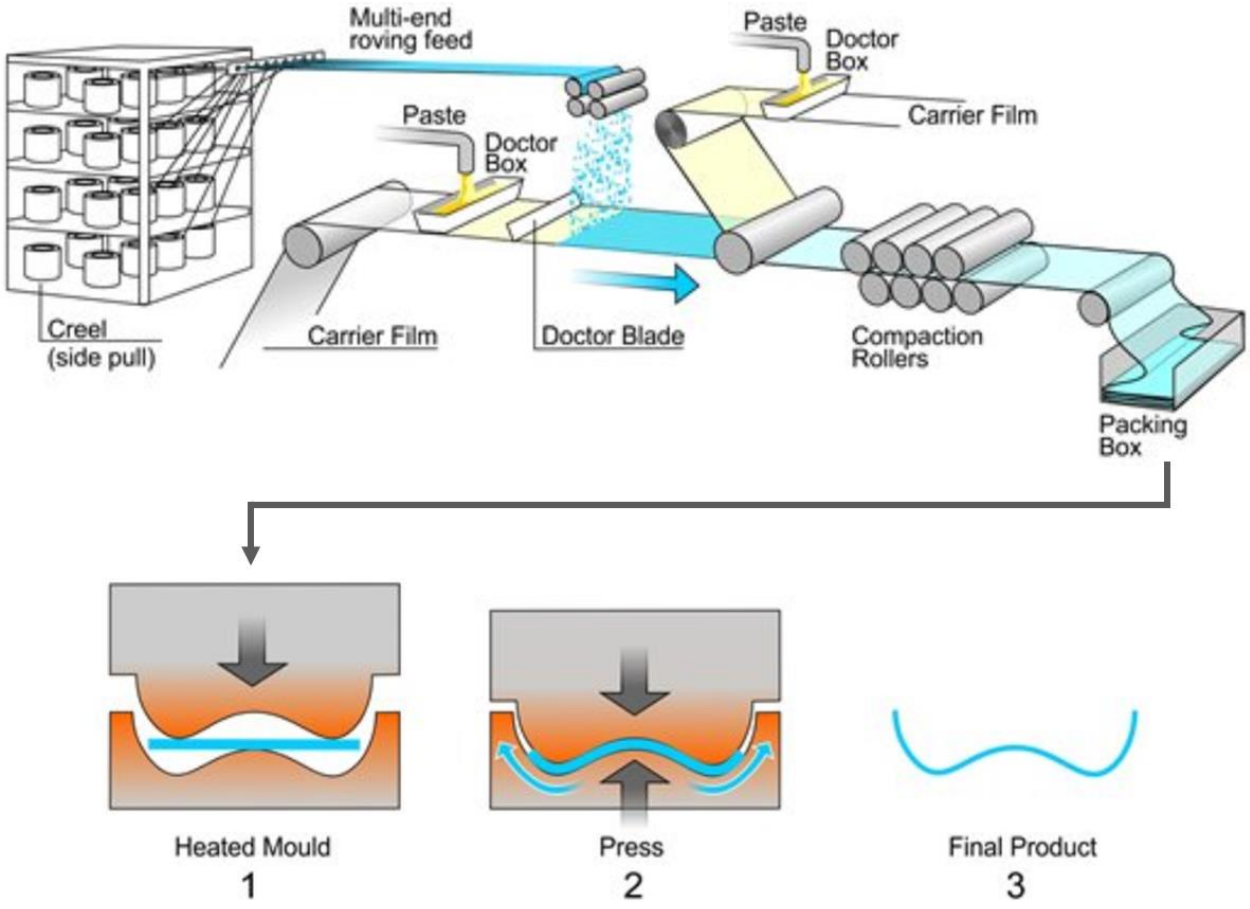

Figure 1 - SMC material manufacturing process and hot compression moulding [13]

The first step in manufacturing SMC is cutting the carbon fibre roving feed into small strands of approximately 25 mm. According to a study by Boylan et al., the SMC constituent that has the most influence on the required moulding force is reinforcement length. Results obtained show that the moulding force increases significantly over 25 mm. As a tradeoff between mechanical properties and material flow during moulding, the industry mostly uses reinforcement of 25 mm in length [14], [15]. These chopped fibres then fall onto a carrier film covered with a thin layer of resin. The resin is evenly spread onto the surface of the film using what is called a doctor box. These boxes collect the mixed resin at the output of the mixing system. Two resin covered films sandwich the chopped fibres before encountering a series of compaction rollers that compress the stack to impregnate the fibres with resin. Finally, depending on the resin chemistry, the produced

prepreg sheets are then stored for 24 to 48 hours to mature. During this time, the resin thickens and allows the sheets to be manipulated by a robot or an operator to be put in a heated mould. Finally, the material is compressed at high pressures of about 1,000 psi and the part cures in minutes to produce the final product [16].

Still allowing high production volumes, bulk moulding compound (BMC) is used in the same way as SMC but the material put in the compression mould, the charge, is in the form of a paste. During moulding, the charge is compressed and flows to fill the mould cavities. BMC parts tend to have lower mechanical resistance than SMC because the charge flow is harder to predict than with sheets that have already been stacked and positioned before moulding. In addition, the fibre length is shorter with BMC than SMC because the material paste requires significantly more flow to fill the mould cavities [17]. This makes BMC's use limited to parts without significant load bearing applications [18].

Another manufacturing process that is currently used in production is high-pressure resin transfer moulding (HP-RTM). In this process, the resin is injected at high pressure in a closed mould where a dry composite preform is placed. Unfortunately, this manufacturing method is not suitable for high production volume because of the higher cycle time. More complex parts tend to be made using HP-RTM, while simple parts tend to use hot compression moulding methods like SMC.

Other composite materials and processes are used in the automotive industry but they do not meet the criteria for structural applications. For interior parts like dashboards, short fibre reinforced thermoplastic injection is used at high production volumes. This manufacturing method allows cycle time to drop below 90 seconds, making it perfect for high production volume. In addition, glass mat thermoplastics (GMT) is used for medium volume production and has become highly automated over the years. It can be compared to SMC in terms of manufacturing method but mechanical properties of the glass and thermoplastic combination do not meet structural requirements [19].

SMC compression moulding offers a lower cycle time and less expensive tooling and material costs than HP-RTM [20]–[22]. Nevertheless, HP-RTM is best suited for high performance and complex structural parts for low to medium volume production cars while SMC ideal for simpler structural parts for high production volume. Global Market Insights Inc. evaluated that

SMC hot compression moulding would soon dominate the automotive composite market as a manufacturing method. This growth is attributed to investment aimed at reducing cycle time, improving ease of manufacturing and offering competitive prices of the process. The same report predicts that the automotive composite market for structural applications will exhibit a compound annual gross rate of 7% until 2024 [10]. On a technical perspective, SMC technology seems to be in the best position to eliminate the industry's dominant problems of cycle time and cost. Finally, this growing industry of high resistance structural parts is at the core of recent advancements in the automotive industry in the last decade.

2.3 Applications of composites in the automotive industry

Among the first production cars to make extensive use of composites was the 1953 Chevrolet Corvette. With its all-fibreglass exterior body, the Corvette had a production volume of only 300 cars during its introductory year. Since then, the Corvette has featured composite body parts and production has increased to an average of 36,250 cars per year for the latest generation [23], [24]. Yet, the Corvette's composite body panels are not considered structural parts, as the car can still operate normally should they be removed or damaged.

Starting in 2013, the BMW i3 features an all-composite passenger cell, shown in Figure 2. The cabin is made from carbon fibre reinforced epoxy resin manufactured mostly through HP-RTM. The BMW i3 sold 31,482 vehicles globally in 2017 [25]. Yet, the BMW i3 is currently the largest composites serial production in the automotive industry, followed by BMW's 7-series [26]. The 7-series uses a hybrid construction method for its cabin, also shown in Figure 2. The use of structural composites in the automotive industry can, therefore, be considered as limited to high performance or luxury cars with relatively low production volumes.

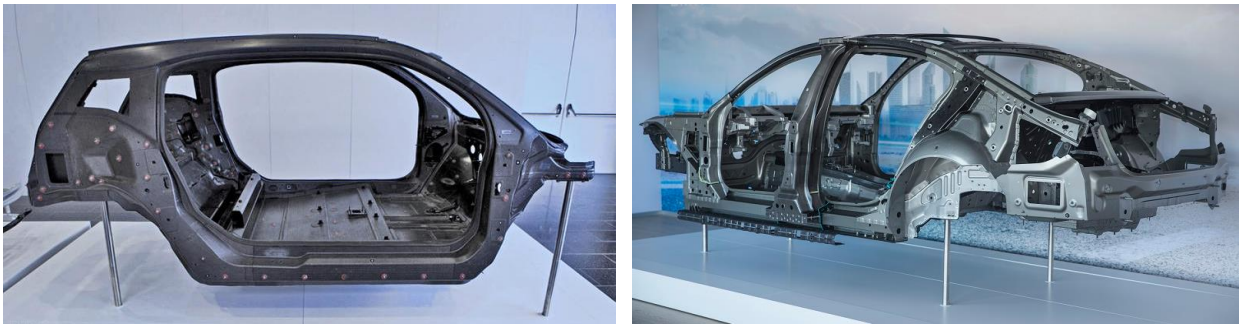

(a) (b)

Figure 2 – Use of structural composites in the automotive industry: (a) BMW i3's cabin made using HP-RTM [27] and (b) BMW's 7-series hybrid-construction Carbon-Core [26]

Figure 3 shows SMC carbon fibre prototype parts intended for mass market vehicles. The picture on the left shows a front subframe manufactured by Magna. The subframe, a primary structural part supporting the motor and wheels, allows weight reduction by up to 34 percent and brings the number of parts from 45 to 6 when compared to the current mass produced metallic version [8]. The picture on the right shows an inner door panel manufactured in a partnership between HYM Haiyuan and Ranger Compositi using the same technology.

(a) (b)

Figure 3 – SMC use in the automotive industry: (a) SMC carbon fibre subframe and (b) inner door panel, JEC Show 2018

Like Magna, Magneti Marelli is currently developing a subframe made of SMC compression moulding. The subframe assembly, shown in Figure 4, is currently being tested on four-door compact sedan vehicles [28].

Figure 4 - SMC front subframe by Magneti Mirelli [29]

2.4 Thermoset resins, the importance of mix homogeneity and characterization methods

The most commonly used matrices for structural applications in the automotive industry are epoxies and vinyl esters for their higher mechanical resistance and thermal performance [30], [31]. Vinyl ester polymers have been widely used for their good mechanical properties, thickening and curing performance as a matrix for SMC [32].

Vinyl ester polymers are a hybrid between polyester and epoxy polymers that feature two catalytic reactions. They are produced by the esterification of epoxy with carboxylic acid, usually bisphenol A and methacrylic acid. The prepolymer is usually dissolved in styrene to decrease the viscosity and to allow the reaction with the methacrylate [33].

In SMC applications, the resin is mixed with a thickening agent to allow the sheets to be manipulated and put into a mould. Physical and chemical thickening methods can be employed. Physical thickening uses crystalline resins but their research difficulty and cost limit their use [32]. In contrast, chemical thickening can be accomplished with isocyanates to form covalent bonds between the hydroxyl and carboxyl groups of the resin, known as urethane linkage [34].

For SMC manufacturing, the resin is made of two major components, part A (vinyl ester monomer, catalyst, inhibitor) and part B (isocyanate). The first reaction is a typical polyurethane reaction which involves isocyanate (Part B) reacting with amines in the vinyl ester resin (Part A)

to thicken the resin. This reaction increases the size of the molecules, notable via the thickening of the resin. This allows rolls of prepreg material to be manufactured and manipulated. The secondary reaction involves vinyl ester crosslinking for part manufacturing and is activated through heat when the product is moulded to its final shape. The increase in thermal energy makes the catalyst sufficiently reactive to initiate the crosslinking reaction of the vinyl ester. This final reaction is what gives the product its properties.

It is important to note that part B, containing mostly a mix of various forms of isocyanate, is very sensitive to humidity [34]. Moisture in the air, a polar compound, reacts with the isocyanate functional group and releases carbon dioxide as a product. This product is undesirable for a resin system because it can create porosity and decrease its mechanical properties. Therefore, during all the manufacturing phase, great care must be given to ensure the resin is stored in an airtight container in a dry environment.

Vinyl ester's mechanical properties and cost fall between polyesters and epoxies. Table 1 lists prices and tensile strength for polyester, vinyl ester and epoxy resin families.

Table 1 – Price and tensile strength comparison of polyester, vinyl ester and epoxy resins

Resin family	**Average price[2] ($/lb)**	**Tensile Strength (MPa)** [35]	**Stiffness (GPa)** [35]
Polyester	2-3	6.4	2.8
Vinyl Ester	3-8	7.6	3.0
Epoxy	5-30	8.1	3.3

Mechanical properties of polyesters do not allow the resin to be used for structural applications. Even though epoxy resins have higher mechanical properties than vinyl ester resins, their higher cost may affect the business case viability in high production volumes. As seen above, BMW uses Huntsman's Araldite LY 3585/Hardener XB 3458 epoxy system for its i3 passenger

[2] Dubreuil, Personal discussion. 2018-10-04. Price listed are a rough estimate. Price will vary greatly depending on the desired properties and purchased volume. Price listed considers a high-volume purchase.

cell, but the car's low production volume and high price, starting at 48,750 $ before taxes, makes it a niche model [36], [37]. In contrast, Magna uses vinyl ester resin for its prototype carbon fibre reinforced polymer front subframe in its development partnership with Ford [38]. The composite part, manufactured using SMC technology, is currently being tested on Ford Fusion models, a car that sold over 200,000 units in 2017 in the U.S. alone with a price starting at 22,838$, about half of BMW's i3 [39], [40].

SMC part manufacturers add multiple additives and fillers to improve the resin properties and bring the cost down. Additives are used to improve performance and alter properties of the resin while fillers are mostly used to reduce cost. Figure 5 breaks down typical SMC resin formulations additive and filler weight content.

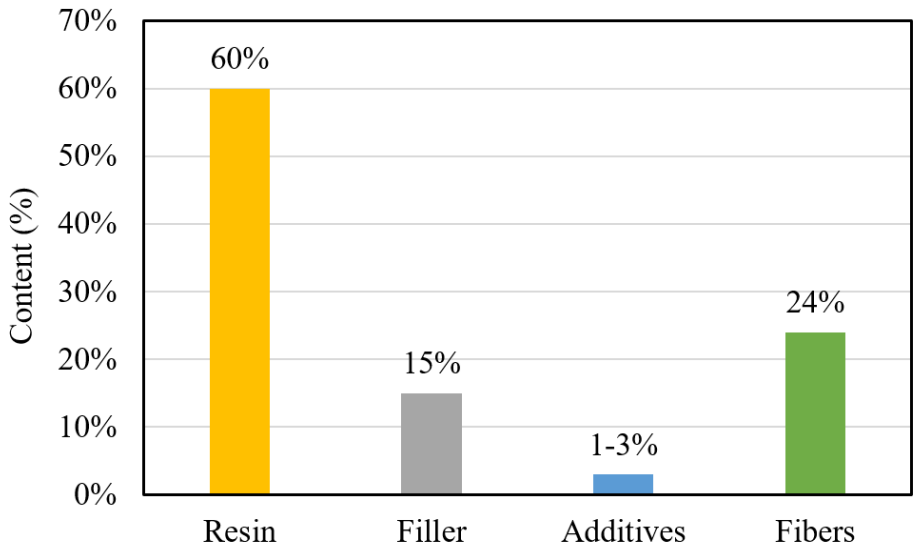

Figure 5 - Typical SMC resin formulations additive and filler content [17]

Filler content is much higher than additives, motivated by the economic advantage they offer. Table 2 lists common additives and fillers with their effect on resin properties.

Table 2 – Common additives and fillers and their effect on resin properties

		Effect on resin properties	Reference
Additive	Nanoclay	Improved toughness, flexural strength and modulus, tensile strength and modulus	[41], [42]
	Phosphorus	Flame retardancy	[43]
	Carbon black	UV protection	[44]
Filler	Glass microspheres	Weight reduction and stiffness increase, reduced shrinkage	[45], [46]
	Calcium carbonate	Increased crosslinking density and stiffness	[47]
	Milled carbon or glass fibers	Improved mechanical properties	[48]
	Talc	Thermal stability and reduced shrinkage	[49]

2.4.1 Mixing homogeneity

Two conditions are required for the polymer to reach the highest degree of polymerization; the components must be present in the right concentration and location [50], [51]. The first condition is dictated by the homogeneity of the mix while the second is a result of good dosage of the resin's constituents. In process engineering, industrial mixing is the control of segregation and is used to obtain a homogeneous distribution of the components in the entire volume [52]. In the field of thermosetting polymers, because slight changes to the formulation can significantly affect the curing and properties of the resin, it is important to make sure that the homogeneity of the resin is sufficient and that the mixing process is well controlled [53].

Depending on the products to be mixed, a wide range of tests can be performed to evaluate homogeneity. Mix homogeneity is a statistical measure of the spatial dispersion of the components and is quantified using the coefficient of variation (CoV) of the products, also known as the intensity of segregation [54]. The CoV is the most commonly used metric to quantify the homogeneity of a mixture [55]. It is calculated by dividing the standard deviation σ_c by the mean μ as,

$$CoV\% = \left(\frac{\sigma_C}{\mu}\right) * 100 \quad (1)$$

the standard deviation of the tested property is calculated by,

$$\sigma_c = \sqrt{\frac{1}{N}\sum_{i=1}^{N}(C_i - \mu)^2} \quad (2)$$

where C_i represents the chosen numerical index, μ is the average of the index's data set and N is the sample size, by the mean. In other terms, the coefficient of variation is a measure of the dispersion of a data set to the mean, or in this case, how equal are the component concentrations in the polymer. The index used for CoV calculations should be associated with the mixture, characterize the final stage of the mixture, be independent of the mixing method and easily determined [56]. The technique used to obtain the index will depend on the materials to be mixed and their properties.

In most industrial processes, a product with a CoV of less than 5% (or. 0.05) is considered adequately mixed [57], [58]. In other terms, a CoV of 0.05 means that the product is 95% homogeneous. For example, a CoV limit of 0.05 is also required by the Canadian Food Inspection Agency for dilute drug mixing processes in the food industry for animals [59].

2.4.1.1 Determination of the index used for CoV calculations

Infrared (IR) spectroscopy is by far one of the most versatile technique to characterize organic compounds. This technique exposes a sample of material to an infrared radiation. The energy absorption of the material with respect to the infrared wavelength is derived and can be related to the substance's chemical functional groups. The machine expresses the results as absorbance or transmittance spectra, both of which are related using,

$$A = -\log(T) \quad (3)$$

where A and T are respectively the substance's infrared absorbance and transmittance at a given wavenumber. More details on the working principle of FTIR can be found in reference [60]. This test method can be used for quantitative monitoring of chemical reactions as well as sample

homogeneity [61]–[64]. More specifically, Fourier Transform Mid-Infrared Spectroscopy (FTmIR), analyzing a sample at wavenumbers from 4000 to 1000 cm^{-1}, is best suited for organic polymers like isocyanate thickened vinyl ester resins and allows the detection of important functional groups. Figure 6 presents the FTIR transmittance spectra of polyvinyl acetate and methyl isocyanate. Polyvinyl acetate has a chemical composition that is very similar to vinyl ester resin.

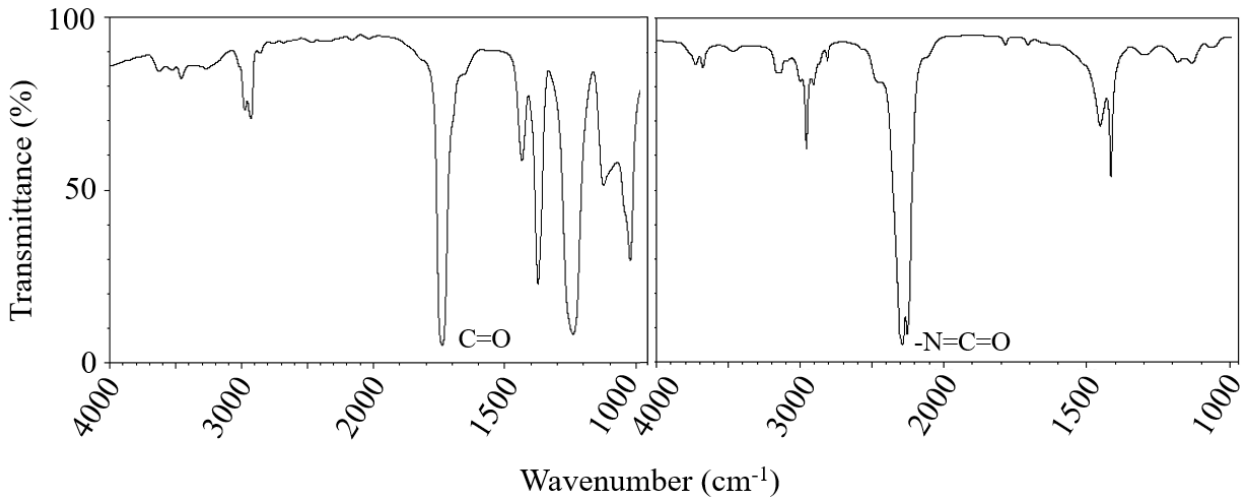

Figure 6 – FTIR transmittance spectra of polyvinyl acetate (left) and methyl isocyanate (right) [65]

Figure 6 shows the characteristic peak of the carbonyl group and isocyanate at 1738 cm^{-1} and 2810 cm^{-1} respectively. In the event of mixing both components together, as would be the case in SMC manufacturing, mostly the same absorbance peaks would be observed in the new spectrum unless rapid chemical reactions occur and modify the composition of the sample. Then, depending on the mixing ratio of both components, the spectrum of one of the components would dominate. In SMC, the chemical thickening agent is added in very low quantity to the resin [66]. This suggests the spectrum of the mixed sample will closely resemble the one for vinyl ester resin with the addition of the major absorbance peaks of the isocyanate infrared spectrum in diminished amplitude.

To use FTIR data to quantitatively evaluate the mixing homogeneity, the Beer-Lambert law is used. The law is expressed as,

$$A = \varepsilon l c \tag{4}$$

where A is the absorbance, ε is the molar extinction coefficient, l is the light path length and c is the concentration, states that the FTIR absorbance of a functional group is proportional to its concentration in the sample [63].

This means the height of a characteristic peak on an FTIR absorbance spectrum graph can be measured and used for quantitative analysis to obtain the coefficient of variation between multiple samples. Figure 7 visually presents the Beer-Lambert law using the linearity of the correlation between FTIR absorbance and the concentration of aspirin dissolved in chloroform.

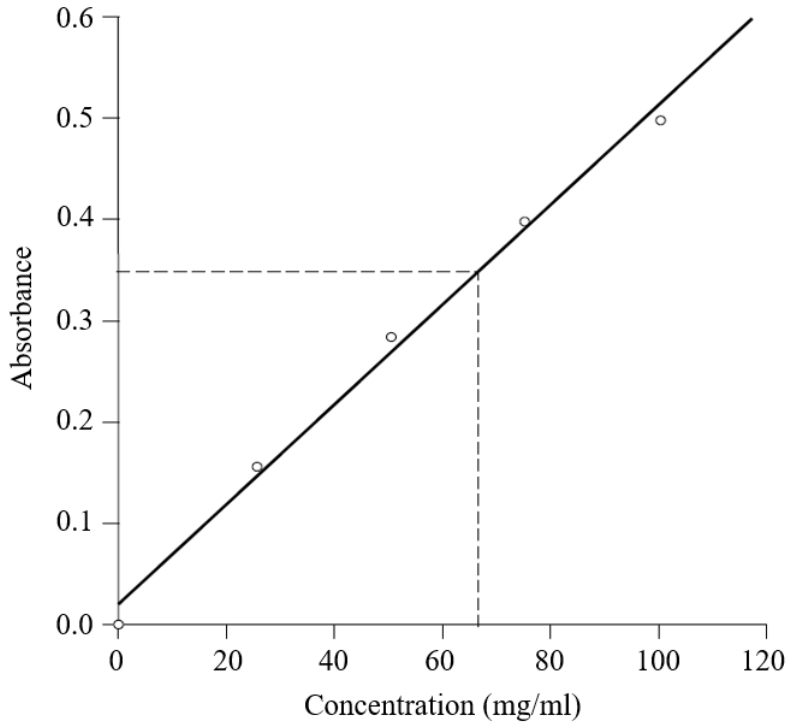

Figure 7 - FTIR calibration graph for aspirin dissolved in chloroform [63]

Applying this correlation to vinyl ester resin and isocyanate, the absorbance peak height of isocyanate at 2810 cm^{-1} can be measured and compared between multiple samples to determine the homogeneity of parts A and B of the resin. The result is expressed using the coefficient of variation (CoV).

Unfortunately, the Beer-Lambert law is only applicable under certain conditions. Non-linearities can be caused if the concentration is too high, if the sample contains solids that scatter the light or if the sample is fluorescent or phosphorescent. SMC vinyl-ester resin systems usually contain solid fillers and additives that could potentially make the Beer-Lambert law inapplicable.

Luckily, the resin does not contain conjugated double-bond systems which suggest it is not fluorescent.

Polymers mix homogeneity can also be evaluated by the mechanical property variations of the cured state. For thermoset polymers, mechanical properties can be directly correlated to the resin/hardener ratio [67]. Therefore, if the mixing is not homogeneous, specimens will show variance in their mechanical properties. On a microscopic scale, badly mixed samples will present areas with a higher or lower concentration of hardener, thus influencing the consistency of the results obtained from mechanical testing. Unfortunately, the test's macroscopic scale does not inform about the intensity of segregation of the products.

A widely spread analytical technique for the characterization of thermosetting materials is differential scanning calorimetry (DSC). DSC essentially measures the energy required to change the temperature of the sample. Usually, this test allows the determination of glass transition and melting temperatures of a polymer compound. Studies have shown the dependence of the glass transition temperature on the composition of a sample [68]. Therefore, DSC analysis results can be compared to a reference sample to evaluate the variance in the mixing ratio. Unfortunately, DSC testing is a relatively slow and expensive test to perform and evaluating the homogeneity of a sample requires a modestly sized sample population to draw meaningful conclusions.

TGA measures the weight loss of a sample as a function of temperature. Applied to thermosetting polymers, this means that TGA testing records the change in mass due to the nature of the matter, monitoring the volatile and solid components. In a similar way to DSC, TGA test results can be used to evaluate the homogeneity of the sample as a different hardener to resin ratio will influence the cure reaction and consequently the weight loss behaviour of the sample. As with mechanical testing, TGA results do not explicitly allow quantifying the concentration of the products.

Other techniques using electrical property measurements can be used to evaluate the mix homogeneity of a two-component product. Unfortunately, it is hard to link the electrical properties of the polymer to its mixing ratio and draw meaningful conclusions because limited information is available on this characterization technique.

Finally, optical tests like spectrophotometry can be used when both components have different colours. For example, Figure 8 shows the homogeneity of two mixed fluids through a

static mixer. The colour difference between the two fluids allows for optical inspection to be used. Spectrophotometers can be used to obtain the red-green-blue (RGB) colour coordinates of a sample and compute the coefficient of variation [69].

Figure 8 - Visual evaluation of the homogeneity of a two-component product mix through a static mixer [70]

Of all testing methods discussed, FTIR spectroscopy is the most suitable for the project because of its versatility and widespread use for chemical characterization of organic compounds. Table 3 lists the advantages and disadvantages and of the reviewed characterization methods.

Table 3 - Advantages and disadvantages of mix homogeneity characterization methods

Characterization method	Advantages	Disadvantages
FTIR Spectroscopy	• Versatile and widely used to characterize chemical compounds • The data obtained can be linked to the concentration of the samples and homogeneity	• Usually employed as a qualitative characterization method
Mechanical testing	• Equipment easily accessible	• It is hard to derive the relations between the mechanical properties of a sample to the homogeneity (intensity of segregation)
DSC	• Results are precise and can be linked to the resin to hardener ratio	• Testing is relatively slow and expensive to perform
TGA	• Results can be linked to the resin to hardener ratio	• It is hard to derive the relations between the TGA results of a sample to the homogeneity (intensity of segregation)
Electrical testing	• N/A	• Cannot be applied to all substances and results cannot be explicitly linked to the mixing ratio and homogeneity of a sample
Spectrophotometry	• Results can directly be associated with the homogeneity of a sample	• Only applies to samples that show colour differences between the components

2.5 Mixing technologies for in-line mixing systems

There are three broad categories for industrial in-line mixing devices: static, dynamic and impingement. Depending on the application and the products, different mixing technologies offer different advantages. The following literature review will focus on static mixers as they are used extensively in the polymer industry [71]. Dynamic and impingement mixing technologies will also be briefly reviewed.

2.5.1 Static mixing

Static mixers are simple mixing devices and consist of blades positioned in-line within a tube where the fluids to be mixed are forced trough. There are no moving parts and the mixing process relies mainly on splitting the flow multiple times. Static mixers do not require an external energy source to operate in the sense that no electrical, hydraulic or pneumatic motor is attached to the mixer. Instead, the energy required to mix both components is drawn from the fluid itself, resulting in a pressure drop across the equipment. A wide variety of mixer geometries are developed for different applications but their working principle remains the same: splitting and/or twisting the flow to produce a multitude of layers [72]. Table 4 below lists the three (3) most used static mixers for industrial processes [73].

Table 4 – Popular types of static mixers

Type/Name	**3D model** [73]
Kenics (twisted blades)	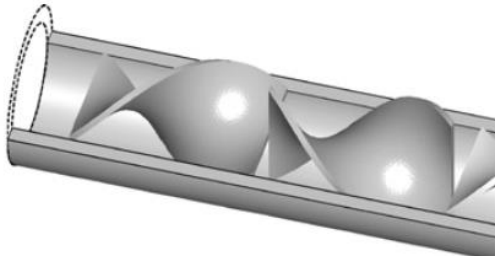
SMX (Static Mixer using crossbars X)	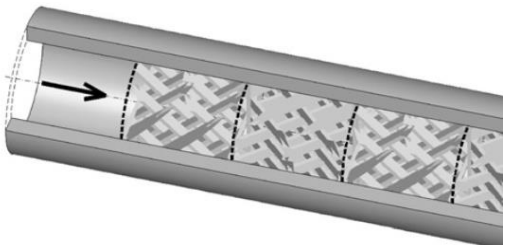
LPD (Low Pressure Drop)	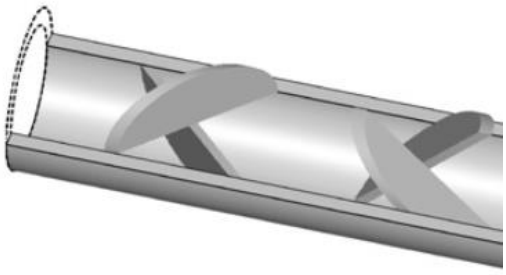

The Kenics mixer consists of a series of right and left-twisted plates, positioned so that each leading edge is at 90 degrees offset to the trailing edge of the previous element.

The SMX mixer is built of small stacked lamellae positioned in an *X* shaped formation. Each lamellae stage is rotated by 90 degrees compared to the previous stage. These mixers come in multiple lamella configurations denoted by n, N_P, N_X and θ which respectively represent the number of lamellae over the height of the channel, the number of parallel lamella along the length of one element, the number of lamella over the width of the channel, and the angle between the lamella. The standard SMX mixer is (2, 3, 8, 90°) as shown in Figure 9 [74].

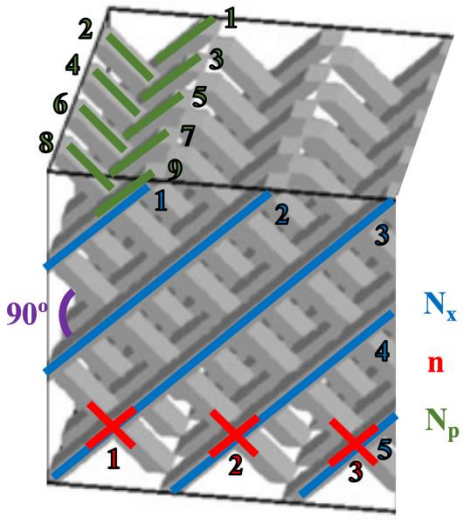

Figure 9 - SMX mixer geometrical configuration (n, N_P, N_X, θ) = (3, 5, 9, 90°)

The LPD mixer is made of a series of semi-elliptical plates positioned at a 90-degree plane to plane offset from one another. Each mixing stage is also rotated by 90 degrees along the pipe axis.

2.5.1.1 Static mixer performance

Many research groups investigated the performance of static mixers using computational fluid dynamics. Among these groups, the most important contributions were performed by Rauline et al. and Meijer et al.

Rauline et al. made a quantitative analysis of the performance of six static mixer geometries including the Kenics, SMX (2, 3, 8, 90°), and LPD by computing the velocity field of the three-dimensional flow using POLY3D^{TM} [54]. The analysis compared the mixers on many metrics that are considered to have an influence on mix homogeneity. The most significant analysis metrics are pressure drop, mean shear rate, interfacial stretching and intensity of segregation. The analysis was performed numerically. Results compared to the literature showed good agreement. A summary of the results obtained by Rauline et al. is presented in Table 5 for the Kenics, LPD and SMX mixers.

Table 5 - Mixing performance analysis of static mixers

	ΔP (MPa)	Mean shear rate (s^{-1})	Interfacial stretching	Intensity of segregation
Kenics	0.71	10	0.57	0.57
LPD	0.75	8.8	0.54	0.60
SMX	1.8	21	4.2	0.13

The pressure drop is the differential pressure between the inlet and outlet of a three-element mixer. Higher pressure drop can be problematic for high flow and high viscosity applications. In addition, as the pressure drop is the static mixer's energy source, it must be considered for efficiency analysis. The mean shear rate measures the mixers' ability to shear or "work" the fluid. Higher shear indicates better performance. Interfacial stretching is the length stretch ratio of a fluid element over a time *t*. A higher interfacial stretching means a greater contact area between the liquids to be mixed [75]. Finally, the intensity of segregation is the spatial distribution of the phases in the sample. For a chemical mixing application in the polymer industry, this metric is significantly important as having an excellent spread of the chemical functional groups ensures the highest degree of the cure can be reached. Results show that the SMX mixer offers the best performance as it shows the lowest intensity of segregation with the higher shear rate and interfacial stretching. However, the ratio of shear rate to pressure drop, which can be used to quantify the efficiency of the mixer because the pressure drop is directly related to the shear rate since the power is lost to friction, shows the Kenics is more efficient.

Moreover, the team developed empirical relations for the pressure drop as a function of mixer length. This allowed them to conclude that the SMX mixer was the most efficient if space is limited to mix the products.

Meijer et al. made computational fluid dynamics flow simulations of the most popular static mixers as a function of the number of mixing elements [73]. Flow simulations of a two-component flow are shown in Figure 10. Each row represents a different mixer geometry while each column shows the cross section of the mixer after various numbers of mixing elements (N_{elem}). Column 1 is a cross-section of the mixer at the fluid entrance where both fluids are clearly visible in black and white with no mixing performed yet. The following columns are the cross sections after 1, 2, 3, 4 and 8 mixing elements.

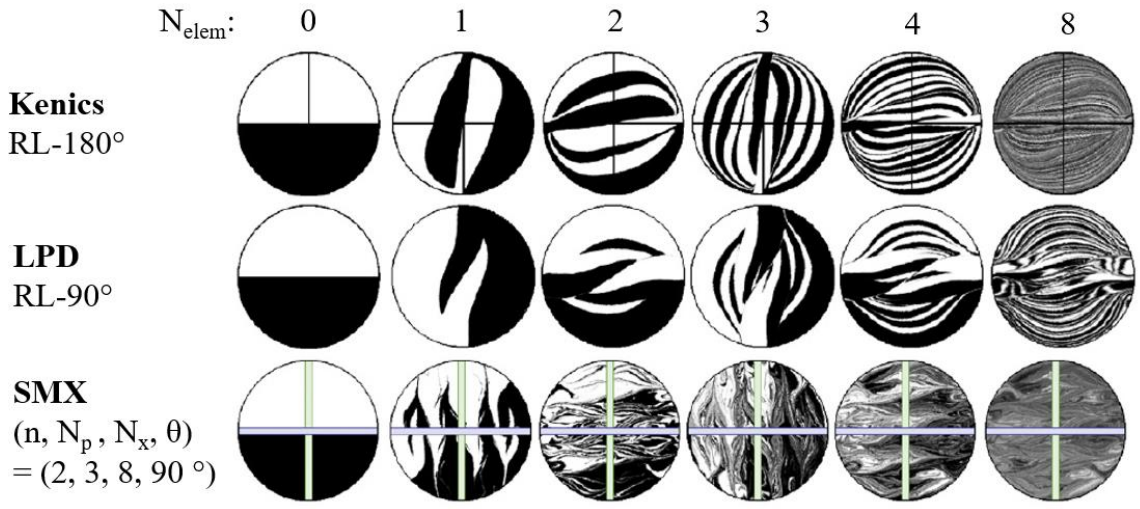

Figure 10 - Mixing profiles and layers as a function of the number of mixing elements [73]

Visually comparing the mixing profiles after eight (8) mixing elements, the SMX mixing profile is more chaotic compared to the Kenics and LPD. Small aggregation areas can be seen on the outer edge of the SMX mixing profile at this stage while the Kenics shows a more predictable and organized mixing pattern. These results correlate with the intensity of segregation presented in Table 5 by Rauline et al. Overall, Meijer et al. also conclude that higher mixing homogeneity can be achieved using the SMX static mixer.

Meijer et al. also qualitatively investigated the number of interfaces produced by the mixers. The higher the number of interfaces produced, the more effective the mixer is at ensuring maximum contact area between the constituents. Results are expressed using two schemes in Table 6. Scheme 1 is based on geometrical analysis while scheme 2 is based on actual interface stretching from their simulations and it refers to what is observed in Figure 10. The group found that the mixing profiles of most mixers do not behave as predicted. For instance, the (1, 1, 3) SMX mixer, with its two mirrored crossing blades, causes two counter-rotating vortices that split the fluid to create two interfaces each of length equal to the diameter *D* of the mixer. This observation depends on the mixer geometry. This alters the mathematical expression that described the number of interfaces produces by each mixing element. Table 6 also lists the dimensionless pressure drop per mixing element. It is defined as the pressure drop through the mixer divided by the pressure drop in an empty pipe of the same diameter as the mixing elements.

Table 6 – Pressure drop and interfacial stretch of different static mixers

Mixer type	**ΔP/element**	**Interfaces produced**	
		Scheme 1: expected	Scheme 2: actual
Kenics (RL-180°)	5.5	$2^{N_{elem}}$	$4^{N_{elem}} - 1$
LPD (RL-90°)	8.5	$3^{N_{elem}}$	$2^{N_{elem}}$
SMX (2, 3, 8, 90°)	38	$8^{N_{elem}} - 1$	$5^{N_{elem}}$

Results show the SMX mixer's higher efficiency at interfacial stretching, a result of the number of fluid interfaces produced. After 8 mixing elements, the number of interfaces produced would be 390,625 for the standard SMX (2, 3, 8, 90°) mixer against 65,535 for the Kenics (RL-180°). For visual interpretation, actual interfacial stretch (Scheme 2) is plotted as a function of the number of mixing elements in Figure 11.

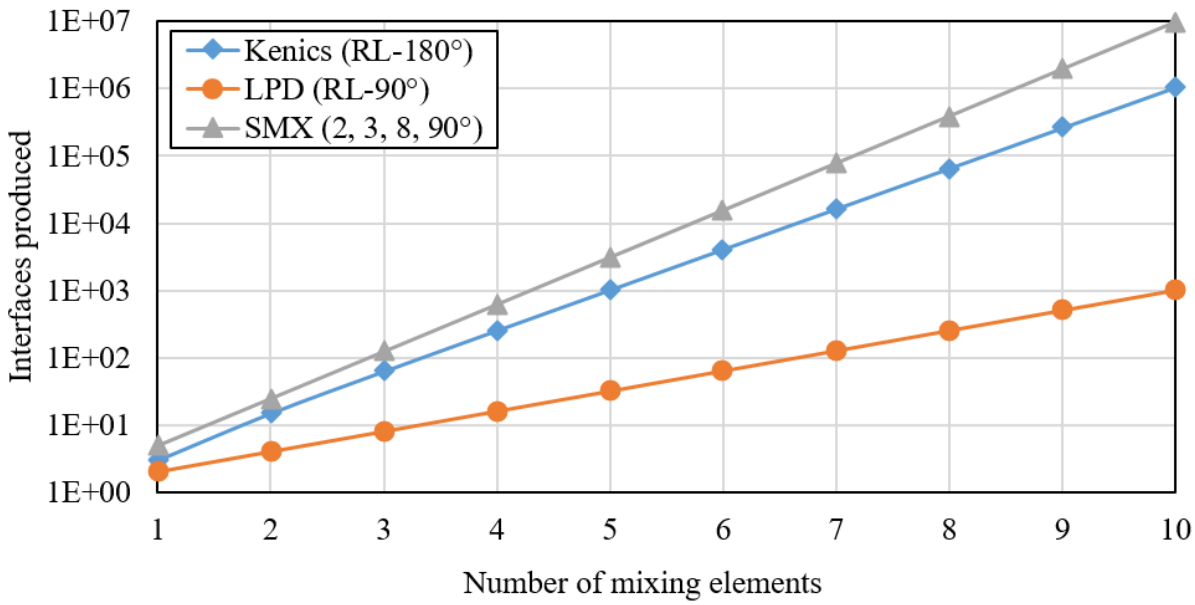

Figure 11 – Actual interfaces produced (Scheme 2) per mixing element

Overall, the literature shows that the SMX mixer is more efficient. However, this comes with the drawback of significantly higher pressure drop. Therefore, the SMX mixers should be used when space is limited and system pressure drop limitations are low. Nevertheless, it should

be kept in mind that high shear may be desirable for mixing but may be undesirable with shear sensitive fluids.

2.5.1.2 Identification of ideal mixer geometry and sizing

Although a lot of research has been done to evaluate the performance of static mixers, mixing homogeneity results will vary depending on multiple factors, the most important being the volumetric and viscosity ratios of the components. High volumetric ratios, usually considered 100:1 or above, require more mixing elements to minimize the intensity of segregation [76]. Likewise, the higher the viscosity ratio, the higher the difference in interfacial stretch between the components, resulting in residual shear stress at the interface that prevents the fluids to mix [77]. Vinyl ester resins used with isocyanate thickening agents have a volumetric and viscosity ratio of approximately 10:1 [78], [79]. A high viscosity ratio is generally considered as anything above 100:1 [76]. This means that vinyl ester and isocyanate is not considered easy nor exceptionally hard to mix.

Ultimately, choosing the ideal mixer geometry and size is what will result in the best trade-off between a maximized mix homogeneity and a minimized pressure drop. It is possible to perform computational fluid dynamic (CFD) analysis using a mixer geometry to simulate the way both fluids will mix. However, this type of analysis is complex and hard to execute with accuracy [80]. Using the literature and empirical data from static mixer manufacturer, the right mixer can be identified, provided that the fluids' properties and application conditions are known. From there, experimental testing and mixer size iterations can allow improving the mixer. However, in most cases, simply adding mixing elements suffices to meet the process criteria.

Static mixers are usually available in reusable and disposable versions [70]. The disposable versions are an interesting solution with polymers. At the end of a manufacturing cycle, the mixer can simply be replaced instead of cleaned, reducing maintenance time and costs.

2.5.2 Dynamic mixing

Dynamic mixers consist of mixing elements that are mechanically agitated by an external power source. In its simplest form, a dynamic mixer can comprise of a shaft and blades submerged in a liquid. One common example is a regular household food processor or blender. In these instances, the mixer works in batches, meaning that one fixed and limited volume of fluid is mixed

at a time. This contrasts with the static mixer where the fluid is mixed continuously as it flows through. This can be a major drawback for an industrial process when large quantities of liquid must be mixed just-in-time for production. Also, this becomes especially critical with reacting polymers because the resin and hardener can react quickly, leaving little leftover time to manufacture the part.

Dynamic mixers are also offered in in-line versions, allowing continuous mixing. Figure 12 shows an in-line dynamic mixer with a two-component flow at the input (lower left) and the mixed output (top) [81]. The energy required for the mechanical agitation of the blades is provided by the electric motor (right). The added mechanical energy provided by the motor will result in less pressure drop when compared to static mixers.

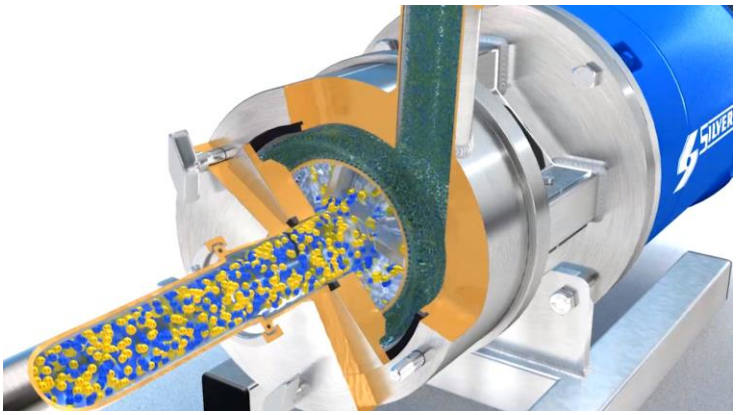

Figure 12 – In-line dynamic mixer by Silverson [81]

Hybrids between static and dynamic mixers are also available. Figure 13 presents two similar static-dynamic mixing heads. Both examples are handheld devices with a motor at the back and a disposable mixing chamber at the output. The term static-dynamic comes from the fact that the blades inside the static mixer are dynamically agitated by an external motor. These mixers are designed to take advantage of the simplicity and easy maintenance of in-line static mixers while adding the energy of the motor-driven mixing blades. In this design, the components to be mixed only meet in the disposable plastic mixer. This eases maintenance cost and complexity by requiring only a change of mixing chamber.

(a) (b)

Figure 13 – Static-Dynamic mixing heads: (a) Static-Dynamic by DOPAG [82] and (b) LC 5/3 by Tartler [83]

One significant drawback of dynamic mixers is the inherently more complex design of the assembly. The addition of moving parts, external motor and energy supply (air, electricity, hydraulics, etc.) and weight make these mixers sometimes a little too complex for certain applications. Even though the addition of a mechanical agitation generally helps to mix the products together, simpler static mixers have been shown to have the ability to adequately mix polymers. Choosing this technology results in higher purchasing and operating costs. Moreover, the moving parts usually make it less durable with abrasive fluids, a common reality with resins containing additives.

2.5.3 Impingement mixing

The last commonly used mixing technology in the field of polymers is called impingement mixing. Figure 14 shows a schematic of a typical impingement mixing head along with a simulation of the mixing chamber. In this process, the two fluids collide at high pressure into a mixing chamber, typically around 80 to 200 bars [84]. This technology was developed for the polyurethanes industry, where conventional valves and actuators were too slow, too hard to clean and required regular maintenance. The sudden pressure drops exhibited by the fluids when entering the mixing chamber creates a lot of turbulence and mixes both products rapidly.

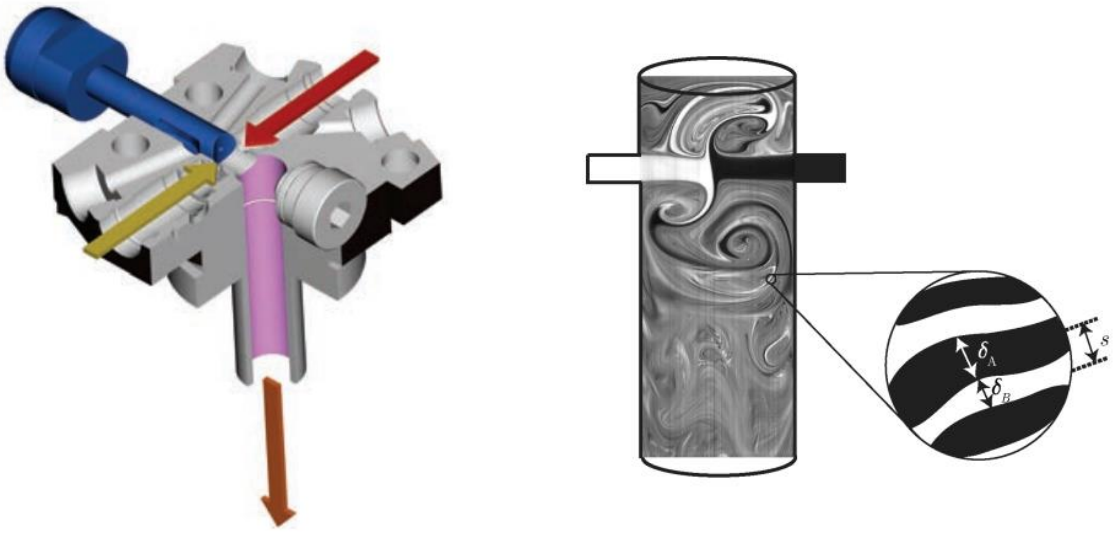

(a) (b)

Figure 14 –Impingement mixer: (a) Schematic of a typical impingement mixing head and (b) Simulation of impingement mixing for a two-component fluid [85]

Although high pressure mixing heads reliably create an even product distribution, they require more complex equipment to supply high-pressure flow. For a mixing chamber with directly opposed jets, the transition to turbulent mixing, a requirement for consistent mix quality, occurs at Reynolds number over 140 [86]. In the case of viscous polymers, achieving such flow requires significant amounts of energy and hydraulic units must be used, complexifying the resin dosing system.

An advantage of the impingement over the dynamic mixer is that cleaning is simplified because there are no rotating parts. Some models include a piston that can push the leftover polymer through at the end of a mixing phase while others have a dedicated solvent inlet for automated cleaning. Impingement mixers are ideal with high flow application, or processes requiring a high number of mixing shots per day, with some mixing units allowing flow rates of up to 8000 ml/sec [87].

Table 7 presents a summary and comparison of static, dynamic and impingement mixers based on their respective advantages and disadvantages.

Table 7 - Comparison of static, dynamic and impingement mixers

Mixing technology	Advantage	Disadvantage
Static	• Simple design • Inexpensive • Wide range of viscosities • Does not require an external energy source	• May create a significant pressure drop
Dynamic	• Reduced pressure drop	• Complex design • High purchasing and maintenance costs
Impingement	• High output flow rate and pressure capabilities • Short fluid residence time for rapid chemical reactions	• High purchasing costs

Limited sources in the literature compare the various mixing technologies together [88]. The design criteria are more influencing the technology choice than the mix quality obtained with a specific technology. The literature shows that with all three technologies, very high homogeneity mixing can be achieved. Ultimately, cost, maintenance and applicability based on the fluids to be mixed will drive the technology choice.

2.6 Pumping technologies for in-line mixing systems

Equally important equipment of an industrial-grade mixing and dosing system are the pumps. This equipment dictates the precision at which both fluids will be injected into the mixing unit. Pump requirements for dosing and mixing systems include high repeatability, pulse-free, low shear, high pressure and abrasive and corrosive fluids capability.

Out of the many pump types that are currently available, all can be categorized into one of the two following groups: centrifugal pumps and positive displacement pump. Centrifugal pumps

use impellers to convert velocity to flow and can pump up to very high flow rates. Unfortunately, these pumps' output flow rate cannot be controlled or adjusted with high precision.

2.6.1 Positive displacement pumps

Positive displacement (PD) pumps use rotating or reciprocating actions to directly push the fluid to the discharge side. The suction, on the other hand, is the wetted part located at the inlet of the pump. Through each cycle of the pump's action, a specific volume of fluid passes from the suction to the discharge, making these pumps very precise and repeatable. The output of the pump can be controlled and adjusted automatically using a feedback loop when combined with a flowmeter. This guarantees a constant and precise flow rate in all conditions. Positive displacement pumps are separated into two categories: rotary pumps and reciprocating pumps.

2.6.1.1 Rotary pumps

Rotary pumps use a rotating mechanical motion to pump the fluid. While the rotor spins, fluid is trapped in the spaces created by the moving parts. Contrastingly, centrifugal pumps use fluid velocity and the pressure differential between the suction and the discharge side to move the fluid. Rotary pumps have the advantages of creating a smooth flow as well as being compact. In addition, they are usually cheaper to acquire and maintain. Regrettably, rotary pumps tend to wear quickly when pumping abrasive fluids because of the tight tolerances between the moving parts. Several types of rotary pumps are available such as the gear, lobe, progressive cavity and peristaltic pumps. Figure 15 shows examples of these for types of rotary pumps.

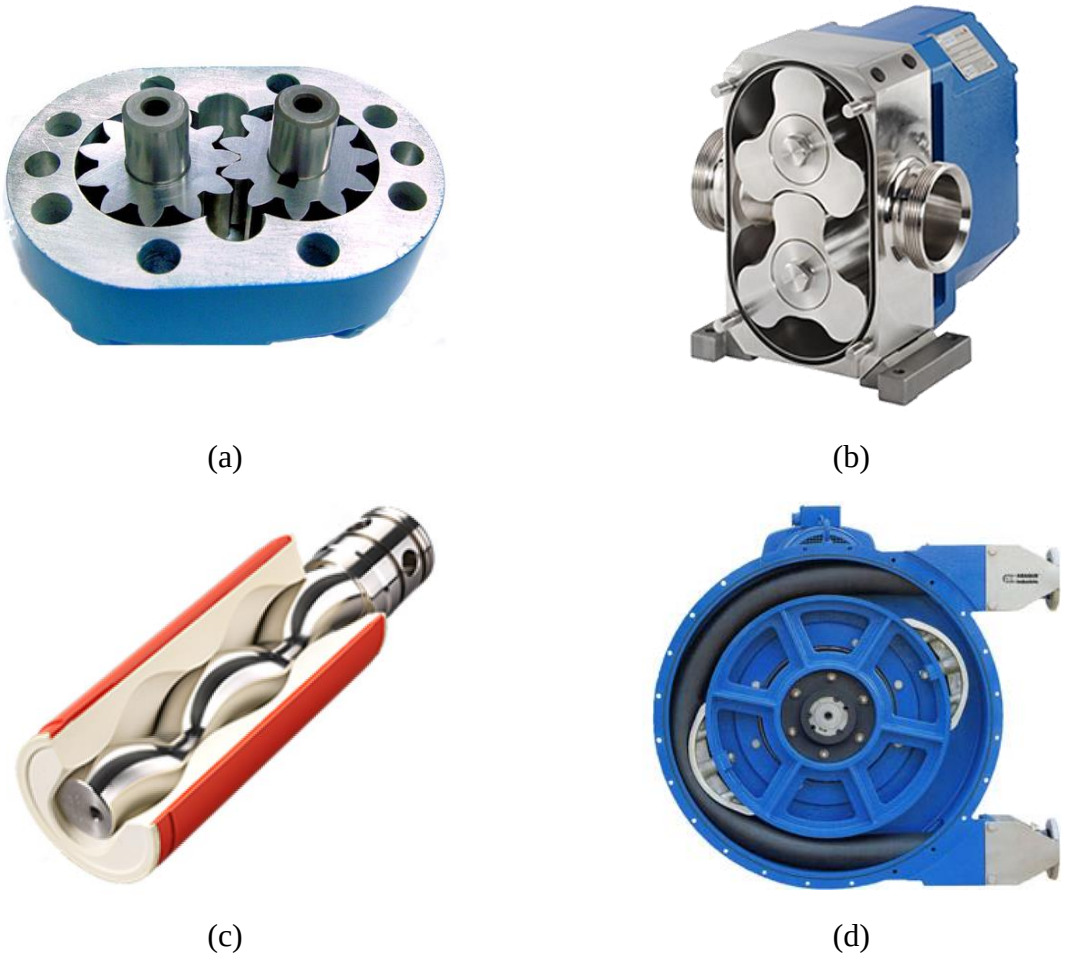

(a) (b)

(c) (d)

Figure 15 – Rotary positive displacement pumps: (a) gear, (b) lobe, (c) progressive cavity and (d) peristaltic

- **Gear pumps**

Gear pumps are made of two wetted meshed gears that are mechanically driven. Each gear tooth brings a constant volume of fluid with it. The pumped flow rate is equal to the number of teeth per gear times the rotational speed of the pump. Ideal for high viscosity applications, gear pumps reduce the impact of pulsations in the flow because each gear has numerous teeth, thus creating many small pulsations that often go unnoticed. The major drawback of gear pumps is that they are not compatible with slurry fluid as they rely on the tight geometrical tolerance in the gear meshing to prevent backflow.

- **Lobe pumps**

Lobe pumps can be considered as a variation of gear pumps. Using the same working principle as gear pumps, they consist of two vanes that are meshed together to pump the fluid around the interior casing. However, unlike gear pumps, the lobes do not touch one another and this is prevented through an external gearbox that is not in contact with the fluid. As a result, lobe pumps are known for their ability to pump fluids with solid contents without being damaged. Figure 15 shows a lobe pump with the front cover taken off. It is possible to notice the small gap between the two lobes that allows this pump to work with abrasive fluids.

- **Progressive cavity pumps**

Also know as Moineau pumps, after the inventor, progressive cavity pumps operate using an ingenious combination of metallic or plastic worm screw rotor inside a rubber stator. The pump's worm screw traps a certain volume of fluid and transports it to the discharge. The rotor and stator assembly are shown in Figure 15. Because the stator is made of soft rubber, these pumps can be used to pump abrasive fluids without damage. However, they cannot run dry for long periods and are very expensive.

- **Peristaltic pumps**

These pumps utilize a roller that compresses a flexible tube to move the liquid. The action is similar to the swallowing motion in the esophagus. The main advantage of this technology is that there is no contact of the fluid with the mechanical parts of the pump. This makes these pumps ideal for pumping harsh materials. When needed, the flexible tube can easily be replaced. In addition, they are self-priming, meaning that the suction end does not need positive pressure to operate, and they can run dry. One drawback is the pulsating flow that is produced at the discharged.

2.6.1.2 Reciprocating pumps

Reciprocating pumps use linear motion on a piston or diaphragm to move the fluid. The reciprocation motion implies there are an upstroke and downstroke to every cycle, resulting in a pulsating flow. One-way check valves are added to the suction and discharge of the pumps to regulate the flow in and out of the system.

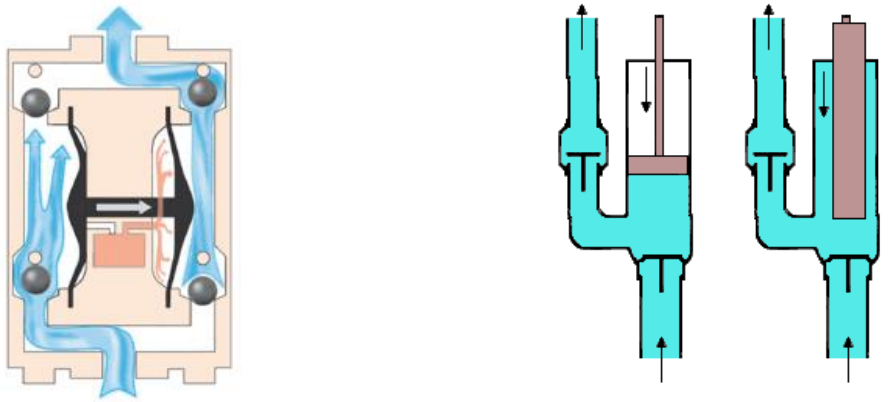

(a) (b)

Figure 16 – Reciprocating positive displacement pumps: (a) double diaphragm pump, (b) piston (left) and plunger (right) pump

- **Diaphragm pumps**

Diaphragm pumps are comprised of an elastomeric membrane that moves in a reciprocating motion to pull and push the fluid in and out the pump. Check valves are located at the suction and discharge of the pump to prevent backflow. In most cases, diaphragm pumps come in double configurations and use two distinct diaphragms that act opposite to one another. The internals of a double diaphragm pump are shown in Figure 16. Since each diaphragm has a charge and discharge phase, combining two diaphragms together allows getting rid of most of the pulsations. As one diaphragm pulls the fluid in, the other is discharging at the discharge and vice versa. Diaphragm pumps are relatively inexpensive and can either be pneumatically, hydraulically or electrically driven.

- **Piston and plunger pumps**

Piston and plunger pumps use almost identical technologies. In both cases, an arm moves linearly back and forth to move the fluid. These pumps excel in high viscosity and high-pressure applications. The working principle is shared with the diaphragm pump. Figure 16 shows a schematic of the minor difference between the plunger and piston pumps. Plunger pumps are better at working with abrasive fluids and can be used at higher pressures because the seal is stationary and tends to wear at a slower rate.

Like diaphragm pumps, piston and plunger pumps usually come in a duplex configuration to limit the pulsating effect. It is also possible, in some instances, to add more than two pistons to limit the pulsating effect and extend the life of the seals due to the slower stroke rate obtained with more pump heads.

Abrasive fluids compatibility depends on the pump technology. Choosing a pump with an intricate mechanism will obviously not work with fluids containing solids. Likewise, chemical compatibility will depend on the material of the wetted parts in the pump. This aspect must be considered both in normal operation and cleaning, where organic solvents are used.

2.6.2 Importance of flow rate linearity

In-line mixing devices have low fluid residence time, meaning that the fluid does not stay long in the mixing chamber [89]. Static mixers are designed for radial mixing, and they are quite effective in removing radial variations in composition and temperature as seen in Figure 8. Radial mixing creates a net velocity profile in the axial direction that approximates piston flow even at low Reynolds numbers. However, the flat velocity profile is a disadvantage when the input composition or temperature varies with time. There is little damping of input disturbances since piston flow provides no axial mixing [90]. This translates to the importance of having a linear and precise flow from the dosing pumps. If the pumps generate a significant amount of pulsations, the composition of the fluid at the inlet of the mixer will vary. The mixer's ability to attenuate this effect by providing axial mixing is limited and the mixed product will likely also present the same composition variations.

From their working principle, positive displacement pumps will almost always produce a certain level of flow rate variation. Luckily, for very sensible applications, there is the possibility

to add flexibility to the system by using pulsation dampeners. Pulsation dampeners are a bladder with an elastomeric membrane that absorbs the pressure surges from the pump's output to level the system's pressure. When chosen correctly, dampeners can remove up to 99% of pressure pulsations depending on the fluid conditions, pumping equipment, system setup and environment [91]. Figure 17 shows the original and dampened pressure as a function of time for a one-inch air-operated double-diaphragm pump. In addition to ensuring a steady flow for chemical metering applications, pulsation dampeners have the added benefit of protecting the instruments and equipment from pressure surges that could cause premature failure.

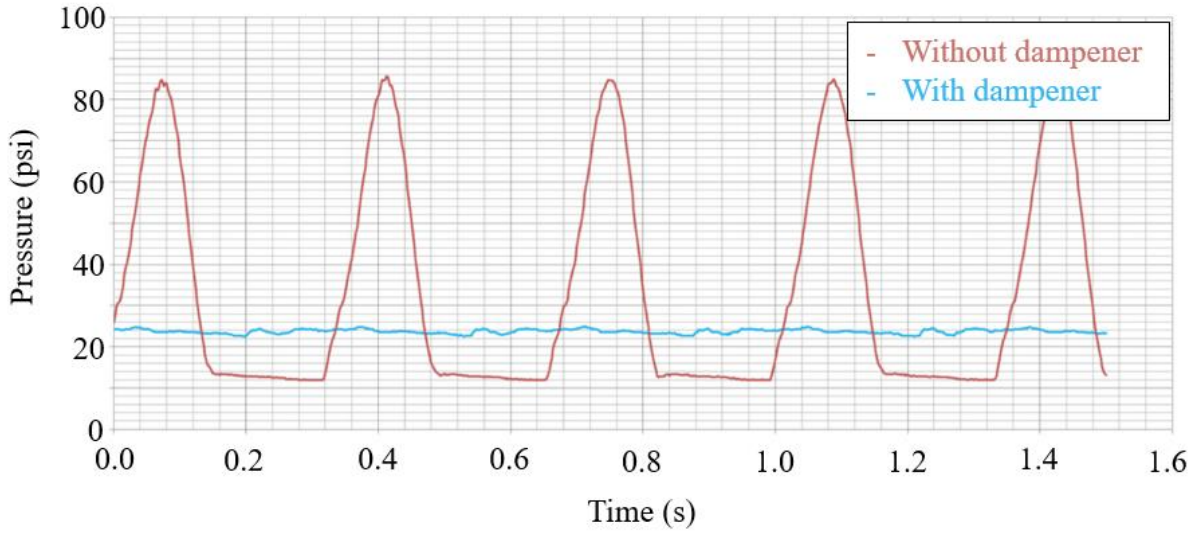

Figure 17 - Pulsation dampening on a 1" air operated double diaphragm positive displacement pump

2.7 Resin metering and mixing systems

A wide variety of metering and mixing systems are available on the market. Because many different industries require them daily, these systems are now offered to cover a wide array of applications. Unfortunately, the applicability and performance of the available systems are limited in some industries. For instance, systems aiming at the food industry will possess high output capabilities and sturdy construction to satisfy very high output and long-term manufacturing forecasts. On the contrary, the pharmaceutical industry will mandate extremely high dosing precision and mixing homogeneity with lower production rates.

For polymer processing, dosing precision and mix homogeneity are very important from a chemical perspective. On top of that, systems must be powerful and reliable to handle products with high viscosities and abrasive characteristics. For composites applications using thermoset resins, a two-component metering and mixing system is usually used to mix the base resin with the hardener.

2.7.1 Hazardous classified locations

Some polymer resin systems release flammable vapours. Under the right conditions, these vapours present risks of an explosion and make the environment surrounding the equipment hazardous. The National Fire Protection Agency (NFPA), an American standard for electrical safety in the workplace, issues standards and guidelines on the use of electrical equipment in a hazardous location in their NFPA 70E document. Canada adopted this standard through the Canadian Standards Association (CSA) in the CSA Z426 standard. Hazardous products can be classified as Class 1 (flammable gases and vapours), Class 2 (combustible dust) or Class 3 (easily ignitable fibres).

Class 1 classification is pertinent with organic compounds and solvent used in this project. Then, depending on the likelihood of the hazardous material being present in dangerous concentrations, Class 1 is subdivided into two Divisions and three Zones. Table 8 defines the two Divisions related to gas or vapours hazardous locations.

Table 8 - Project relevant flammable gas and vapour classification definitions in Canada

Division and Zones Classification	**Definition** [92]
Division 1	The explosive mixture of gas or vapour and air may exist under normal operating conditions.
Division 2*	The explosive mixture of gas or vapour and air may exist under abnormal conditions such as accidental rupture of a vessel or container or failure of a ventilating system.

* Normally, a Division 2 location is assumed to surround a Division 1 location unless the hazard is prevented from spreading beyond the Division 1 location by a solid, vapour proof (for gases and vapours) or dust-tight (for dust and fibres) partition wall without any openings (e.g. doors or windows).

As a result, classified locations standards impose electrical equipment to be certified for safe use within a certain volume around an open container as shown in Figure 18.

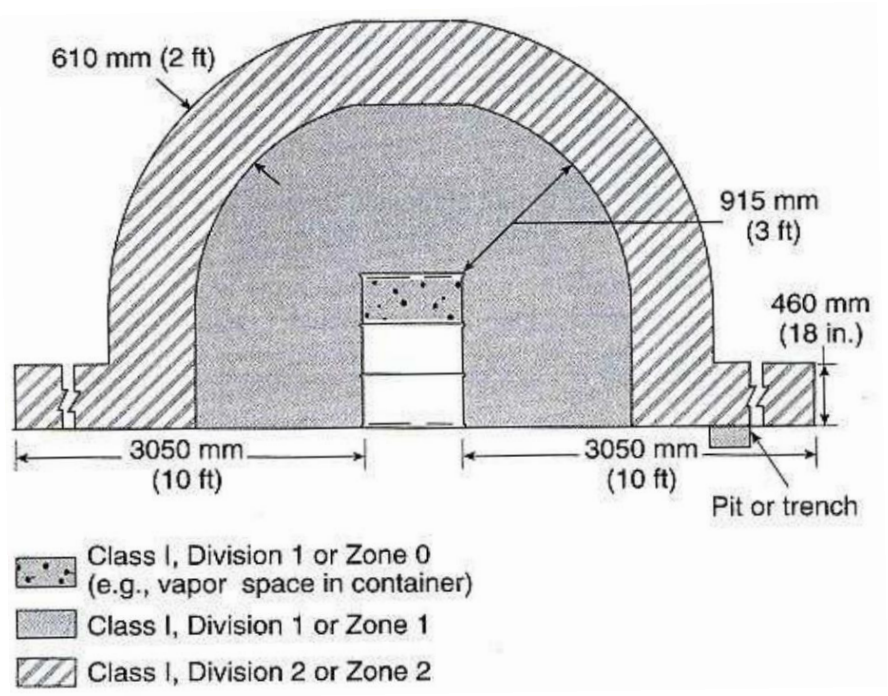

Figure 18 - Electrical area classification around an open container in a ventilated area

Electrical equipment located within three feet of the open container in any direction and down to the floor must be certified for use in Class 1 Division 1 locations. The same principle goes for Division 2 which is the volume surrounding Division 1 extending out another two feet in any direction and down to the floor with another five feet by 18 inches high on the ground.

2.7.2 Resin abrasiveness

As reviewed in section 2.4, resins used for SMC manufacturing can contain around 15% fillers and 3% additives. These fillers and additives are generally non-reactive and non-soluble dry powders that can be very abrasive. Some of the most common SMC resin fillers and additives include hollow and solid glass microspheres, milled carbon and glass fibres and calcium carbonate, all abrasive materials with relatively high hardness.

Studies on the influence of fillers and additives particle size and content in resins on wear rate show the damage such fluids can cause on metal surfaces over time [48], [93]. More specifically, it has been confirmed that signs of wear caused by abrasion are most significant in areas of tight clearances within gear pumps for example [94]. Therefore, many pump technologies and equipment used in metering and mixing systems must be chosen to accept such abrasive fluids. A talking example is the use of gear pumps as their operation and precision rely on tight tolerances between the meshing gears and housing as shown in Figure 15. The same observation holds true for gear flowmeters as they are essentially passive gear pumps.

2.7.3 Two-component metering and mixing systems

The following section presents the capabilities of five commercially available two-component in-line metering and mixing systems. The systems were selected because their technical specifications were closest to this project's metering and mixing application. The systems are shown in Figure 19 and their technical data is listed in Table 9. Most of the performance data for the metering and mixing systems are available on the manufacturer's website. However, in many cases, answers to more technical questions were obtained by directly contacting the companies' representatives. The technical questions emphasized the system's ability to process highly abrasive fluids and on certification to operate in classified hazardous locations, two common requirements with SMC vinyl ester resin systems.

(a)

(b)

(c)

(d)

(e)

Figure 19 – Commercially available two-component metering and mixing system: (a) Mahr MarMax, (b) Tartler Nodopur, (c) Cannon B-System, (d) Meter Mix PAR200 and (e) DOPAG Compomix

Table 9 - Reviewed metering and mixing system technical data

	Mahr MarMax	Tartler Nodopur	Cannon B-System	Meter Mix PAR 200	DOPAG compomix
Reference	[3]	[4]	[95]	[5]	[5]
Viscosity (cP)	up to 85,000*	Virtually no limit*	5,000	Up to 1,500,000*	1 to 50,000*
Mixing ratio	100:100 to 100:1*	100:10 to 10:100*	1:1 to 50:1*	1:1 to 20:1*	100:5 to 100:100
Flow rate (ml/min)	50 to 4,000*	100 to 13,000*	1000 to 400,000*	161 to 2,910	2,000 to 20,000
Highly abrasive fluids capability	No	No	No	Yes[$]	No
Mixing technology	Static or Static-Dynamic	Static-Dynamic	Dynamic	Static or Dynamic[$]	Static or Dynamic[$]
Pump technology	Gear	Gear	Gear	Gear, Single acting piston[$]	Gear
Wetted parts material	Stainless Steel, PTFE	Stainless Steel, PTFE	Carbon steel, Stainless Steel[$]	Aluminum, Stainless Steel[$], Viton, PTFE[$]	Aluminum, Stainless Steel[$], Viton, PTFE[$]
Class 1 Div. 1 Hazardous locations certified	Yes[$]	No	Yes[$]	No	Yes[$]

*Depending on equipment selection at purchase
[$] Optional

The first system is built by Mahr, a German company that specializes in metrology and metering systems. The MarMax metering system features two high precision metering gear pumps with gear flowmeters. Available options include day tanks with agitator and temperature control. The mixing is performed by a static-dynamic mixing gun (not shown in the picture). The system is versatile and allows wide flow rate and mixing ratio ranges. However, the system cannot handle

[3] Flowers, Personal communication, November 14th, 2018

[4] Fesel, Personal communication, October 19th, 2018

[5] Ripberger, Personal communication, November 14th, 2018

fluids with abrasive fillers as it uses gear pumps to accurately dose the fluids. In addition, the base model is not certified to operate in Class 1 Division 1 hazardous locations. This feature is only available as an expensive option.

The Nodopur is made by Tartler, a German company, and is very similar to the MarMax system in terms of performance. The system features gear metering pumps and a static mixer. The flow rate and mixing ratio capabilities are similar to the MarMax system. The main drawbacks are that it is not designed to handle abrasive fillers and is not certified to operation in Class 1 Division 1 classified locations.

Next is the B-system by Cannon, an Italian company. This machine has limited viscosity capabilities and a lower mixing ratio range than the first two systems. It offers a higher flow rate range which might be a limitation for low-speed research and development SMC manufacturing lines. Moreover, it cannot handle abrasive fluids but can be certified to operate in Class 1 Division 1 classified locations as an option.

Meter Mix, a German company, makes the PAR 200 and offers a lower and narrower flow rate range capability than the previous systems. However, it is the only system that can be modified to process abrasive fluids. This can be achieved by replacing the base gear pumps with single acting piston pumps. Unfortunately, the single action of the piston means that the system cannot continuously dispense mixed resin to the production line. The system offers some of the highest viscosity capacity of any system but cannot operate in Class 1 Division 1 hazardous locations.

The last system, the Compomix, is made by DOPAG, another German company. Like most systems, it uses gear metering pumps and therefore cannot process abrasive fluids. It is available with Class 1 Division 1 classified location certification as an option. Otherwise, it offers a static or dynamic mixing unit and like Cannon's B-system, its flow rate capacity is higher and might limit small production speed applications.

Overall all systems have stainless steel and PTFE wetted parts stock or available as an option. These materials have excellent chemical compatibility with a wide range of chemicals and organic solvents. In the case of a typical SMC vinyl ester resin, chemicals like styrene, isocyanate and acetone are most concerning. Nonetheless, stainless steel and PTFE offer outstanding chemical

resistance to these products. Moreover, stainless steel has a hardness of 70 on the Rockwell B scale, the highest of most metals available for processing equipment like. This normally means that it will have the added advantage of showing increased wear resistance, but it is highly dependent on the surface treatment applied [96].

2.7.4 Summary of current systems limitations

It is important to note that the technical data shown in Table 9 cannot be achieved with any given configuration of the system. The design of the metering and mixing system must be adjusted and tailored to the specific fluids through equipment selection and sizing when purchasing the system. In addition, some performance data are not compatible with one another. For example, to be able to accurately meter and mix high viscosity fluids, the flow rate capabilities must be limited to avoid increased pressure drops in the piping.

There is no reviewed system that can handle abrasive fluids while being certified to operate in Class 1 Division 1 classified locations. This proves to be an important limitation for vinyl ester SMC resin formulations as they contain styrene and a high content of abrasive filler and additives.

Another important aspect to consider is that although all systems used positive displacement pumps, which are very precise, not all systems use flowmeters to control the pumps output using a feedback loop. Moreover, all systems use independent pumps to meter each component. This means that a slight lag in the feedback loop or even a slight motor speed variation will immediately affect the mixing ratio.

Finally, Table 9 shows there is a great innovation opportunity to develop a new in-line metering and mixing system that overcomes currently available system limitations.

2.8 Summary and knowledge gaps

The literature review first covered the application and manufacturing processes of composites in the automotive industry before summarizing the available methods for resin mix homogeneity evaluation. Then, the different mixing and pumping technologies were studied along with an overview of the commercially available metering and mixing systems.

The automotive industry has been using composites material for more than 50 years. However, only now do we see OEM starting to invest in developing solutions for the use of composite materials for structural parts of high-volume production vehicles. For structural parts, carbon fibre reinforced epoxy or vinyl ester resins seems to provide adequate mechanical properties for these applications. Two major manufacturing processes stand out; resin transfer moulding and hot compression moulding.

Static mixers seem to offer adequate mixing while having a simple design, low cost and easy maintenance. However, the literature review does not allow to predict with accuracy the mix homogeneity obtained using a specific mixer and only compares most static mixer technologies together to facilitate geometry choice for a given application.

Currently, available in-line metering and mixing systems do not meet the requirements for the continuous mixing abrasive resins in Class 1 Division 1 hazardous location. Moreover, currently available systems use independent motors for each of the pumps. This does not guarantee that the mixing ratio will be maintained following a rapid increase or decrease in output flow rate as one motor could potentially change its rotational speed faster.

2.9 Project objectives

The first objective of the project is to demonstrate that adequate mix homogeneity can be obtained using a commercially available static mixer with the partners vinyl ester resin formulation.

The second objective of the research project is to develop a new metering and mixing system that meets all the partner’s requirements. Deliverables of this objective include a complete 3D model along with the complete part list and costs. Then, the system must be assembled.

As a third and final objective, the newly developed system will be tested and validated. Resin samples will be mixed using the system and homogeneity will be evaluated using the same methods used in the first objective.

CHAPTER 3 DEMONSTRATION OF THE PERFORMANCE OF A STATIC MIXER TO OBTAIN AN HOMOGENEOUS RESIN SAMPLE

The objective of this chapter is to demonstrate that adequate mix homogeneity, measured through the CoV, can be achieved with a static mixer. In order to meet the objective, three items are verified in this chapter. First, verification is done to determine if FTIR spectroscopy can be used to evaluate the homogeneity of a resin sample (item one). Then, the performance of a static mixer to obtain a homogeneous resin sample is evaluated (item two). Finally, the impact of mixing ratio variation on mix homogeneity is qualitatively evaluated to assess the axial mixing capabilities of a static mixer (item three).

Item three assesses the static mixer's ability to attenuate flow rate variations that may be caused by the pumps. As seen in the literature review, a lot of research has been made on velocity profiles in static mixers. All have concluded that static mixers are ideal for radial mixing and only provide a limited amount of axial mixing. More specifically, the aim is to qualitatively evaluate the static mixer's axial mixing capabilities, or the mixer's ability to mix the fluid lengthwise in the direction of the flow. This aspect is important regarding the pump technology choice for the new system to know whether or not flow rate pulsations will significantly affect the product's mix homogeneity.

The chapter first describes the materials and equipment used. Then, the procedure associated with each of the three items needed to achieve the chapter's objective is detailed. These items are the recommended procedure for FTIR analysis, the validation of the performance of the static mixer to obtain a homogenous resin sample and the qualitative evaluation of the axial mixing provided by the static mixer, notable via the influence of mixing ratio variations on mix homogeneity. Finally, a conclusion summarizes the results for the three items.

3.1 Materials

The resin used was provided by the industrial partner. It is a two-component vinyl ester resin (part A) with an isocyanate thickening agent (part B) used for SMC manufacturing. Part A is a typical unsaturated bisphenol-A epoxy vinyl ester resin in styrene while part B is a combination

of polymethylene polyphenyl isocyanate and 4-4 diphenylmethane diisocyanate[6]. Many additives and fillers are incorporated in the resin but their exact nature and content are kept secret by the industrial partner. However, these additives and fillers are inert and do not influence the mixing and reaction of both components. The presence of styrene makes this resin Class 1 Division 1 explosive following CSA's standards. The necessary safety precautions were taken to comply with the regulation during storage and handling of the products. The technical information of parts A and B are presented in Table 10.

Table 10 – Parts A and B technical information

Process variable	Part A	Part B
Viscosity (cP)	1050	195
Density (g/ml)	1.068	1.234

3.2 Equipment

Resin components were mixed together using a Kenics RL 180 static mixer (7700704, Nordson EFD) shown in Figure 20. The mixer is made of brass inlet and outlet NPT fittings with nylon tube housing and 24 acetal mixing elements. This mixer was chosen for its simple geometry and proven efficiency for mixing various two-component products. It was sized by the manufacturer based on the flow rates and viscosities of the products to be mixed. The mixer offers good performance and limited pressure drop compared to the SMX mixer. An SMX static mixer will be tested with the final system. The system will offer better pressure capabilities than the experimental setup presented below.

[6] Pachha, Personal discussion. November 19th, 2018.

Figure 20 - Kenics RL 180 static mixer

Positive displacement pumps were used for the A and B components. For part A, a high precision resin injection piston was used (5000 cc, Radius Engineering Inc.). This piston can dose the resin from 1 to 500 ml/min at ± 1 ml/min. For part B, two different positive displacement pumps were employed: a laboratory scale syringe pump (KDS 200, KS Scientific) and a peristaltic pump (7553-80 motor and controller with 7015-20 pump head, Cole-Parmer). All three pumps are shown in Figure 21.

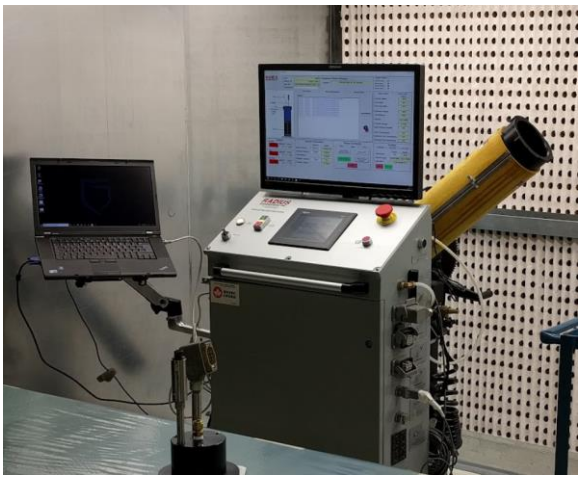

(a)

(b)

(c)

Figure 21 – Pumps used during testing: (a) Resin injection piston, (b) laboratory scale syringe pump, and (c) peristaltic pump

The mixing tests were performed at CTA's composites laboratory. It is equipped with the appropriate ventilation to manipulate resin containing organic volatiles. On the other hand, FTIR analysis was performed at cegep Édouard-Montpetit's chemistry laboratory using a Perkin Elmer UATR Two machine, shown in Figure 22. Data collection was done using the company's software v.10.4.4. File conversion was done with the Spectragryph 1.2.10 while spectral analysis and graphs presented in this work were generated with Microsoft Excel 2016.

Figure 22 - Perkin Elmer UATR Two

3.3 Procedure

3.3.1 FTIR spectroscopy as a technique to evaluate the homogeneity of a resin sample

To evaluate the homogeneity of the resin mixture, the coefficient of variation (CoV) is used on a metric that is linked to the mixing ratio of both components. Following the literature and guidelines from the industry, a resin sample that has a CoV of less than 5% is considered homogenous.

Attenuated Total Reflection Fourier Transform Infrared Spectroscopy (ATR-FTIR) is used to collect the metric used for CoV calculations. ASTM E168 and ASTM E1252-98 test standards are used to collect and analyze the FTIR data [97], [98]. First, the spectrum of both the A and B components were collected to know their individual spectrum. Then, both components were hand mixed in a cup at the volumetric mixing ratio stated by the industrial partner, or 20,5:1 (A:B). This allowed evaluating if the characteristic infrared absorbance peaks of the different components could be resolved in the spectrum of the mixed sample. According to the industrial partner, mixing both components by hand for two minutes yields adequate homogeneity. Based on the results from the individual and mixed spectra, the IR absorbance peak used as the metric is identified for further CoV calculation.

To validate the linearity of the correlation between the mixing ratio (part B concentration) and the absorbance, six samples with various mixing ratios were hand mixed in a 120 ml glass jar.

Results should obey the Beer-Lambert law to allow FTIR absorbance peak height to be used for homogeneity calculation. The composition of the samples used for the Beer-Lambert law validation is listed in Table 11.

Table 11 - Beer-Lambert law sample composition

Sample #	Mass part A (M_A)	Mass part B (M_B)	Mixing ratio (M_A/M_B)	$M_B/(M_A+M_B)$
	[g]	[g]		[-]
1	25,010	0,000	N/A	0,0000
2	24,060	0,976	24,652	0,0390
3	23,865	1,150	20,752	0,0460
4	23,394	1,620	14,441	0,0648
5	22,709	2,304	9,856	0,0921
6	20,718	4,296	4,822	0,1717

The six samples presented in Table 11 include the mixing ratio stated by the industrial partner (M_A/M_B = 17,7:1). The quantity $M_B/(M_A + M_B)$ is the concentration of part B in the sample.

Hand mixed samples used to validate the use of FTIR spectroscopy were mixed in 120 ml glass jars. Five (5) FTIR spectra are collected to calculate the homogeneity of the sample using the CoV, as shown in Equation 1. Figure 23 shows the approximate position of the samples collected.

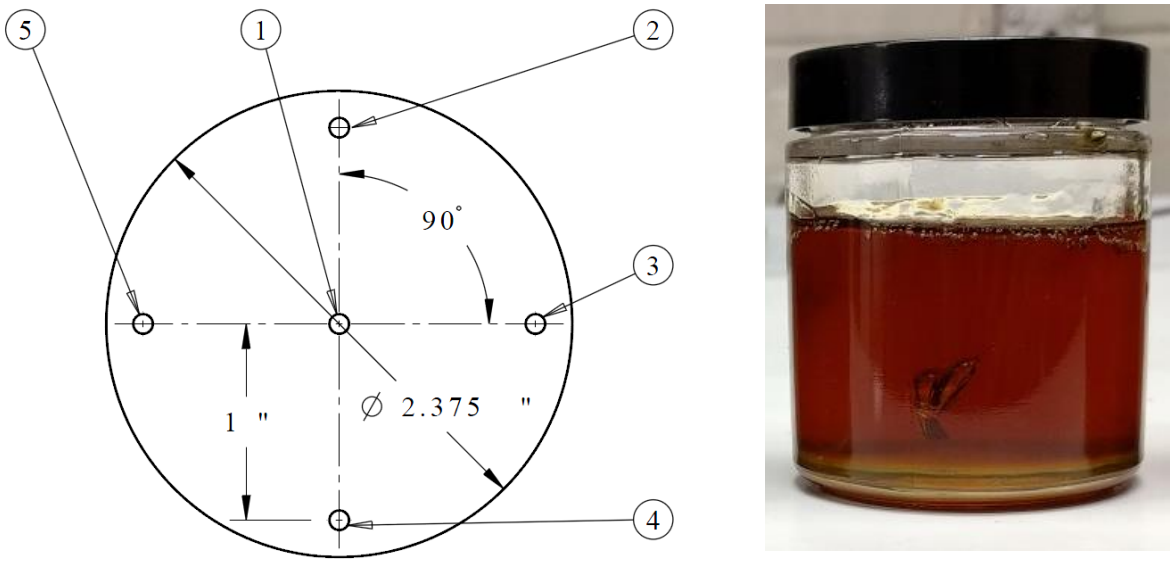

(a) (b)

Figure 23 – (a) FTIR sample positions and (b) mixing jar

FTIR spectra collected by ATR-FTIR present slight amplitude variations that can be caused by sample preparation or data collection. To adjust for this amplitude variation, the IR absorbance peak of interest used for CoV calculation is normalized using other easily resolved peaks. These peaks must not be characteristic of the mixing process (i.e. they must not be involved in the chemical reaction between parts A and B). This ensures that the CoV results for homogeneity evaluation are independent of the normalization process. To identify the peaks used for normalization, FTIR spectra were collected over a period of 48 hours, or more specifically 1, 2, 3, 4, 24 and 48 hours after the mixing occurred.

Moreover, depending on the chosen chemical functional group associated with part B of the resin used for CoV calculations, the amplitude of the FTIR absorbance peak may vary over time. The reactivity of parts A and B will influence the homogeneity calculations obtained because the amplitude of the absorbance peak will be modified over time. It takes approximately three minutes to complete one FTIR spectrum data collection. The time delay between the analysis of the first and fifth sample can, therefore, be significant in terms of amplitude variation caused by the reaction of both components. Time compensation calculations are added to the data analysis by using the reaction rate of the chosen absorbance peak. As the mixing is performed at CTA ($t = 0h$) and the FTIR analysis at cegep Édouard-Montpetit ($t = 1h$), the mixed samples have approximately one hour to react before the first FTIR sample is collected ($\Delta t = 1h$). From there, all samples required for homogeneity calculations are collected within one hour (from $t = 1h$ to $t = 2h$). The reaction rate is determined by measuring the amplitude variation of the chosen absorbance peak from the first hour after mixing to two hours after mixing. The speed of the reaction is assumed to be linear and the amplitude of the absorbance peaks for a given sample are compensated for the time since the first FTIR spectrum has been collected. In other words, the amplitude of the absorbance peak from the first FTIR reading taken at $t = 1h$ after mixing is not time compensated. The next reading, taken approximately three minutes later, is compensated so that the amplitude of the absorbance peak can be compared with the first sample taken. The same logic applies for the following readings. Only when the data have been normalized for amplitude variations and time-compensated can the CoV be calculated for a mixed sample.

With the results obtained from the FTIR data collection, amplitude normalization and time-compensation methods, it will be possible to conclude if FTIR can be used to collect reliable data. Then, the homogeneity of a mixed sample will be calculated using the CoV.

3.3.2 Performance of a static mixer to obtain a homogeneous resin sample

For the second item, the syringe pump and injection piston are employed to generate a linear flow rate. The speed of each pump is adjusted so that the volumetric mixing ratio of 20,5:1 is respected. The flow then passes through the Kenics RL 180 before exiting into a V-shaped container. The V-shaped container is used to facilitate the resin collection and limit the additional mixing that could be obtained from the resin falling and being transported into a glass jar. The linear geometry of the V-shaped container was thought to limit the risk of diffusion mixing over the time used for transportation. During transportation from CTA to cegep Édouard-Montpetit, the V-shaped container was tightly covered with a bagging film to prevent contamination, spills and resin flow. The V-shaped container was pulled by a 12 volt direct current motor with variable speed, as shown in Figure 24.

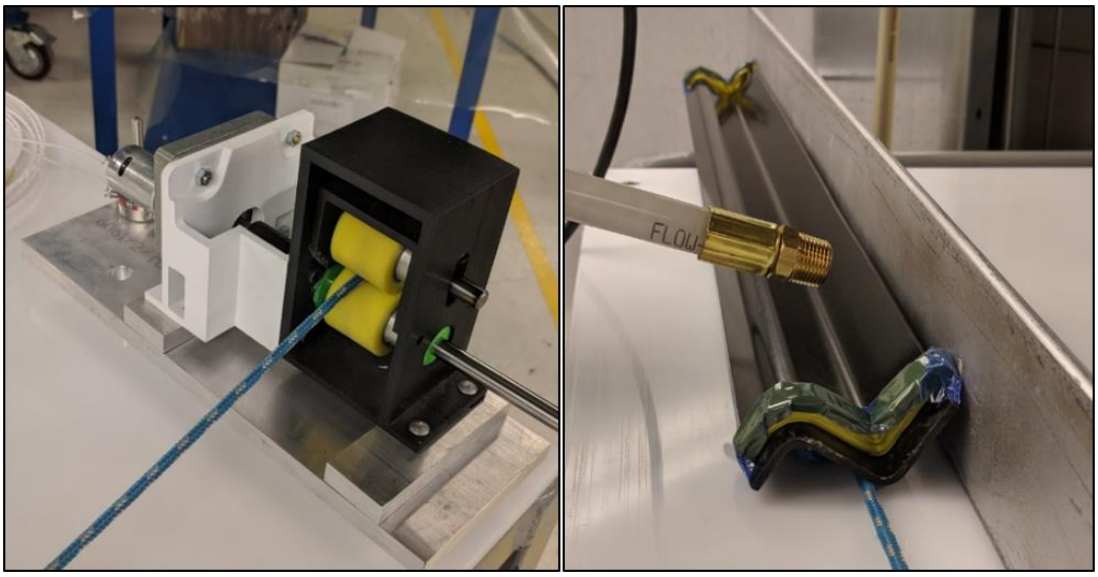

(a) (b)

Figure 24 - V-shaped sample collector: (a) Puller and (b) output of the static mixer into the V-shaped container

FTIR data were collected at five different positions along the container using the same analysis method described in 3.3.1. The position of each measurement is presented in Figure 25.

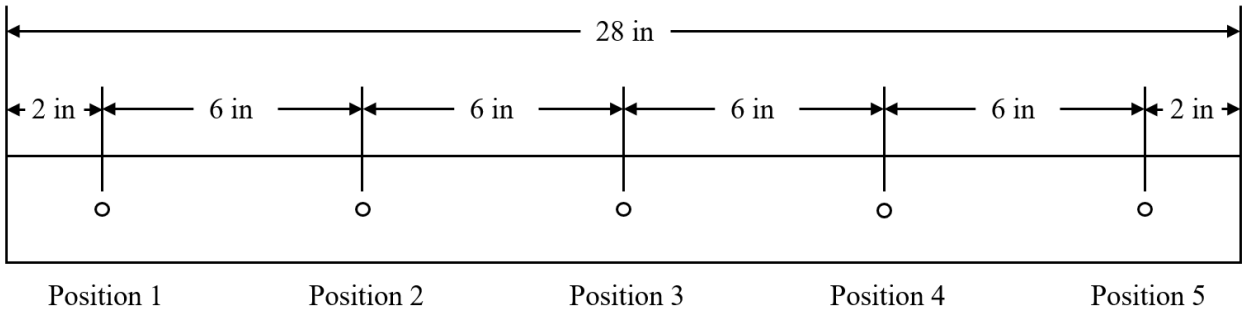

Figure 25 - Sampling positions within the V-shaped container to validate the performance of the static mixer

3.3.3 Qualitative evaluation of the impact of mixing ratio variation on mix homogeneity

For the third item, the peristaltic pump and injection piston is employed to generate a pulsating flow rate. The resin was mixed using the Kenics RL 180 static mixer and samples were collected in the moving V-shaped container. Using the pump's pulse frequency, the speed of the puller was adjusted to get at least two complete pulse cycles along the length of the V-shaped container. Samples were collected every three-fourths of an inch over the length of the container, totalling 36 FTIR readings (*n*) as shown in Figure 26.

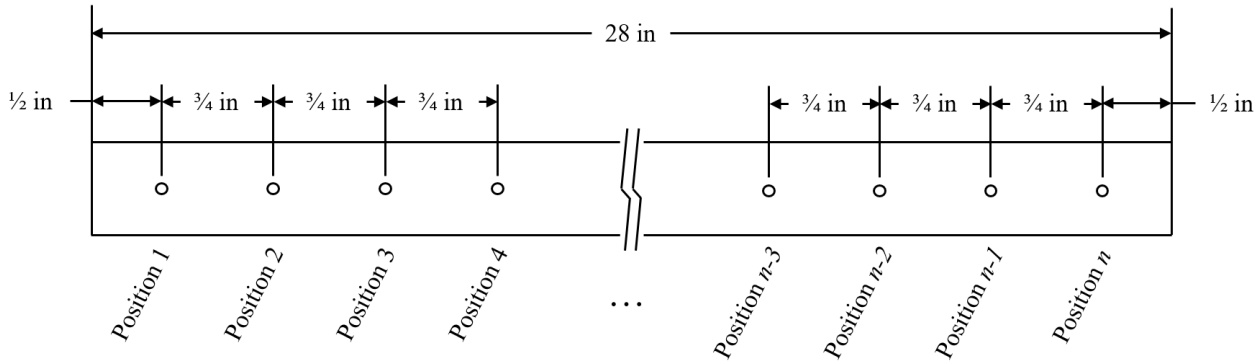

Figure 26 - Sampling positions within the V-shaped container using the static mixer and the peristaltic pump

FTIR spectra were collected for each of the 36 positions and the amplitude of the absorbance peak was normalized and time-compensated as with previous tests. Only the peristaltic pump used on the B side created flow rate pulsations to make sure the mixing ratio varied over time at the inlet of the mixer.

3.4 Results and analysis

3.4.1 FTIR spectroscopy as a technique to evaluate the homogeneity of a resin sample

Figure 27 shows an overlay of the FTIR spectra of parts A and B of the resin system. The x-axis is the wavenumber and is directly proportional to the energy. The left of the spectrum, at high wavenumbers, is of higher energy than the right. The y-axis is the absolute infrared absorbance of the sample. The absorbance peak of isocyanate, R–N=C=O, stands at a wavenumber of 2200-2300 cm^{-1} of part B.

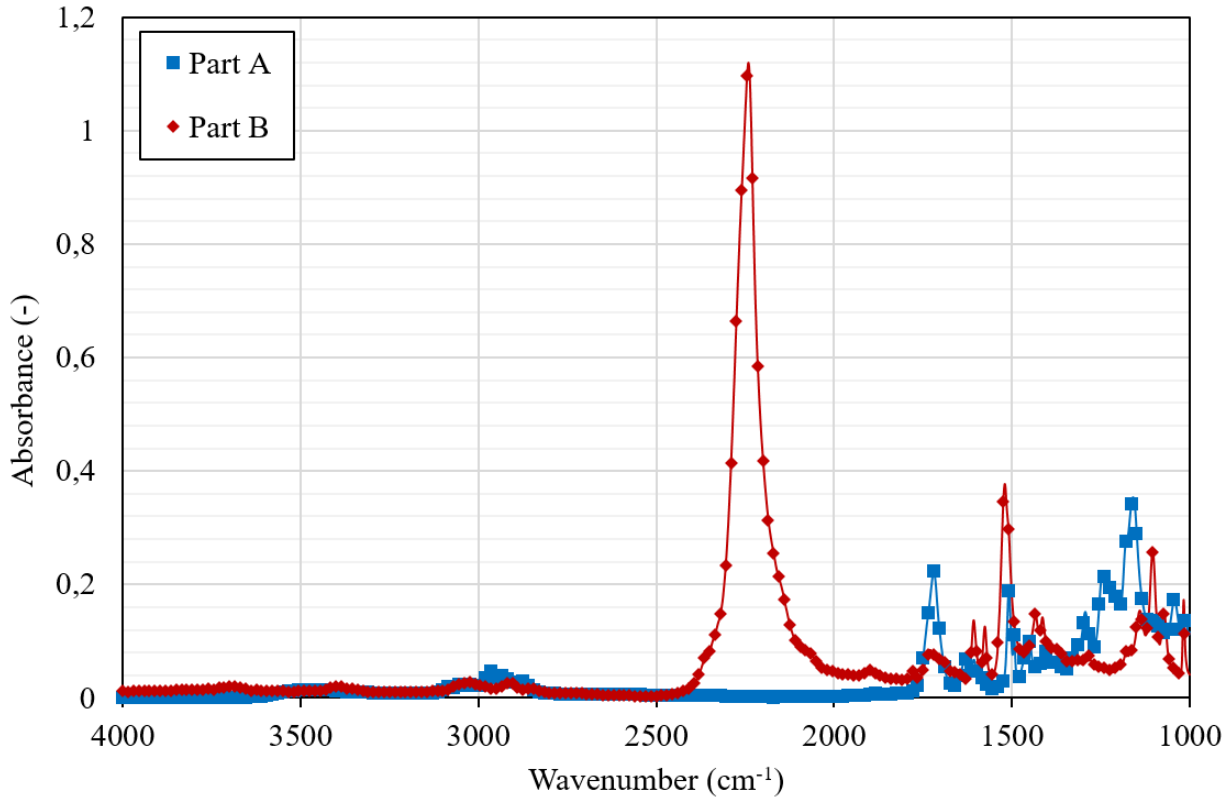

Figure 27 - Overlay FTIR spectra of parts A and B

The isocyanate peak is well defined as it does not overlap with the peaks of any other functional groups and has a high amplitude. If the isocyanate peak fell aligned with an important

peak from part A, deconvolution would need to be used to resolve overlapping bands and allow analysis. This would increase the uncertainty and diminish the reliability of the analysis.

Immediately after mixing, the isocyanate starts reacting with the amines present in part A. This reaction creates a new bond between the amines and the carbon of the isocyanate and breaks the double bond between the nitrogen and the carbon. This reaction changes the functional group, modifying the infrared spectrum and shifting the absorbance peak position slightly. The new urea group created, R_2–N–(C=O)–N–R_2, does not absorb at the 2200-2300 cm^{-1} wavenumbers, causing a decrease in peak height over time. This phenomenon is slightly visible in the lower zoom range of Figure 31, where an overlay of the FTIR spectra of a mixed sample is presented over time.

Because the absorbance peak of isocyanate is only caused by part B, meaning that it cannot be found in the spectrum of part A, it will be used as a metric to evaluate the mix homogeneity of parts A and B. However, this is true only if the Beer-Lambert law is respected. The isocyanate absorbance peak height as a function of mixing ratio is presented in Figure 28. FTIR results were normalized for amplitude variations and time-compensated for the reactivity of parts A and B over time. The data point intersecting the y-axis is the amplitude of the absorbance peak of isocyanate in the spectrum of part B only.

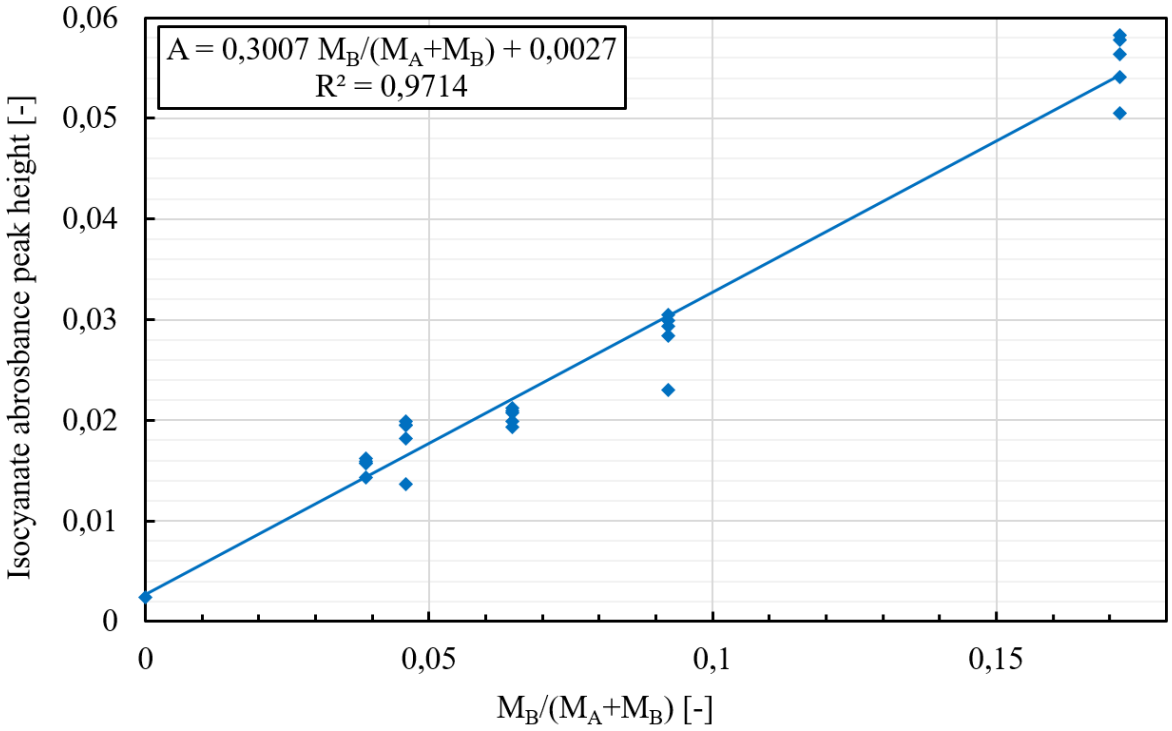

Figure 28 - Beer-Lambert law isocyanate absorbance peak height versus mix concentration

The results of Figure 28 show the linearity of the concentration versus absorbance for the isocyanate and resin system. The equation of the linear trendline is,

$$A = 0{,}3007\ \frac{M_B}{M_A + M_B} + 0{,}0027$$

where A is the amplitude of the isocyanate absorbance peak and M_A and are respectively the mass of parts A and B used in the sample.

The trendline has a linear regression coefficient of 0,9714, confirming the strong linearity of the correlation. Beer-Lambert's law is applicable because the resin used for analysis is not phosphorescent nor fluorescent, the concentration of isocyanate is low and it did not contain solid fillers or additives during testing.

The next sample was mixed using a volumetric mixing ratio of 20,5:1. Figure 29 plots the FTIR spectra at five positions of a hand-mixed sample with zoom ranges to highlight regions of interest.

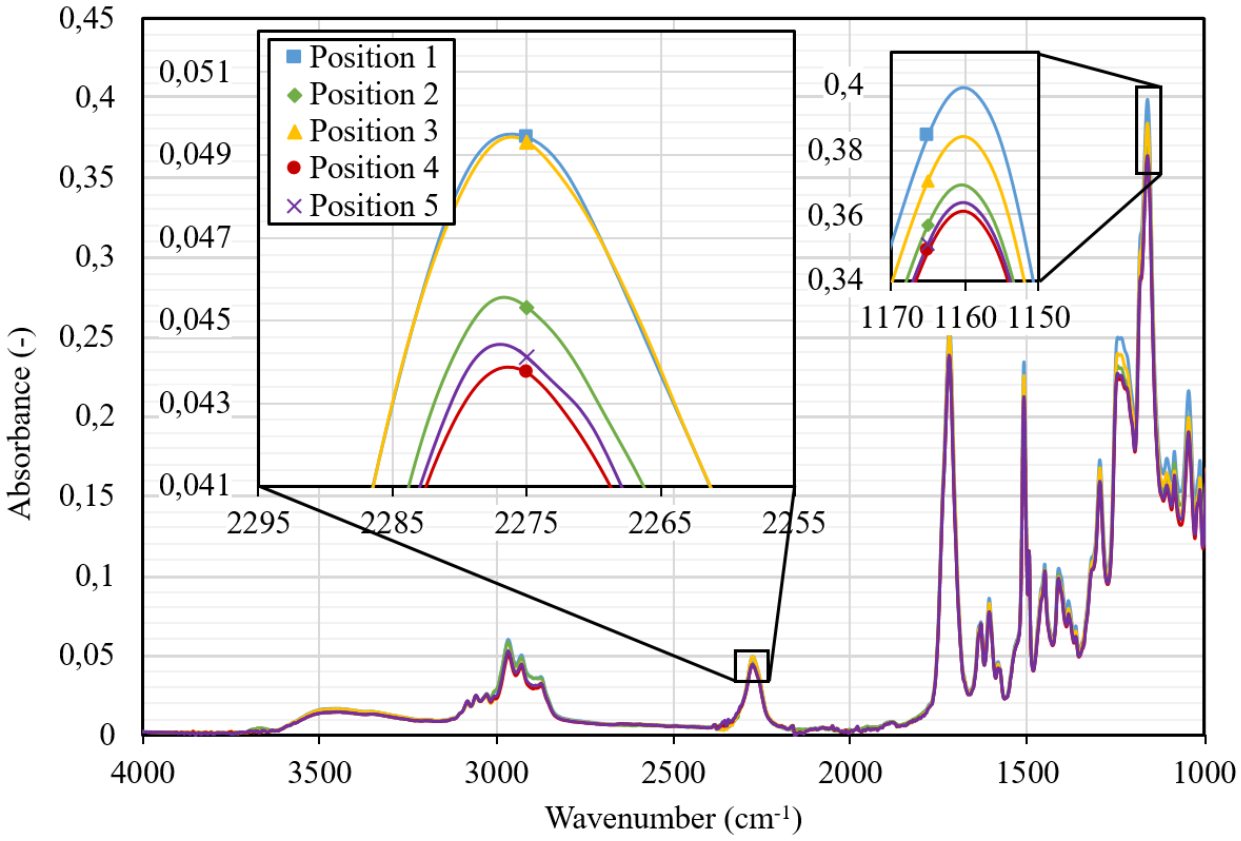

Figure 29 - FTIR spectra of samples mixed by hand for 2 minutes, data collected 1 hour after mixing

Figure 29 shows the absorbance peak of isocyanate (2280 cm^{-1}) in the left zoom range. As predicted, the peak height difference of the isocyanate peak between the five positions seems to correlate with the amplitude variation at wavenumber 1160 cm^{-1} shown in the right zoom range. In fact, this amplitude variation is visible throughout the whole spectrum. To evaluate the cause of this amplitude variation, Figure 30 below shows FTIR spectra of position 5 of the hand mixed sample with parts A and B of the resin unmixed.

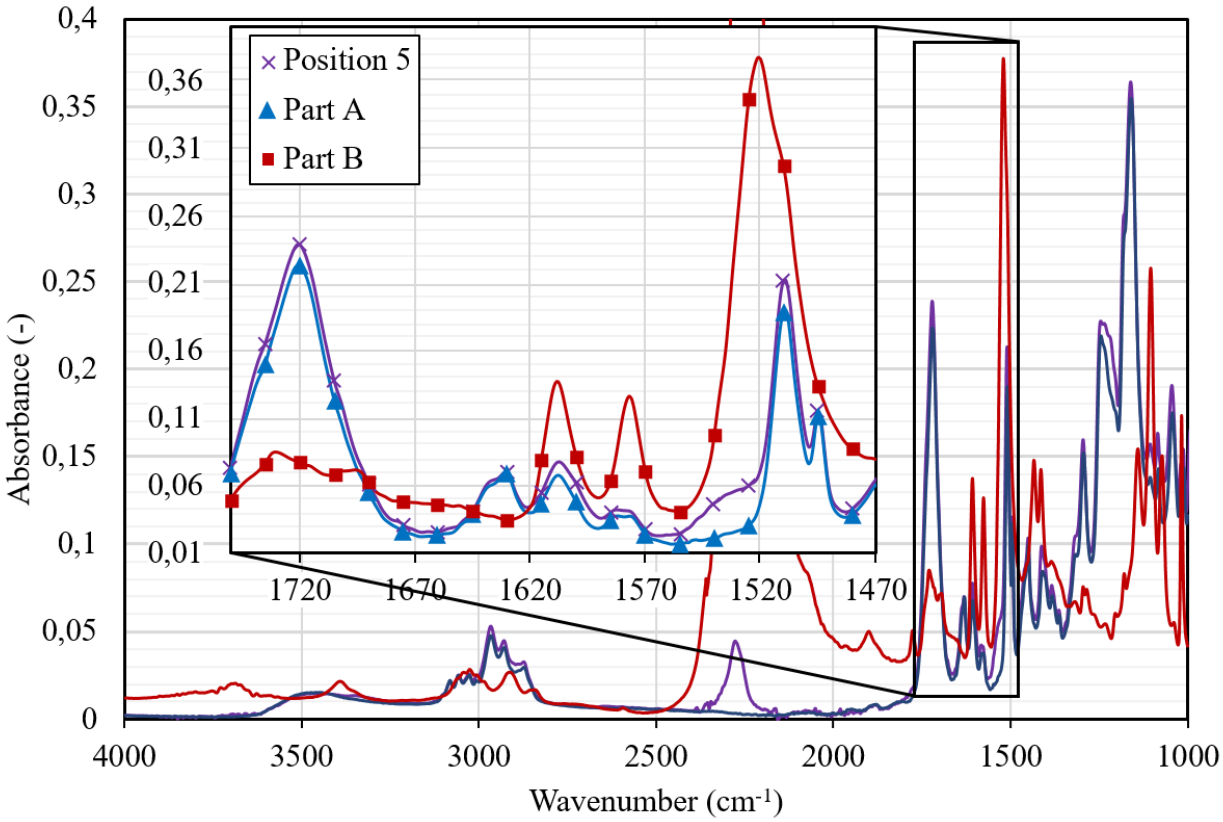

Figure 30 – Overlay FTIR spectra of hand mixed sample with parts A and B of the resin

Figure 30 allows to better understand what happens when both components combine. First, because of the high A:B volumetric mixing ratio of 20,5:1, the FTIR spectrum of part B does not significantly alter the FTIR spectrum of the mixed sample, except at wavenumber 2280 cm^{-1} where the isocyanate absorbance peak is located. In fact, the absorbance peaks at 1720 cm^{-1} and 1510 cm^{-1}, shown in the zoom range, are not significantly modified between part A only and the mixed sample, even though part B of the resin has a strong absorbance peak at 1510 cm^{-1}. This may be explained either by the fact that part B is added in too low quantity to have significant influence or because the mixing of both components modifies the molecular group associated with this wavenumber through a chemical reaction.

The previous observations mean that the amplitude variation observed between the various readings in Figure 29 is mostly explained by other factors than the mixing of both components itself. Sample preparation or data collection can influence the amplitude of the spectrum. For example, sample thickness or trapped air can be the cause of this result. To eliminate the influence of this amplitude variation on the data analysis, the absorbance peak height of isocyanate was

normalized using the absorbance peak height of other easily resolved peaks, a commonly used technique in FTIR analysis. Three peaks were identified to be suitable for normalization. The peaks' locations are 1160, 1510 and 1720 cm^{-1}. The normalization is performed with these three distinct functional groups to ensure that the technique yielded consistent results. However, to ensure that the three peaks were not modified or involved in a chemical reaction with part B of the resin, FTIR spectra analysis of the mixed sample was performed over time. Results are presented in Figure 31.

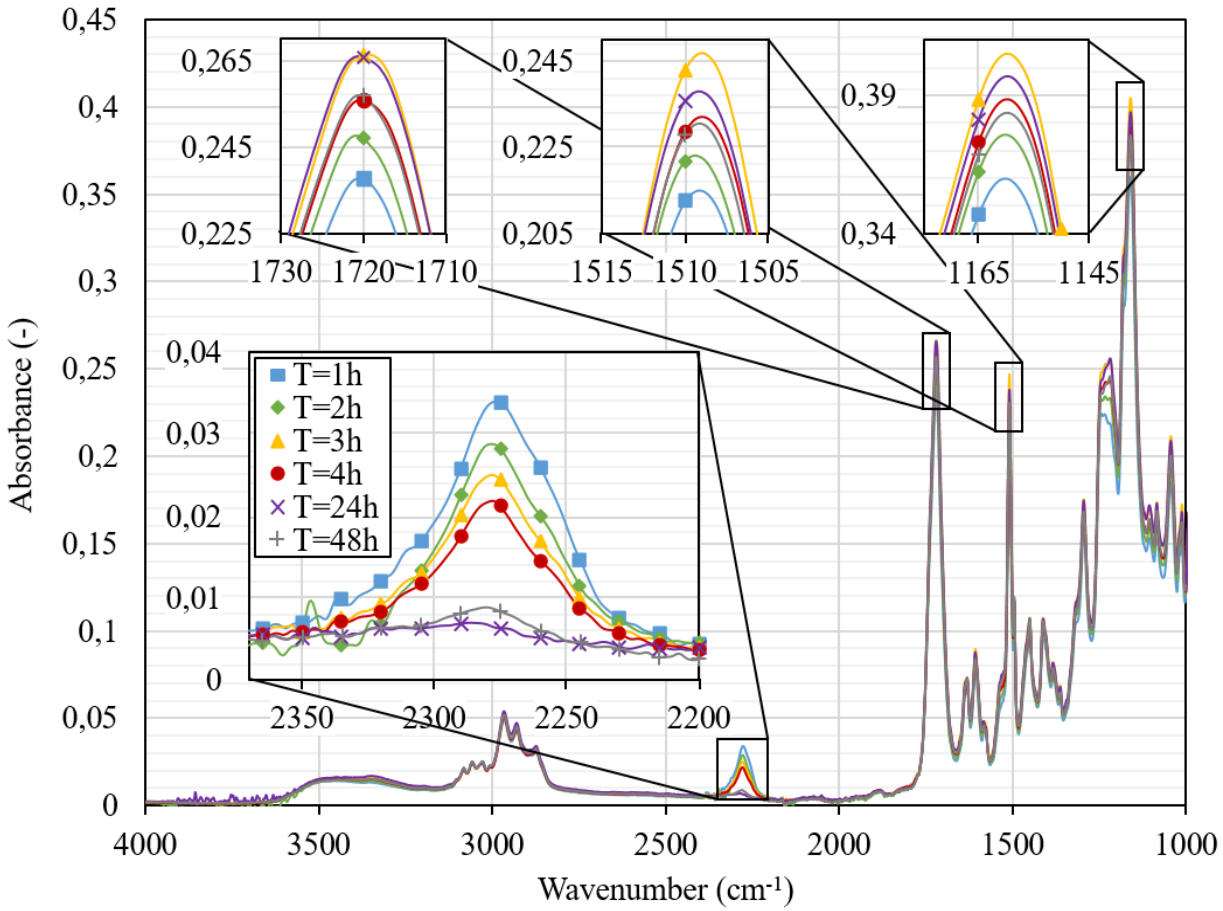

Figure 31 – FTIR spectra evolution of a mixed sample over 48h

Figure 31 shows that the three chosen peaks vary in amplitude over the course of the reaction between parts A and B. However, the variation is similar for the three peaks, even though some peaks are more influenced by the absorbance spectrum of part B as shown in Figure 25. Likewise, the evolution of peaks 1720, 1510 and 1160 cm^{-1} does not match the evolution of the isocyanate at 2280 cm^{-1}. This suggests that there is no correlation between the reaction of parts A

and B of the resin and the amplitude variation observed at the peaks located at 1160, 1510 and 1720 cm^{-1}. The amplitude of the isocyanate absorbance peak can be normalized by all three identified peaks and averaged before being used for CoV calculations.

The amplitude decrease of the isocyanate peak can be seen in the lower left zoom range of Figure 31. A total of five samples were collected at one hour and two hours after mixing to obtain the rate of amplitude decrease. Results are plotted in Figure 32.

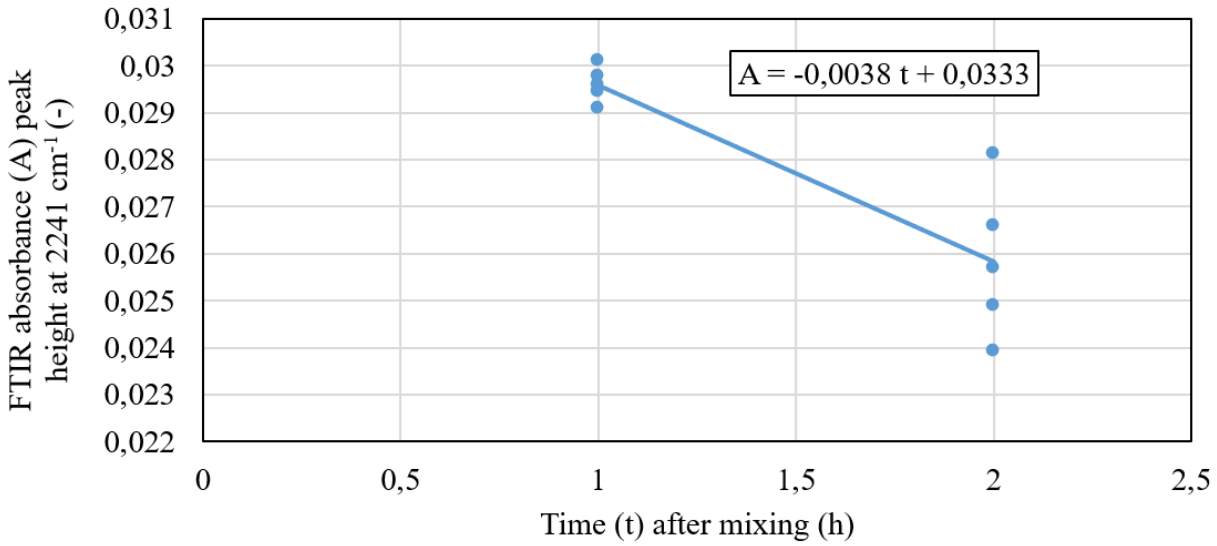

Figure 32 - Amplitude of the isocyanate absorbance peak at one and two hours after mixing

A linear trendline was fitted to the data to obtain the rate at which the isocyanate absorbance peak decreases from one hour to two hours after mixing. Using the equation of the linear regression trendline,

$$A = -0{,}0038\,t + 0{,}0333 \tag{5}$$

where A is the FTIR absorbance peak height of isocyanate at 2241 cm^{-1} wavenumber and t is the time after mixing occurred in hours, the amplitude of the isocyanate absorbance peak can be modified as a function of time for CoV calculations. Looking at the isocyanate absorbance peak decrease from 1 hour to 48 hours after mixing in the lower left zoom range of Figure 31, an inverse funcion would be more adequate to model the peak decrease over time. However, for the purpose of this work, the linear approximation is precise enough for analysis.

Table 12 lists the raw, time compensated and amplitude normalized isocyanate absorbance peak height (2281 cm^{-1}) of the hand mixed sample. The coefficient of variation is calculated for raw and modified data sets. The time compensation is performed on the normalized results. The final CoV of the sample is obtained by taking the average of the time-compensated and normalized CoV.

Table 12 – Raw, time compensated and normalized isocyanate absorbance peak height and CoV of hand mixed samples

			Sample position					
Data type			**1**	**2**	**3**	**4**	**5**	**CoV**
		Raw	0,0495	0,0456	0,0494	0,0439	0,0444	**5,24%**
			0,0495	0,0458	0,0500	0,0447	0,0455	**4,68%**
Time compensated	Normalized	1720 cm-1	0,192	0,190	0,198	0,188	0,191	**1,85%**
		1510 cm-1	0,211	0,213	0,221	0,211	0,214	**1,72%**
		1160 cm-1	0,124	0,124	0,130	0,124	0,125	**1,91%**
		Average of time-compensated and normalized CoV						**1,83%**

The sample mixed by hand has a coefficient of variation of 5,24% without time compensation nor normalization. This CoV value falls outside the set tolerance of 5% for acceptable variation in the mixing process. However, with time compensation, the CoV is reduced to 4,68% and falls within the acceptable limit. Then, with the addition of normalization for amplitude variation, the CoV is 1,85%, 1,72% and 1,91% using each of the three peaks (or an average of 1,83%). The normalization technique gives similar results, suggesting that the chosen peaks are constant and not altered by part B of the resin system. Therefore, as suggested by the industrial partner, hand mixing the resin sample for 2 minutes is adequate as the concentration variation of part B is 1,83%.

These first tests suggest that FTIR spectroscopy can be used to accurately evaluate the mixing quality of a resin sample. The absorbance versus concentration graph for isocyanate and resin (parts A and B) is linear and comply with the Beer-Lambert law. The absorbance peak of isocyanate can easily be resolved in the mixed product. From there, the absorbance peak height is measured. Results are then time-compensated for the reaction rate of parts A and B of the resin using Equation 5 and normalized for amplitude variations using three peaks located at 1160, 1510 and 1720 cm^{-1}. The final CoV for the sample is obtained by taking the average of the time-

compensated and normalized CoV. Ultimately, the coefficient of variation (CoV) is used as a metric to express the homogeneity of the sample. If the CoV is lower than 5%, the product is considered homogeneous enough for the intended application.

3.4.2 Performance of a static mixer to obtain a homogeneous resin sample

An overlay of the FTIR spectra of five evenly spaced positions of the sample mixed using the static mixer is shown in Figure 33 below.

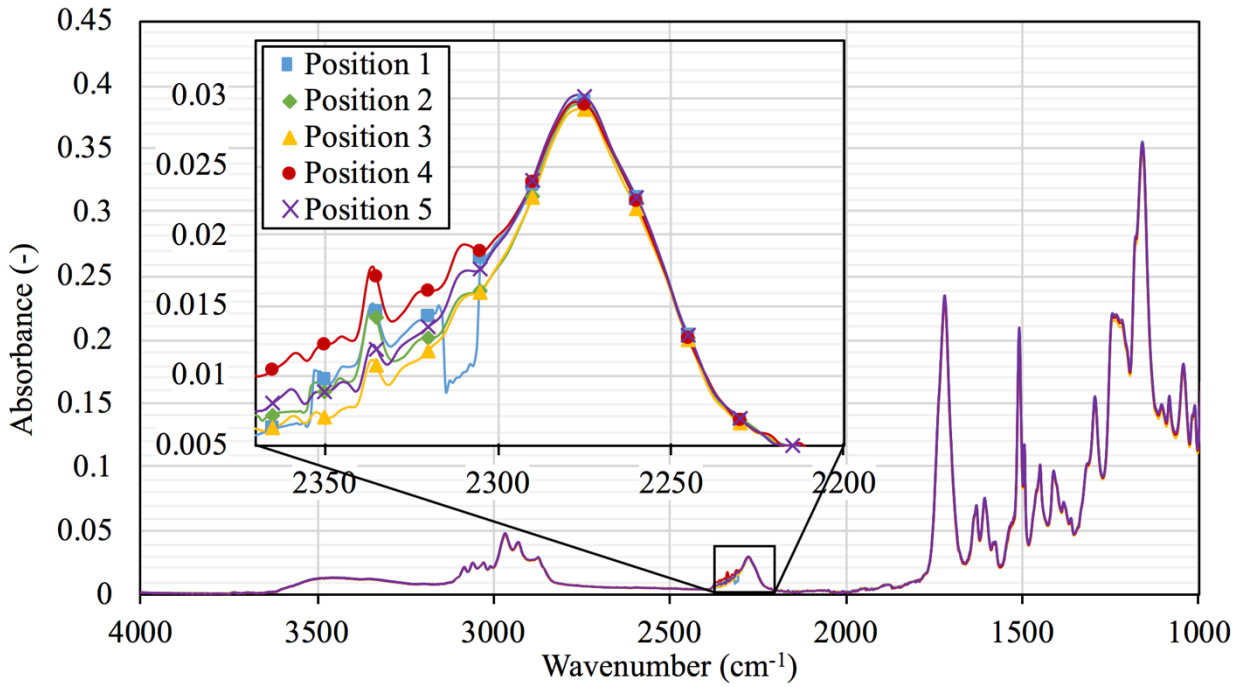

Figure 33 - FTIR spectra of samples mixed with the static mixer, data collected 1h after mixing

Looking at Figure 33, it is possible to notice noise in the 2300 to 2340 cm^{-1} wavenumber range. This noise is probably caused by CO_2 (O=C=O) level differences between the background scan and the analyzed spectra. Luckily, the noise does not align with the isocyanate absorbance peak and seems to have no influence on the results. Using the same data analysis method as with the hand mixed samples, CoV results are presented in Table 13.

Table 13 – Raw, time compensated and normalized isocyanate absorbance peak height and CoV of samples mixed using the Kenics static mixer

Data type			Sample position 1	2	3	4	5	CoV
		Raw	0,0298	0,0294	0,0291	0,0296	0,0301	**1,13%**
			0,0298	0,0296	0,0295	0,0301	0,0308	**1,64%**
Time compensated	Normalized	1720 cm-1	0,127	0,127	0,128	0,130	0,131	**1,38%**
		1510 cm-1	0,144	0,143	0,147	0,148	0,147	**1,38%**
		1160 cm-1	0,0837	0,0835	0,0850	0,0856	0,0869	**1,49%**
		Average of time-compensated and normalized CoV						**1,41%**

Table 13 shows that CoV of the raw data is 1,13%. Adding the time compensation and normalization for amplitude variation, the CoV averages 1,41%, well below the 5% limit. It is interesting to note that the CoV increased when adding the corrective terms. This is not alarming because the results obtained from the raw data are not reliable. Again, the normalization technique is conclusive as the coefficients of variation based on all three normalizing peaks are consistent with one another. Compared to the sample mixed by hand with a CoV of 1,83%, the static mixer seems to produce slightly higher homogeneity at a CoV of 1,41%.

The previous results conclude that the Kenics RL 180 static mixer with 24 mixing elements produces adequate mix homogeneity for this specific mixing application. During the validation of the performance of the in-line mixing system, an SMX type mixer will be tested. Based on the literature review, SMX mixers should produce samples with higher mix homogeneity to the expense of a greater pressure drop. A different type of static mixer will be tested with the completed system to get more comprehension of the performance of different static mixer geometries and hopefully improve the results obtained here. Yet, results of this section give enough confidence that static mixers can be used in the in-line metering and mixing system. In any case, resin samples will be mixed using the newly developed system and FTIR analysis will be performed to assess the mix homogeneity. Validation testing details and results are presented in Chapter 5.

3.4.3 Qualitative evaluation of the impact of mixing ratio variation on mix homogeneity

Figure 34 shows the approximation of the flow rate generated by the peristaltic pump as well as the isocyanate absorbance peak height at the various positions throughout the V-shaped collected. The chart's x-axis is the sample number across the V-shaped container and refers to Figure 25. The primary y-axis is the normalized and time-compensated isocyanate absorbance peak height. The secondary y-axis is the approximate flow rate of the peristaltic pump in ml/min. The flow rate simulation was derived from the pump's rotational speed, average flow rate and observed pulse pattern. The flow rate of the pump was recorded by dispensing resin into a cup for a period of 10 pulses. Then, the fluid was weighed, multiplied by the density and divided by the sample collection time. This gave an average flow rate of 12.8 ml/min. Next, the pulse frequency was calculated by multiplying the motor speed by the number of rollers on the shaft. This method was considered accurate enough for a qualitative analysis with the purpose of determining if there was a match between the mixing ratio variation at the inlet of the mixer and the isocyanate levels in the mixed samples. The amplitude of the pump's flow rate variation and waveform was modelled through visual analysis only. The waveform was approximated as a smoothed square wave. Physically, this model makes sense with the mechanical operation of the pump's rollers. The flow will be linear while the rollers do not obstruct the pump and will quickly drop to zero when the rollers obstruct the outlet.

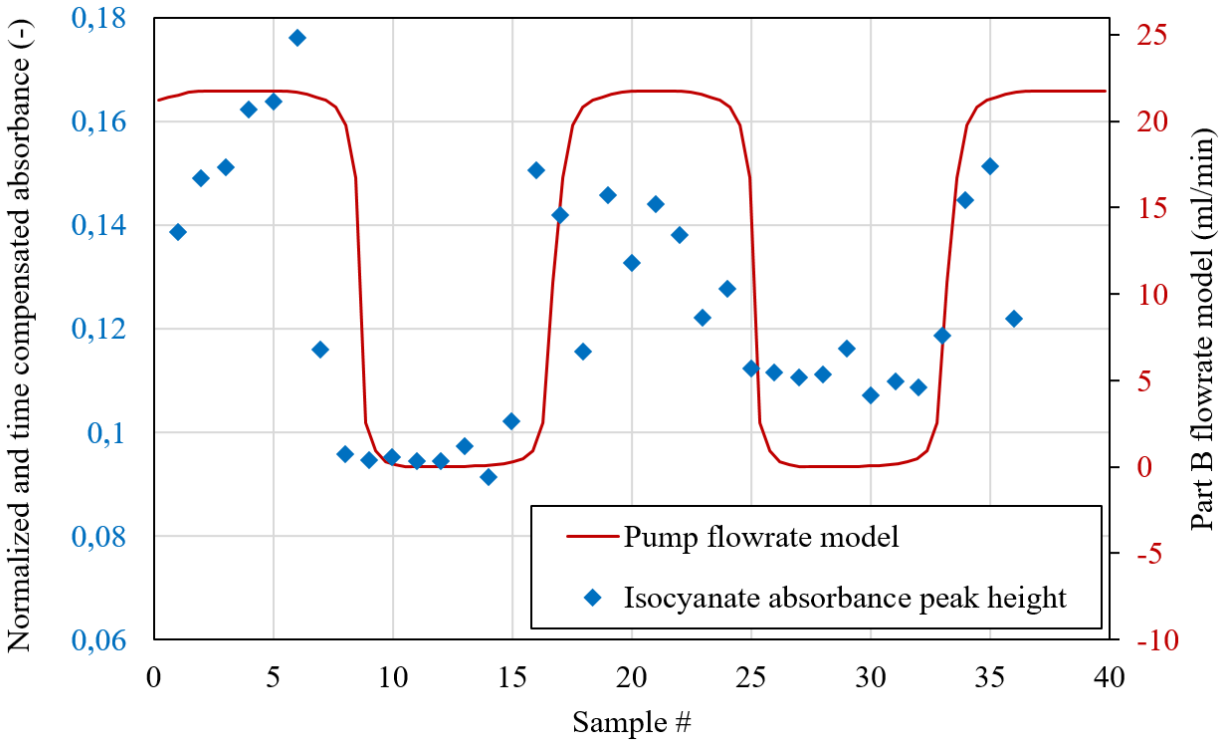

Figure 34 - Overlay of isocyanate absorbance peak height and pulsed flow rate model

Figure 34 shows the match between the flow rate model and the isocyanate concentration found by FTIR. Each of the 36 isocyanate peaks recorded by FTIR along the length of the V-shaped container together shows the isocyanate concentration fluctuations. The frequency of the isocyanate absorbance variations matches with the pump's flow rate model. To estimate the degree of axial mixing through the static mixer, the coefficient of variation for the 36 readings was calculated. Results are presented in Table 14.

Table 14 – Isocyanate absorbance peak height coefficient of variation

	Average	**Standard deviation**	**CoV (%)**
Isocyanate absorbance peak height (-)	0,124	0,0228	18,4

Table 14 shows that the sample's isocyanate absorbance peak height using the peristaltic pump and static mixer combination is 18,4%, an indication of low mix homogeneity caused by significant mixing ratio variations at the inlet of the static mixer. Interestingly, although the flow rate model estimates a flow rate relative variation of 100% from 0 to 22 ml/min, the coefficient of variation of the isocyanate absorbance peak height is 18,4%. This suggests that, although limited,

the static mixer generates some amount of axial mixing to dampen the mixing ratio variations present at the inlet.

The results agree with the literature which states that static mixers offer a limited level of axial mixing. Unfortunately, because the pumps flow rate variation model is qualitative, it is impossible to quantify the level of axial mixing provided by the static mixer. To quantitatively evaluate the impact of a varying volumetric ratio on the mix homogeneity, the pump's flow rate variations would need to be quantified using a flowmeter. Nonetheless, despite the limitations of the experiment, the results help to understand the risk of having volumetric mixing ratio variations with the prototype mixing system. For this reason, considerations will be made regarding the choice of the pumps for the design phase, as detailed in section 4.2.4.1.

3.5 Conclusions

The tests presented in this chapter allowed to reach the target objective and sub-objectives. Many conclusion and observations were made possible, namely:

- FTIR spectroscopy can be used to evaluate the mixing homogeneity of a resin sample. A method was developed to obtain the CoV of a sample. The infrared absorbance peak of isocyanate, present in part B of the resin only, can easily be resolved in the spectrum of a mixed sample. From there, normalization for amplitude variation and time compensation for the peak height decrease caused by the chemical reaction of part A and B is performed. Results are then used to compute the coefficient of variation of the data set. The method is detailed further in section 3.4.1.
- The Kenics RL180 static mixer with 24 mixing elements yields adequate mix quality. The coefficient of variation of the mixed samples is 1,41%, below the acceptable 5% threshold set for this mixing application and most industrial processes. This suggests that an SMX static mixer would perform well in the in-line mixing system as it offers more performance on all metrics to the expense of higher pressure drop. Therefore, depending on the pressure capabilities of the prototype in-line mixing system, a Kenics or SMX static mixer will be chosen.

- The use of the Kenics RL180 static mixer with 24 mixing elements produces a more homogeneous resin sample than thoroughly hand mixing for 2 minutes, the reference according to the industrial partner.
- A pulsed flow rate, or mixing ratio variation, at the inlet of the static mixer, has a great influence on the homogeneity of the mixed sample. This suggests that very low axial mixing is produced, agreeing with the literature. Special considerations will be taken to limit the flow rate variations that may be caused by the pumps in the completed system.

CHAPTER 4 DEVELOPMENT AND MANUFACTURING OF A PROTOTYPE IN-LINE METERING AND MIXING SYSTEM

Following the literature review of Chapter 2 on some of the current metering and mixing systems and their capabilities, this chapter presents the development of the proposed metering and mixing system along with its innovative features.

First, the design requirements are presented. Then, the preliminary and detailed design are described using the system's process and instrumentation diagram and 3D model. Finally, a walkthrough of the manufacturing of the system is illustrated.

4.1 Requirements

4.1.1 Process requirements

The first step is to determine the output capacity of the in-line mixing system to identify the right equipment size. Based on the partner's SMC development line speed and width, prepreg sheet weight target and fibre mass fraction, the metering and mixing system required resin production rate is obtained. Then, using the resin's mass mixing ratio, the flow rate of parts A and B is calculated. Mixing ratio precision requirements are presented in Table 15. Part A must be precise at ± 1.8 % while part B's precision is limited to ± 1.6 %. The minimum mixing ratio is obtained by dividing the minimum of part A allowed by the maximum of part B allowed, and vice versa. Volumetric mixing ratio is obtained using the density of parts A and B of 1,0676 and 1,2342 kg/L respectively.

Table 15 - Mixing ratio precision requirements

	Parts by mass		Unit mass mixing ratio	Unit volumetric mixing ratio
	A	**B**	**A:B**	**A:B**
Minimum	108	6.3	17,14:1	19,82:1
Nominal	110	6.2	17,74:1	20,51:1
Maximum	112	6.1	18,36:1	21,23:1

The resin chemistry is engineered and adjusted for a volumetric ratio of 20,5:1. However, with future development and improvements with the resin chemistry, the mixing ratio may change.

For this reason, the industrial partner requested the system to have an adjustable mixing ratio from 5:1 to around 30:1.

The system's output flow rate range is presented in Table 16 below. The nominal flow rate is based on target SMC production speed once the system will be operational. Maximum and minimum figures were imposed by the industrial partner to give the system versatility in case the process is modified in the future.

Table 16 – System's operating range

	Flow rate (ml/min)		
	A (± 1.8%)	**B (± 1.6%)**	**Total**
Minimum	572	28	**600**
Nominal	1441	71	**1511**
Maximum	1907	93	**2000**

4.1.2 System requirements

The system is developed to dose two-component resin systems. Table 17 lists the fluid properties that have an impact on the system design.

Table 17 - Resin system properties

Property	**Part A**	**Part B**
Viscosity (cP)	1050	195
Temperature (°C)	20 to 30	20 to 30 °C
Density (kg/l)	1,0676	1,2342
Chemical composition	Vinyl ester resin, peroxide, styrene	Isocyanate
Cleaning solvent	Acetone	Acetone
Abrasive fillers and additives	Glass microspheres, talc, nanoclay	N/A

The viscosity of the fluid has a significant impact on the pressure drop across the system, which dictates the sizing of all the equipment. Higher viscosity fluids mean higher pressure drop, which in turn requires more powerful pumps, sturdier valves and instruments. Again, because the industrial partner is still in the research and development phase of their carbon SMC material, the fluid properties may be modified. For this reason, Magna requested the system to be able to work with a resin of viscosity of 1050 cP (current resin) to 5000 cP.

4.1.3 Additional requirements

In addition to the process and system requirements, the system needs to reflect a set of design guidelines intrinsic to the intended application.

4.1.3.1 Reliability

The intended operating framework of the new system is in the automotive industry which implies a significant challenge in terms of design reliability. Ford, one of Magna's partner for the new SMC prepreg material, built 6.4 million cars in 2016 [99]. Of course, only a limited number of these cars will include composite structural parts soon. Yet, it would be safe to assume that at least 5% of all manufactured cars will feature a composite part. This translates to 320,000 composite parts manufactured per year. Assuming the in-line metering and mixing system operates seven hours a day, five days a week, and that each car requires one 15kg composite part (front subframe for example), a minimum of twenty resin metering and mixing systems with this project's target production rate are required worldwide to supply to the demand. These numbers are based on approximations and are simply used to show the production scale such resin mixing system could face during its useful life if the technology goes into production at a global scale. Therefore, downtime due to system break must be avoided as much as possible which shows the importance of a reliable system.

There is a research field dedicated to predicting the reliability of a new system [100]. However, the scope of this work limits the prediction of reliability to common sense and only focuses on equipment selection. It is important to always opt for robust and reliable equipment that is meant to be used in high volume industrial applications. This increases the costs of the equipment but overall affects the reliability of the system. For instance, two different one-inch sanitary stainless-steel ball valve are shown in Figure 35. One is manufactured by an amateur brewing hardware company for about $30 USD while the other is from a food processing and pharmaceutical equipment supplier for $80 USD.

(a) (b)

Figure 35 – 1" Sanitary Stainless Steel Ball Valves: (a) amateur brewery application [101] and (b) industrial food and pharmaceutical applications [102]

Visually, the valve manufactured for industrial applications looks sturdier and designed for higher pressure applications. Moreover, it can easily be disassembled for cleaning because of its modular design, which is not the case with the amateur brewing model. The above example is applicable to almost all industrial equipment making up metering and mixing systems.

4.1.3.2 Cleaning and maintenance

Like all systems, the proposed prototype must be easy to clean and maintain. This requirement is especially true when working with reactive polymers. The industrial partner says part B of the resin, the isocyanate, will age if it comes in contact with moisture. On the other hand, part A of the resin contains both the monomer and catalyst but the reaction is prevented by an inhibitor. This inhibitor has a limited lifetime and the resin will start to cure on its own after approximately two weeks. If the resin is not cleaned properly or left stationary inside the system for too long, the polymerization reaction will harden the resin in place and the system's components will have to be replaced. Hence, it is crucial to select equipment that is designed to be cleaned-in-place (CIP) with a solvent flush or easily disassembled for manual cleaning. Fortunately, if the system is used regularly, the resin will not have time to age and will not require frequent cleaning. Nevertheless, dead areas of the system, where fluid velocity is low, may require regular cleaning.

4.1.3.3 Chemical compatibility

The system's wetted parts (components in contact with the process fluid) must be chemically compatible with the process fluids and cleaning agents. The chemical compatibility of various metals and polymers with chemicals of interest for this project is presented in Appendix A.

Combining the chemistry of the resin system and cleaning solvent, stainless steel and polytetrafluoroethylene (PTFE or Teflon®) are ideal materials.

4.1.3.4 Classified locations

As covered in 2.7.1, all electrical equipment must be certified to operate in hazardous classified locations. Frequently, industrial equipment suppliers sell electrical equipment that is already certified. Otherwise, if a certain type of electrical equipment is not available with the appropriate certification, pneumatic or hydraulic alternatives must be used. For low current equipment like instrumentation, intrinsic Zener safety barriers can be used. These safety barriers are installed in the control panel, which is located outside the classified location, and limit the voltage and current to the instrument located within the explosive area. Figure 36 shows a layout diagram of the intrinsic safety barrier and instrument located in a hazardous location.

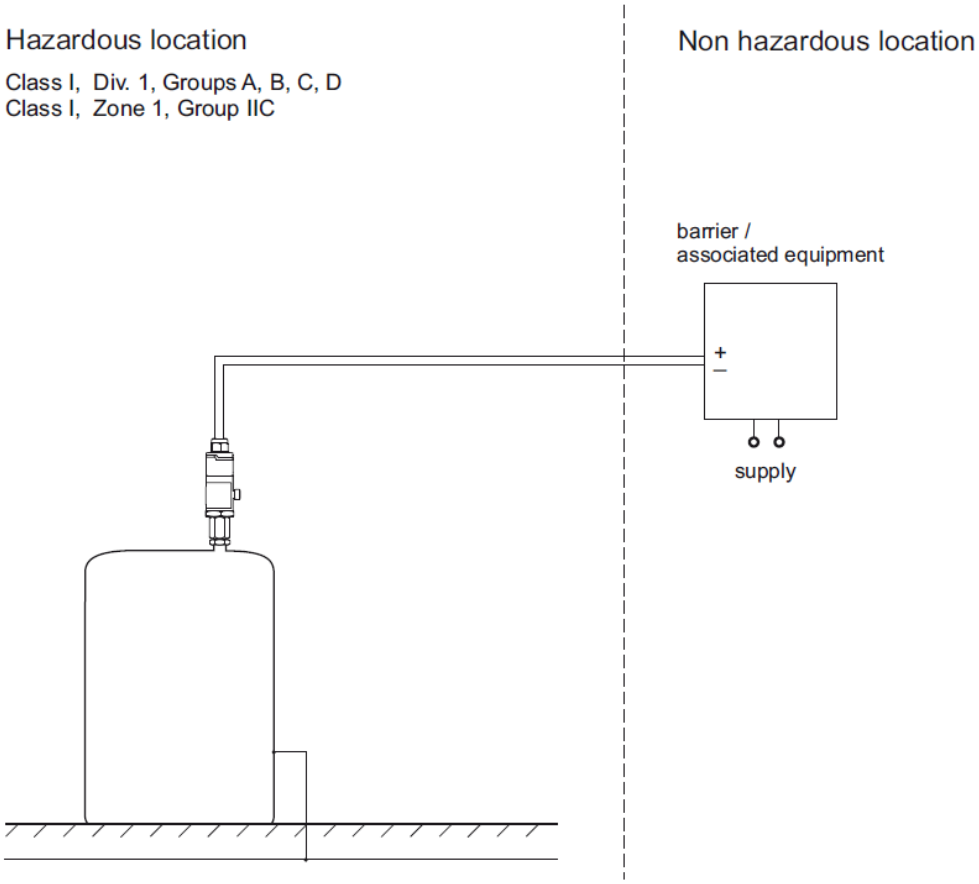

Figure 36 - Use of an intrinsic safety barrier for instrumentation located in a hazardous location The safety barrier, installed in the control panel, falls outside the hazardous location [103]

4.1.3.5 Safety

The safety of the operators is essential. Common safety considerations are required during the development phase of the system. Easily accessible areas of the system should not have sharp edges and pinch zones. Likewise, in the event of a system failure, there should be no risk of injury to the operator through contact with the chemical substances.

4.1.3.6 Automation and integration with the SMC prepreg line

The system needs to be able to operate continuously and independently. This means that the resin and thickening agent coming from storage tanks must be fed to the metering system, metered to the right mixing ratio, mixed and dispensed to the prepreg line for SMC manufacturing automatically. In addition, as seen in Figure 1, SMC prepreg manufacturing lines feature two doctor boxes that are used to spread the resin in a thin film in which a specific resin level must be kept. Automated features, from resin metering and mixing to doctor box level monitoring, must be controlled through a programmable logic controller.

The number of automated features of the new system should depend on the project's budget, schedule and available resources. Interest is focused on less frequent operations like system startup, shut down and cleaning procedure, all of which can request the need of an operator.

4.2 Preliminary design

The objective of the preliminary design is to identify the equipment required to build a complete and working system. During the preliminary steps, the design is detailed up to the process and instrumentation diagram (P&ID) and the ideal technologies are identified for all equipment. Using the system's requirements, various iterations of the P&ID were created and modified through meetings and design reviews with the industrial partner until a consensus was achieved. Figure 37 shows the final iteration of the P&ID while Table 18 lists all components included in the system. The system is divided into three areas; resin preparation, metering system and mixing and delivery.

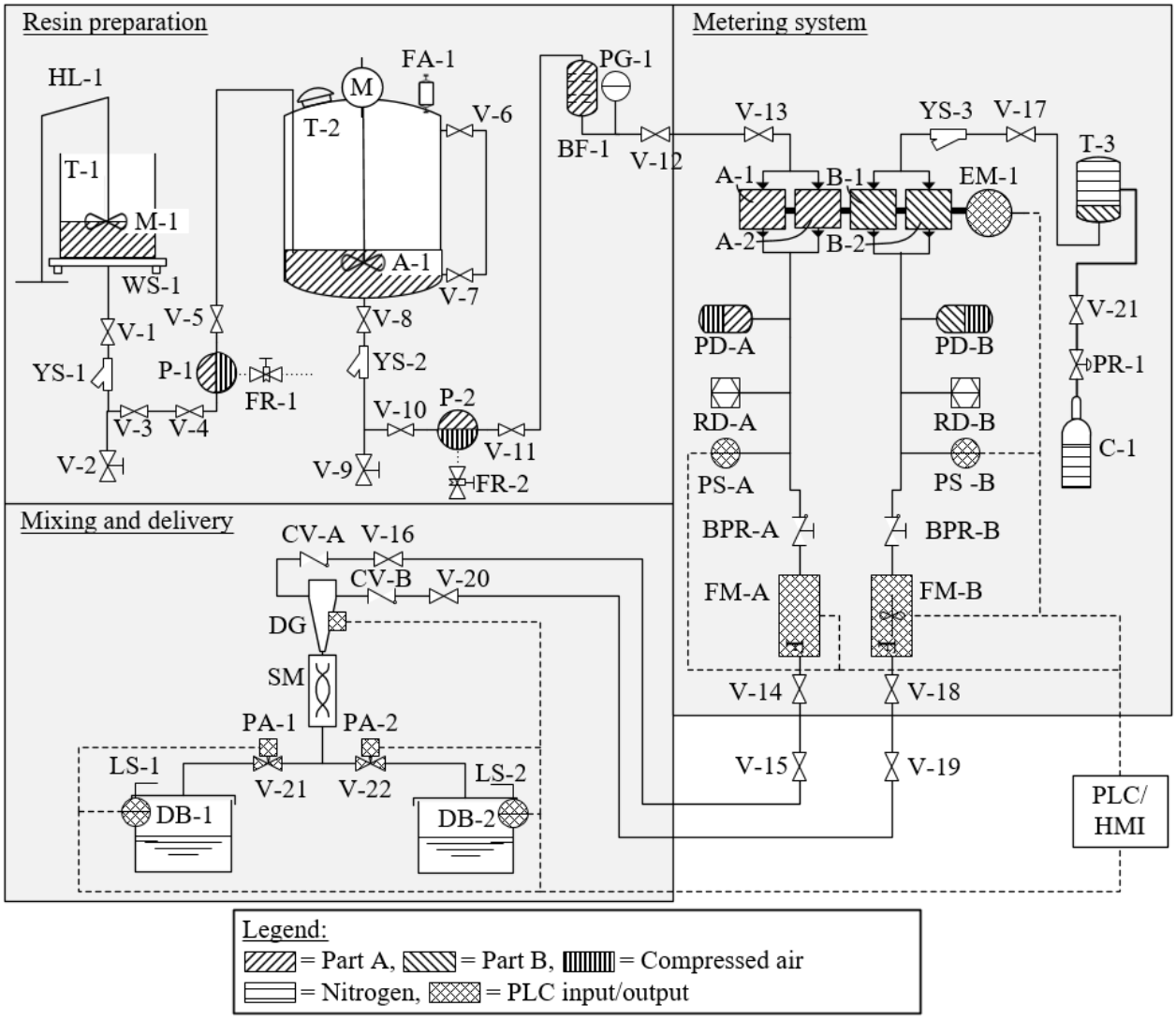

Figure 37 - In-line metering and mixing system process and instrumentation diagram: resin preparation, metering system and mixing and delivery areas

Table 18 - In-line metering and mixing system component identification

Part number	Description	Part number	Description
A-1, A-2	Part A Pump Plunger	P-1	Transfer Pump
B-1, B-2	Part B Pump Plunger	P-2	Feeding Pump
BF-1	Bag Filter	PA-1, PA-2	Pneumatic Actuator
BPR-A, BPR-B	Backpressure Regulator	PD-A, PD-B	Pulsation Dampener
C-1	Nitrogen Cylinder	PG-1	Pressure Gauge
CV-A, CV-B	Check Valve	PLC	Programmable Logic Controller
DB-1, DB-2	Doctor Box	PR-1	Pressure Regulator
DG	Dispense Gun	PS-A, PS-B	Pressure Sensor
EM-1	Electric Motor	RD-A, RD-B	Rupture Disk
FA-1	In-line Flame Arrestor	SM	Static Mixer
FM-A, FM-B	Flowmeter	T-1	Mixing Tank (Part A)
FR-1, FR-2	Air Filter and Regulator	T-2	Day Tank (Part A)
HL-1	Hydraulic Lift	T-3	Day Tank (Part B)
HMI	Human Machine Interface	V-1 to V-22	Ball Valve
LS-1, LS-1	Level Sensor	YS-1 to YS-3	Y-strainer or In-line Filter
M	Day Tank Agitator Motor	WS-1	Weighing Scale
M-1	High Shear Mixer		

The project's scope covers the mechanical design, equipment sourcing, procurement, assembly and testing of the new system. This chapter includes the preliminary and detailed designs and assembly of the metering system, mixing and delivery sections of Figure 37. The preliminary and detailed designs of the resin preparation area are also presented. The assembly and testing of the resin preparation area was the industrial partner's responsibility. The testing of the new system is presented in Chapter 5.

4.2.1 Resin preparation

The equipment located in the resin preparation area of Figure 37 is used to prepare and feed part A of the resin to the metering system. First, the resin along with its multiple fillers and additives are incorporated in tank T-1 using a high shear mixer M-1. The tank has an open top and the high shear mixer is lowered in the resin using a hydraulic lift HL-1. The high level of shear created by the mixer helps disperse the particles and minimizes the creation of agglomerates. Tank T-1 is mounted on a precise weighing scale WS-1 to accurately measure the mass of additives and fillers that are added. A valve V-2 is located at the lower point of tanks T-1 and T-2 to empty them in case of a system failure or for cleaning purposes. Then, when a certain volume of resin has been

prepared and mixed with its fillers and additives, the fluid is transferred to a larger day tank (T-2) via pump P-1. Because flow rate precision and linearity are not required at this step, an air-operated double diaphragm (AODD) pump is used. The AODD pump is relatively inexpensive and can pump highly abrasive fluids. The air inlet for the pump has a filter and regulator to control the pump's output rate. Day tank T-2 features an electrically driven agitator to keep the particles in suspension in the resin. Y-strainers (YS-1 and YS-2) are positioned at the outlet of each tank to collect debris that could be present in the resin to protect downstream equipment. The day tank also features an in-line flame arrestor FA-1 for safety in case the flammable vapours contained in the tank ignite. The tank is level monitored using a clear side tube located between valves V-6 and V-7. Finally, using another air-operated double diaphragm pump, the resin from tank T-2 is pumped through a bag filter BF-1 before entering the metering system. A pressure gauge is positioned right before the metering system to monitor the fluid pressure at the inlet of the system.

4.2.2 Metering system

The purpose of the metering system is to pump both components with the right mixing ratio and flow rate. It features an assembly of plunger pumps that are all driven by the same motor through a single shaft. Plunger pumps were identified as the best technology as they are designed to pump high viscosity and abrasive fluids to high precision. The two first plungers, A-1 and A-2, dose part A of the resin and the next two, B-1 and B-2, dose part B. Each plunger is sized to give the right mixing ratio. To change the output speed of the system, the motor speed is adjusted. The main advantage of this configuration is to mechanically guarantee that the mixing ratio will remain unchanged during production speed changes. Details and working principle of the pump are presented in 4.2.4.1. Part B of the resin enters the system and is filtered using Y-strainer YS-3. The isocyanate is contained in a nitrogen pressurized tank T-3. The nitrogen is contained in a pressurized cylinder C-1 and released in tank T-3 using a pressure regulator PR-1. The nitrogen is used to provide sufficient inlet pressure for the metering system as well as avoid moisture contamination of the isocyanate. Pulsation dampeners PD-A and PD-B are positioned at the outlet of the pumps to attenuate any leftover pulsations that may still be present to get a flow rate that is as linear as possible. The pulsation dampeners are located closest to the pumps' outlet to maximize their efficiency. Immediately after are two overpressure safety mechanisms. The first is a pressure sensor (PS-A and PS-B) that continuously monitors the pressure in the system. The signal is sent

to the PLC and the control logic is set to stop the motor as soon as an overpressure is recorded. As a secondary safety feature, a rupture disk (RD-A and RD-B) is installed and designed to break before the weakest equipment of the system. The latter safety system is used as a last resort and therefore the pressure sensor's overpressure setting is set lower than the disk burst pressure. Next are back pressure regulators (BPR-A and BPR-B) to maintain a minimum upstream pressure. This pressure requirement ensures smooth operation of the pump and will be explained in 4.2.4.1. The metering system ends with two flowmeters (FM-A and FM-B) and outlet valves V-14 and V-18.

4.2.3 Mixing and delivery

The lower left corner of Figure 37 is where both components mix to then get dispensed into the two doctor boxes for SMC prepreg material manufacturing. Both components exit the metering system to make their way to the dispense gun DG-1. This equipment is positioned right before the in-line static mixer SM-1 and is designed to facilitate cleaning by combining both components at the last second using a manifold. The dispense gun opens and shuts using a double acting air actuator. Right before the dispense gun are two check valves (CV-A and CV-B) to prevent backflow of one the components. The two components then enter the static mixer before the mixed output gets split to feed each of the two doctor boxes (DB-1 and DB-2). On the way, two springs loaded normally opened pneumatic actuators (PA-1 and PA-2) allow the automatic control of the flow splitting to both doctor boxes. Each pneumatic actuator is attached to an encapsulated ball valve. The valves are normally opened to prevent overpressure situations if the emergency shut off is activated. Finally, both doctor boxes are equipped with a contactless ultrasonic level sensor (LS-1 and LS-2).

4.2.4 Equipment technology choice

4.2.4.1 Pumps and pulsation dampeners

The main challenge was to integrate a pump technology that allows processing abrasive fluids while being able to operate in Class 1 Division 1 classified location and produce a linear flow rate. Plunger pumps are offered with stainless steel and PTFE wetted part for excellent chemical compatibility. However, they generate significant flow rate pulsations because of their reciprocating action. The working principle of a plunger pump is presented in Figure 38.

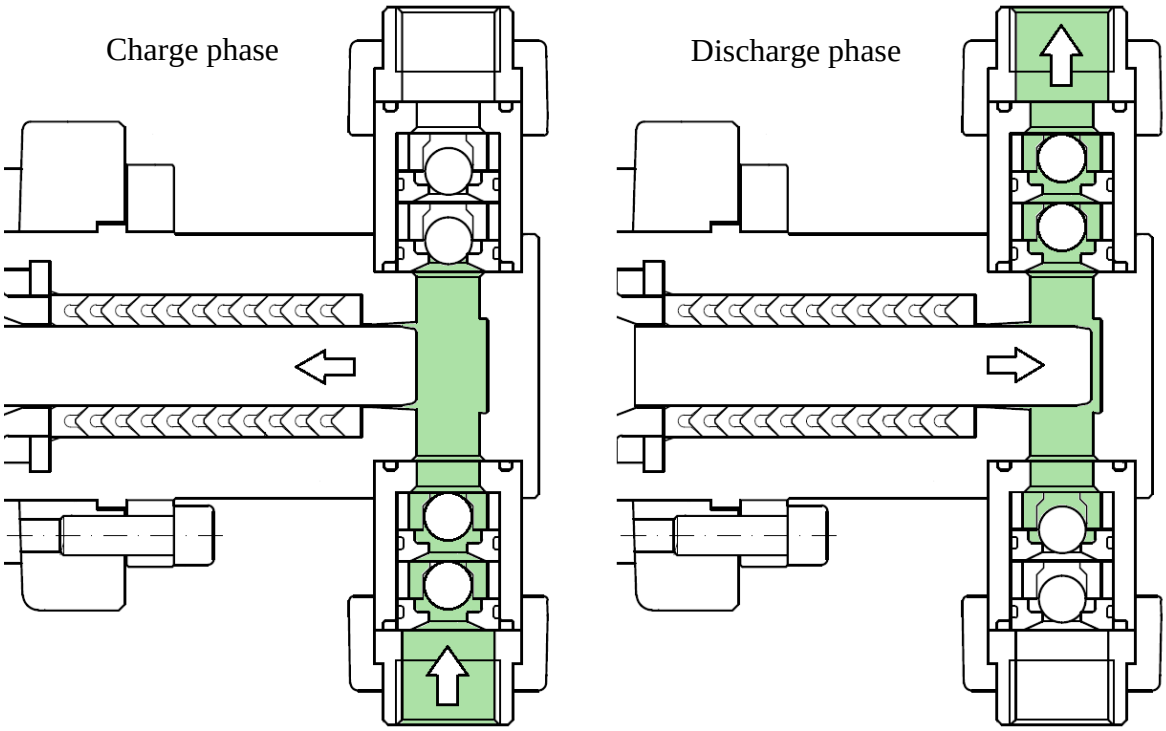

Figure 38 - Working principal of a plunger pump - Image courtesy of TKM LLC

Based on the results from section 3.4.3, where the impact of a pulsed flow rate on mix homogeneity was evaluated using a static mixer, flow rate pulsations must be avoided. Otherwise, the mixing ratio will not be constant and the homogeneity of the product will decrease drastically. Therefore, to limit the amplitude of the flow rate variations, two plunger pumps are used per component, for a total of four plungers. Within a pair, the reciprocating motion is set out of phase by 180°. In theory, while one plunger draws fluid at the inlet, the other one dispenses fluid at the outlet and vice versa. Nevertheless, because the plungers are usually driven by an eccentric shaft, their linear speed describes a sine wave. This means that there will still be a point where the flow rate goes to zero when both plungers change directions. Ideally, more plungers could be used per component to limit the pulse action further but this would rapidly increase the purchasing and maintenance costs as well as increasing the overall size and weight of the pump assembly. As a trade-off, an assembly of two plungers per component can be used with the combination of pulsation dampeners at the outlet. To adjust the mixing ratio, each plunger is equipped with an adjustment screw that controls the plunger's travel length.

Pulsations dampeners are simple devices that use a flexible membrane to attenuate the pressure variations in the fluid. On one side of the membrane is the process fluid and on the other

is a pressurized gas like dry air or nitrogen. When the pump generates a pulse at the outlet, the fluid pressure increases slightly and acts on the membrane, which in turn compressed the gas on the other side. Then, during a fluid pressure trough, the opposite action occurs. The gas pressure pushes the membrane back towards the process fluid. The result is a smoothing of the process fluid's pressure, which, from the incompressibility of the fluid, linearizes the flow rate in the system. Each dampener must be pre-charged with 80% of the operating fluid pressure [91].

4.2.4.2 Flowmeters

The flowmeters use two different technologies for parts A and B. A Coriolis flowmeter is used on the A side while a gear flowmeter is used for the B side. The working principle of both flowmeters is not described in this work. The Coriolis flowmeter features no moving parts and is ideal for fluids containing solid particles. In addition, because of its single bore design, the instrument can easily be cleaned in place with a solvent flush. The gear flowmeter is used for the isocyanate as the fluid contains no particles that risk breaking or clogging the meshing gears. Moreover, gear flowmeters offer enough precision and are a cheaper alternative to the Coriolis technology. Both flowmeters are certified to operate in Class 1 Division 1 classified locations.

4.2.4.3 Pressure sensors

Two sanitary tri-clamp pressure sensors that are Class 1 Division 1 certified are used. The sensor has a flush diaphragm to facilitate cleaning.

4.2.4.4 Valves

Three-piece encapsulated ball valves, as shown in Figure 35, are used throughout the system. Their design makes these valves easy to disassemble and clean. Moreover, when set to the open position, the bore inside the valve has a constant diameter, eliminating tight areas where the resin could accumulate. The wetted parts and valve body are made of 316 stainless steel with PTFE gaskets.

4.2.4.5 Piping

For chemical compatibility purposes, the system features sanitary 316 stainless steel piping with tri-clamp connections and PTFE gaskets. This technology was recommended by the industrial partner and is the industry standard for chemical processing applications. The main advantages are

the constant diameter bore that facilitates cleaning and the ease of assembly of the tri-clamp connections. Because the mating faces are flat, piping and instrumentation can be removed without requiring axial play, contrary to threaded standards like National Pipe Thread (NPT) or Joint Industry Council (JIC). Also, the absence of thread allows the components to be orientated in any direction. Figure 39 shows a sanitary pipe with tri-clamp connection and PTFE gasket. The constant bore diameter at the mating face can be observed.

(a) (b)

Figure 39 - Sanitary tri-clamp piping connection with PTFE gasket: (a) assembled [104] and (b) disassembled [105]

4.3 Detailed design

Pressure loss calculations were performed for equipment sizing. For confidentiality reasons, calculation details are omitted from this document. The calculations were done considering the piping length and system layout during the final installation at the partner's facility. Moreover, component viscosity and flow rate considered the worst-case scenario. Using a parametric excel spreadsheet, pipe size was modified to limit pressure drop but also limit unused resin loses. Pressure drop calculation includes head loss, vertical elevation and fittings like elbows, valves and tees using the resistance coefficient method [106], [107]. In some most complex cases, the pressure drop across certain equipment is provided by the manufacturer. Otherwise, conservative estimates were made. Pressure drop results are presented in Table 19.

Half inch piping was used for the B side and one inch for the A side all the way to the dispensing gun. From there, the mixed resin is carried in half-inch disposable nylon tubing to the doctor boxes. In some occasions, some equipment or instruments were not available in half inch sizes and piping section changes were required. This is the case for the pressure sensors and rupture disks, which were only available down to one inch.

Table 19 - Pressure drop calculations from the outlet of the metering pump to the outlet of the static mixer

	Part A	**Part B**
Viscosity (cP)	5000	195
Flow rate (ml/min)	1907	93
Reynold's number (-)		
Pressure drop (psi)		
Head loss	131	89
Fittings and equipment	78	69
Vertical elevation	4	5
Total pressure drop (psi)	**213**	**163**

To demonstrate the sensibility of the pressure drop calculations, simply choosing half-inch piping for part A from the metering pump's outlet to the entrance of the dispense gun would bring the total pressure drop to 1532 psi. This significant increase is due to the system installation layout at the partner's facility. The resin must travel long piping lengths from the metering system to the mixing and delivery system.

4.3.1 Computer-assisted design (CAD)

The following figures present the 3D CAD of each of the three sections of the P&ID presented in Figure 37. On each figure, component identification of Table 18 is overlaid. Figure 40 first shows the resin preparation area.

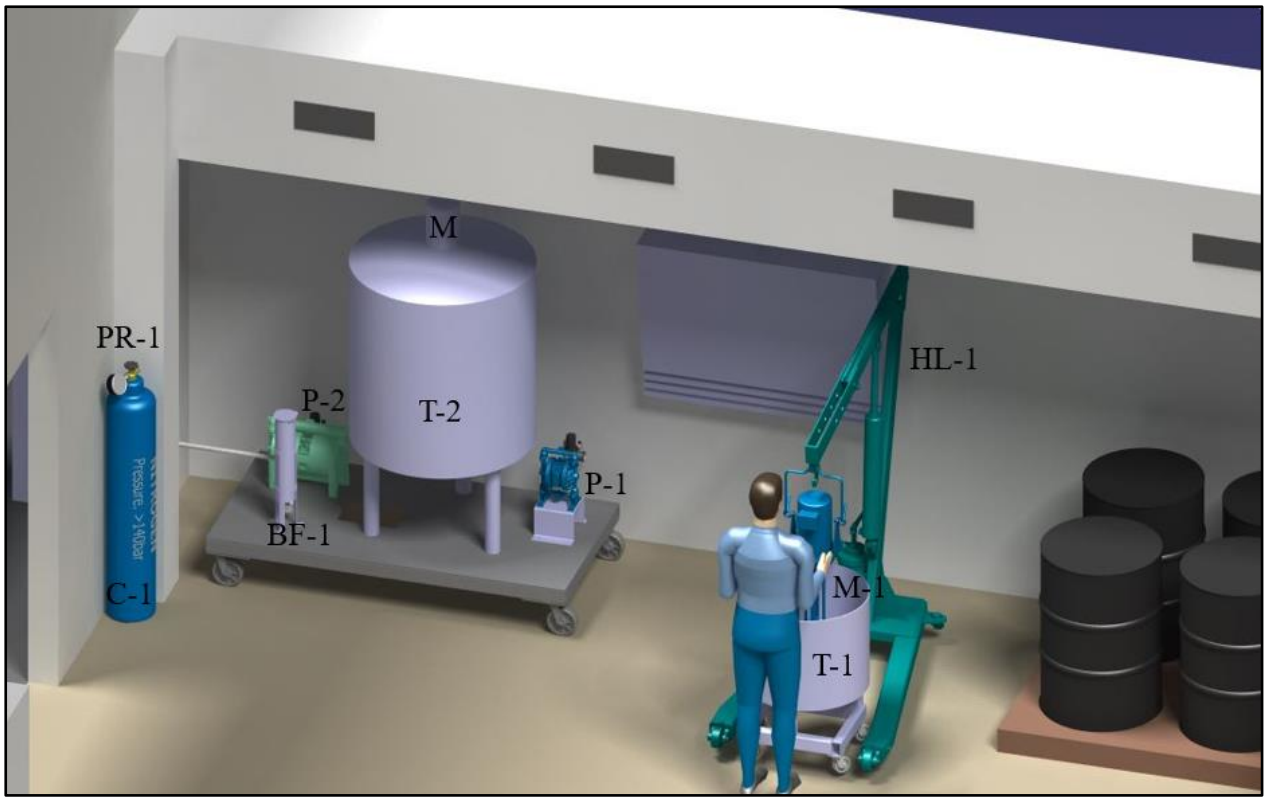

Figure 40 - Resin preparation 3D CAD

Figure 41 shows a 3D model of the metering system. The equipment is mounted on a skid to facilitate relocation of the system if desired.

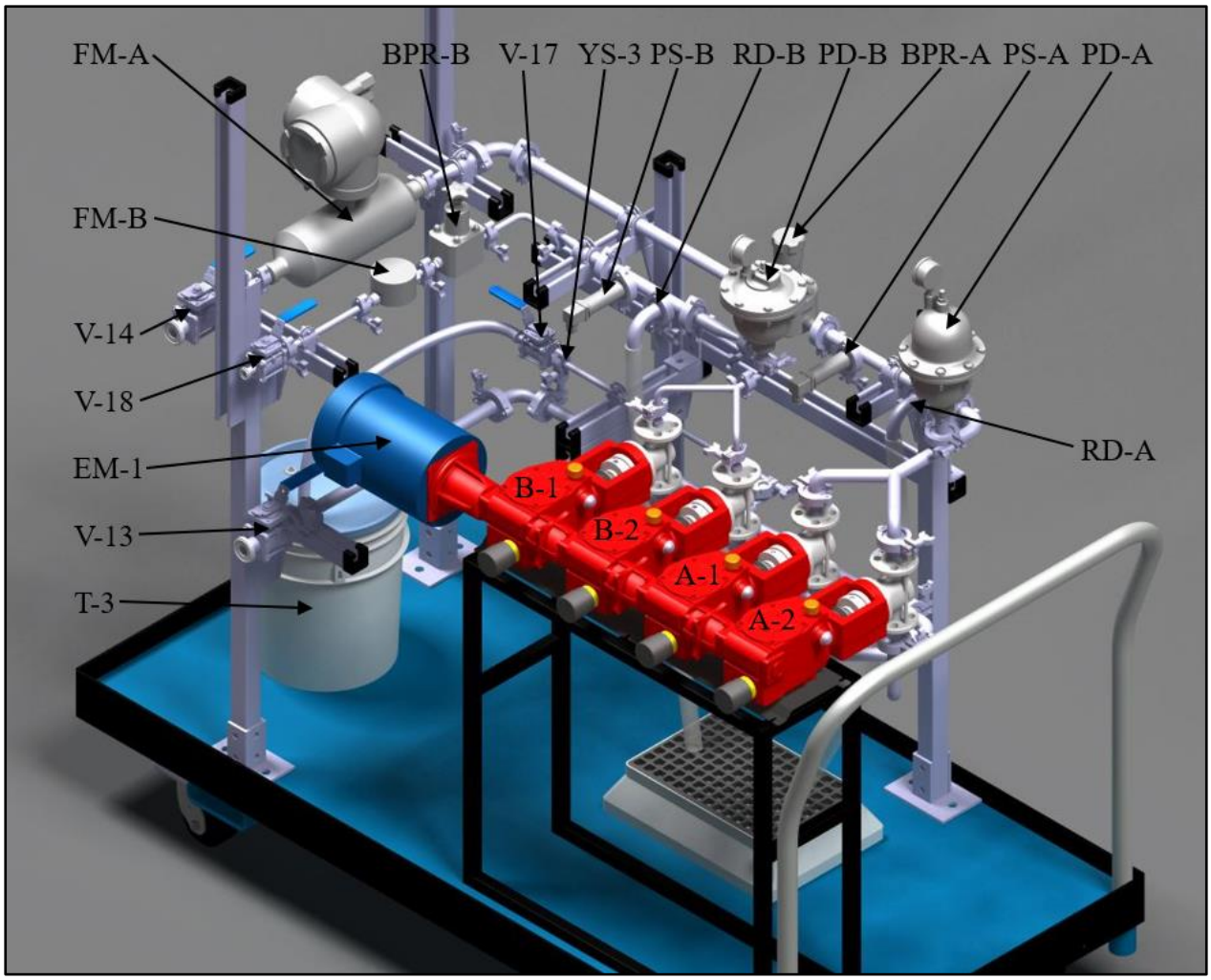

Figure 41 - Metering system 3D CAD

The skid features two-inches high sidewalls with a silicone seal to prevent potential system leaks to spread on the floor. Likewise, a soft clear tubing connects the outlet of the rupture disks to a polypropylene collecting pan. The isocyanate tank is mounted on the skid. The plunger pump multiplex assembly is shown in red in the foreground with the single electric motor in blue. At the discharge side of the pump can be seen, in sequential order and on both fluid sides, the pulsation dampeners, rupture disks, back pressure regulators and flowmeters. The resin enters the system from V-13 and V-17, passes through the pumps from the bottom, before exiting the metering system from valves V-14 and V-18. Then, the resin makes its way to the prepreg line, where the mixing and delivery equipment is located. The mixing is performed as close to the outlet of the system to limit mixed resin in the piping. Figure 42 shows the mixing and delivery section of the system.

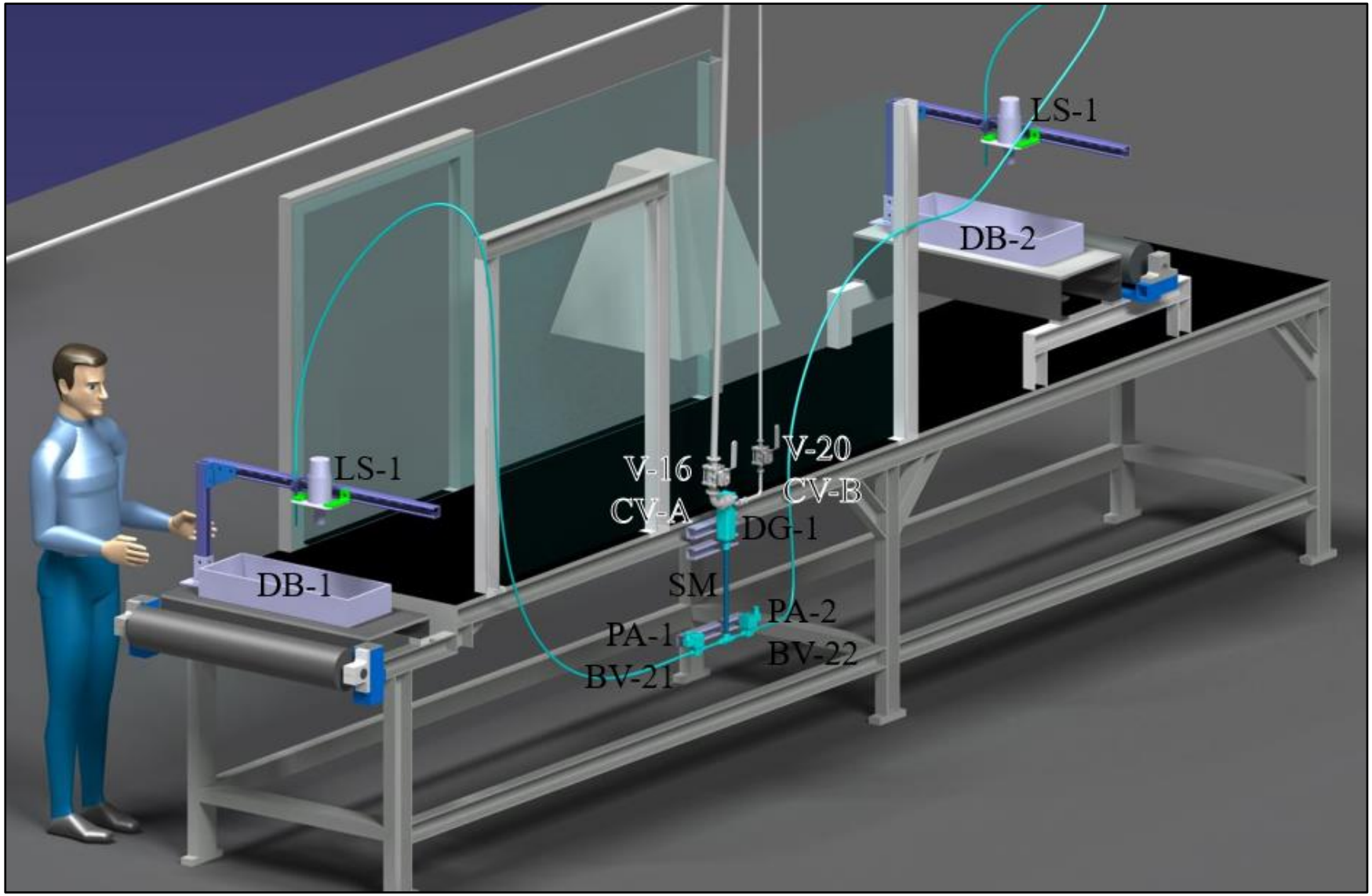

Figure 42 - Mixing and delivery 3D CAD

The resin coming out of the metering system arrives at the mixing and delivery section from the top of the prepreg line. Both resin components then go through the dispense gun and static mixer before the flow is split into two and directed to each doctor box.

The 3D model allowed to validate the positioning of the equipment to avoid interference and ensure all components were easily reachable for maintenance.

4.3.2 Automation and control logic

The system is equipped with various instruments (inputs) and controllable equipment (output) to automate the system. The inputs and outputs are listed in Table 20 below.

Table 20 - Programmable logic controller (PLC) inputs and outputs list

	Instrument/equipment
Inputs	Pressure sensors (PS-A and PS-B)
	Flowmeters (FM-A and FM-B)
	Level sensors (LS-1 and LS-2)
Outputs	Metering pump motor (EM-1)
	Dispense gun (DG-1)
	Air-actuated ball valve (PA-1 and PA-2)

The system has three distinct operating modes: normal, calibration and manual. In all cases, some manual operations are required prior to starting the system. Such manipulations include opening manual ball valves at the inlet and outlet of the skid, filling the day tanks T-2 and T-3, starting the metering system's feeding pump P-2 and pressurizing tank T-3 with nitrogen.

For all operating modes, some control logic is always applied. First, the overpressure safety control logic is always running when the pump is turned on. If the pressure sensors record an overpressure, the metering pump motor will stop and the dispense gun and ball valves to both doctor boxes will remain open. Second, the PLC is programmed to prevent the motor to operate if there is not at least one outlet path opened. More specifically, at least one of the valves BV-21 and BV-22 and the dispense must be opened. If the PLC does not register an outlet path of the resin, the metering pump cannot be started.

4.3.2.1 Normal mode

The normal mode consists of three chronological sequences; startup, normal and shut down. Normal mode allows the system to operate on its own and is started and stopped with one action on the HMI. During the startup sequence, doctor box one is filled up to a certain level before a proportional-integral (PI) control feedback loop activates using the reading from the contactless ultrasonic level sensor. This allows the pump speed to self adjust and keep the resin level in the doctor box to the desired height. At that point, the prepreg line's lower resin film starts. Doctor box one is filled first to have the upper and lower resin fronts meet at the end of the line. After a certain delay, the chopped carbon fibre is dropped on the lower resin film before doctor box two starts filling. In normal mode, the pump speed and the status of valves BV-21 and BV-22 are adjusted automatically to keep the resin level in each doctor box at the setpoint or going over the upper and lower limits. In addition, flowmeters independently measure the flow rate of each component to validate the accuracy of the pumps and the mixing ratio. The shutdown sequence uses the opposite control logic to the startup sequence.

The doctor box level control logic is a combination of two algorithms. The first algorithm involves the resin level in each doctor box separately. To do so, upper and lower limits are set at 3,1 and 2,9 inches respectively. These limits represent the acceptable tolerance for the resin level. At every code execution, the resin content recorded by the level sensor is compared to the lower and upper limits. If the resin is below the lower limit, the valve associated to the other doctor box is shut if its resin level is not also below the lower limit. As a result, this action directs all the flow to the first doctor box for its level to go over the lower limit. Likewise, if the resin level in a doctor box goes over the upper limit, its associated valve is shut to prevent it from filling more only if the other doctor box is not also over the upper limit. At any time, both valves cannot be shut otherwise no flow path would be available for the system.

The second algorithm is used to control the system's total flow rate through the pump's speed and is comprised of three scenarios. In each scenario, a PID control feedback loop is used to adjust the pump's speed to modify the resin level error from the three inches set point. In the first case, both valves to either doctor box are opened. The PID is used on the average error from both doctor boxes combined. For example, if doctor boxes one and two are at 3,05 and 2,95 inches respectively, their average error is zero and the PID is not active. However, if the levels are 3,1 and

3,05 inches, the average error from the setpoint is 0,075 inches and the PID is activated to reduce the motor speed in order to bring the average error to zero. The same logic applies if the average height of both doctor boxes falls below the setpoint. For the complete block diagram of the doctor box level control logic, please refer to Appendix B.

4.3.2.2 Calibration mode

The calibration mode is used to adjust the system's mixing ratio. When the system is started in calibration mode, the mixing ratio is shown on the human-machine interface (HMI) and instructions are given for the operator to adjust the pump's plunger travel length to get the exact flow rate for each component.

4.3.2.3 Manual mode

Manual mode is used to manually operate every output of the control panel. From there, the pump speed can be adjusted and the system can be started for an indefinite duration or until a set volume has been dispensed.

4.3.3 HMI

Figure 43 below shows the six (6) HMI screens. The interface was made by David Murray and Marie-Christine Caya from CTA following guidelines on the desired features and layout provided.

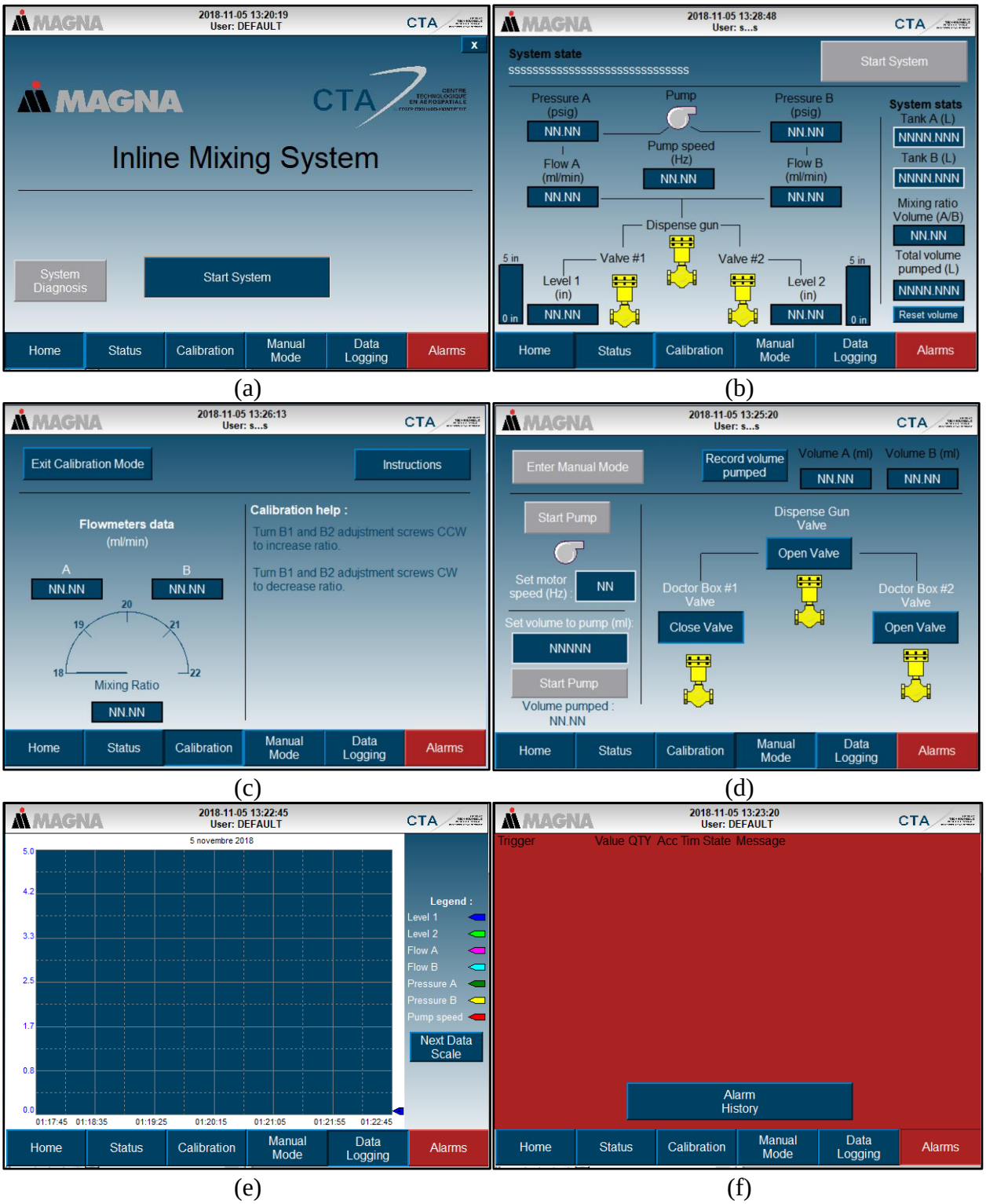

Figure 43 - HMI Screens: (a) Home, (b) Status, (c) Calibration, (d) Manual Mode, (e) Data Logging and (f) Alarms

4.3.3.1 System alarms and warnings

Table 21 lists the system alarms and warnings of the system's PLC.

Table 21 - System alarms and warnings

	Cause	Action
Alarms	Overpressure recorded	Pump stopped
	Doctor box overflow	Pump stopped
	Mixing ratio out of limit	Pump stopped
Warnings	Doctor box low resin level	Pump speed increased
	Mixing ratio slightly out of limit	Warning message for mixing ratio adjustment
	Low tank resin level	Warning message for tank refilling

4.3.4 System technical and performance data

Similarly, to Table 9, which summarizes the technical and performance data of commercially available metering and mixing systems, Table 22 below does the same with the system developed in this project.

Table 22 - Developed system theoretical technical and performance data

	System capabilities
Viscosity (cP)	30 to 9000[1]
Pressure (psig)	up to 300[2]
Volumetric mixing ratio	0,8:1[3] to 320:1[4]
Flow rate (ml/min)	50 to 2500[5]
Abrasive fluids capability	Yes
Mixing technology	Static
Pump technology	Multiplex Plunger
Wetted parts material	Stainless Steel, PTFE
Class 1 Div. 1 certification	Yes

[1]The minimum viscosity is dictated by the gear flowmeter, which is not precise at viscosities below 30 cP; [2]The minimum pressure required has not been validated; [3]At 125 ml/min maximum; [4]At 2227 ml/min maximum; [5]At a volumetric mixing ratio of 20,5:1

It is important to note that the listed performance data of the system can be achieved in its current configuration. Like with commercially available systems, modifying the equipment size would allow the system to meet a new set of performance specifications in terms of pressure rating, mixing ratio and flow rate.

4.4 Manufacturing

Assembly of the system began with the metering skid. During this time, the control panel was subcontracted to Automation Machine Design, an engineering firm located in Saint-Hubert, Canada. Then, the resin mixing and delivery section of the system was manufactured.

4.4.1 Metering system

Figure 44 shows the assembly of the metering system. All equipment and instruments were ordered and delivered to CTA and the complete system was assembled in-house. Piping support and pump frame were manufactured at CTA. The skid was purchased from an industrial equipment supplier and was then modified to accommodate this project's requirements. Sturdier chemically compatible wheels, spill prevention sidewalls, pump, piping and instrumentation support frame and forklift channels were installed by the team at CTA.

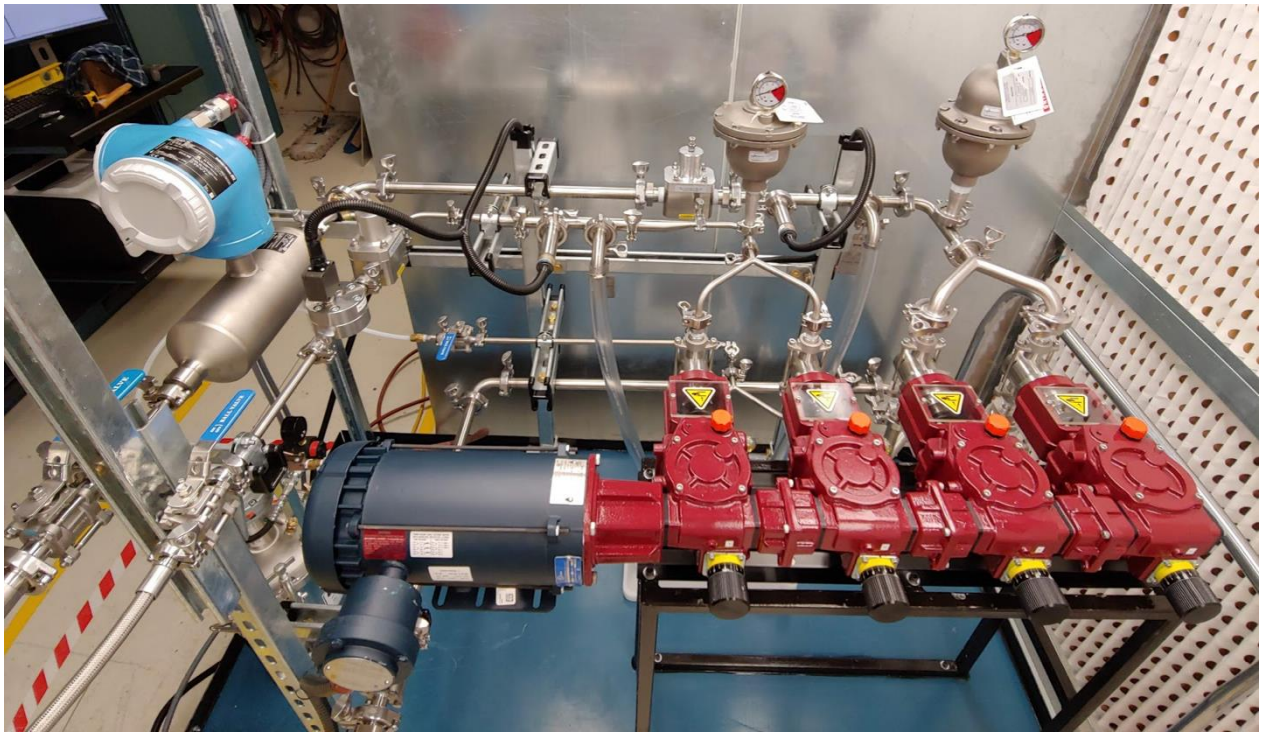

Figure 44 – Metering system assembly

4.4.2 Mixing and delivery system

The mixing and delivery system assembly is presented in Figure 45. Because the system was tested at CTA's facility, the mixing and delivery system could not be installed on the prepreg line for the testing phase. Instead, a temporary testing apparatus was built and acted as a mock-up of the final system installation layout seen in Figure 42 to allow the system to be tested normally. Temporary buckets were used as doctor boxes and ball valves were fitted at the bottom of each bucket to simulate resin usage from the prepreg line.

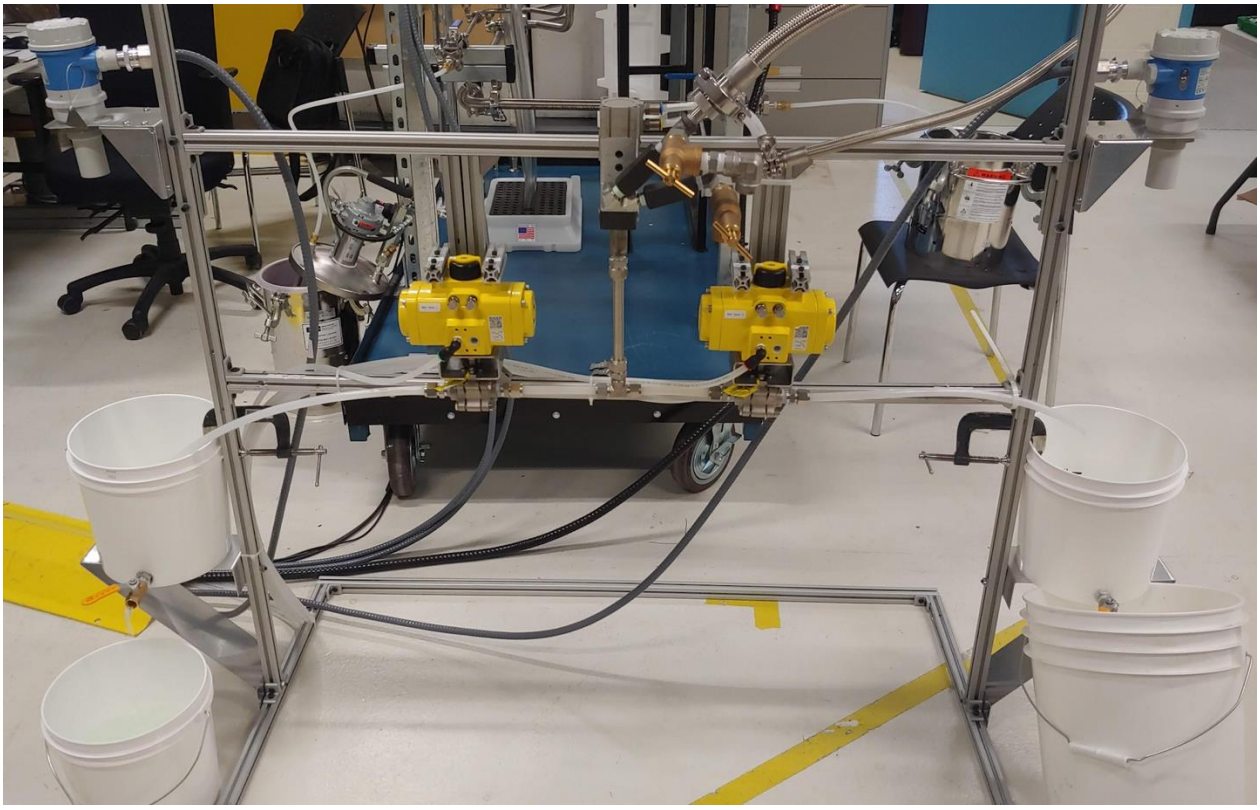

Figure 45 - Mixing and delivery system mock-up

4.4.3 Control panel

The control panel manufactured by the subcontractor is shown in Figure 46 below. The HMI and PLC programs were developed in-house by David Murray and Marie-Christine Caya.

Figure 46 – Control panel

The control panel features a touchscreen HMI, an emergency shut-off switch, a rearming button, a stack light and buzzer. The pneumatic equipment, mounted on the side of the control panel, was installed in-house. An air filter-regulator-lubricator and shut off valve is mounted on the left of the panel. The right side contains the pneumatic actuators. There are two single pneumatic actuators for the two ball valves that direct the flow to either doctor box and a double pneumatic actuator for the dispense gun. Stack light colour code definitions are presented is presented in Table 23.

Table 23 - Stack light colour code definition

	Steady	Flashing
Green	System is in normal operation	System is in manual or calibration mode
Amber	System in transition (start sequence or stop sequence)	Action needed (low resin level or mixing ratio out of range)
Red	System is stopped	System alarm (E-stop or overpressure)

CHAPTER 5 VALIDATION OF THE SYSTEM'S PERFORMANCE

This chapter validates the new system's performance and evaluates the flowmeters' precision, control logic, flow rate linearity, cleaning and mix homogeneity.

5.1 Flowmeter precision validation

Testing started with the validation of the flowmeters' precision as they allow to calibrate the system's mixing ratio, a crucial and strict requirement. To do so, the resin components were individually dispensed in a cup while the flowmeters measure the flow over time. The weight of the dispensed resin was compared to the instrument's flow result. Coriolis (Part A) data is compared with the manufacturer's theoretical precision in Figure 47. Figure 48 presents the same results for the gear flowmeter (Part B). The validation experiment was performed at three output speeds throughout the machine's operating range; 388 ml/min (10 Hz), 1514 ml/min (39 Hz or nominal) and 2329 ml/min (60 Hz) total for parts A and B combined at a volumetric mixing ratio of 20,5:1. At each speed, a minimum of three samples was collected.

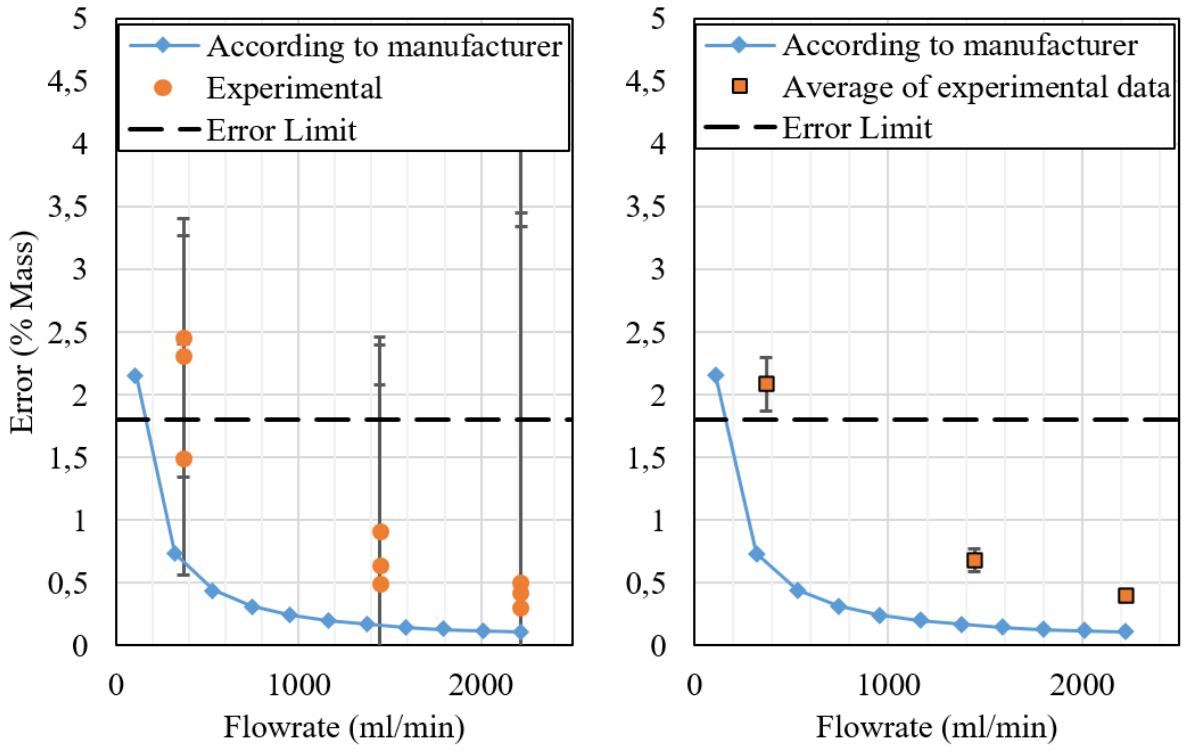

Figure 47 - Coriolis flowmeter precision validation: (a) Experimental data with error bars for the individual measurements and (b) Average of experimental data with error bars representing the standard deviation for each flowrate

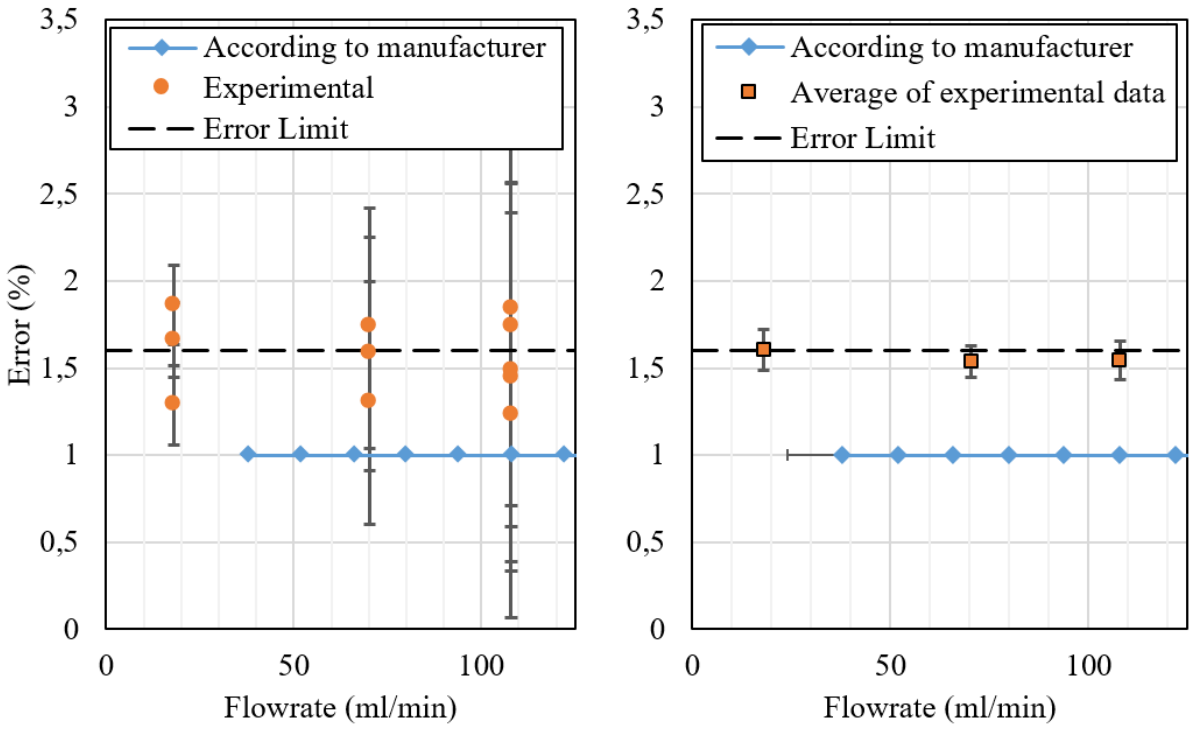

Figure 48 - Gear flowmeter precision validation: (a) Experimental data with error bars for the individual measurements and (b) Average of experimental data with error bars representing the standard deviation for each flowrate

The Coriolis flowmeter records mass flow rate that is then converted into a volumetric flow rate using the resin density supplied by the industrial partner. The uncertainty on the density value was unknown but was considered negligible for this analysis. The error bars for the experimental data include the uncertainty on the flow rate recorded by the flowmeter on the PLC as well as human reaction time to start and stop the recording. On the other hand, the uncertainty on the experimental data comes from the precision of the scale used to weigh the resin samples. The human reaction time was considered to be 200 milliseconds at both the start and the stop of the recording on the PLC. The uncertainty caused by the weighing scale precision is constant at ± 0,01 g. However, at higher flow rates, the error caused by the human reaction time increases rapidly. Therefore, the error bars for the individual measurements are wider at higher flow rates. The error bars could be reduced by collecting samples for longer times. However, limited resin and isocyanate supplies were available at the time of testing. As expected, for both part A and part B,

the experimental precision of the flowmeter is lower than the one stated by the manufacturer for these process conditions. Sources of errors like PLC sample rate or flow rate pulsations might be the cause of this discrepancy. Nevertheless, the Coriolis flowmeter's precision presented in Figure 47 is adequate for this project as it falls below the 1,8 % requirement at the nominal flow rate of 1440 ml/min. For the gear flowmeter in Figure 48, the error is not below the 1,6 % requirement. Yet, the highest recorded error during testing was 1,86 % which is not far from the desired error limit. This project's part B operating range of 28 to 93 ml/min is not entirely covered and falls in the lower range of the flowmeter's state operating range of 37 to 3785 ml/min. This may be the cause of the higher error. Ideally, a flowmeter with a lower operating range would likely allow the precision to be increased.

Even though the flowmeters' precision does not always fall within the set limits over the system's total operating range, the mixing ratio is still guaranteed to be constant. This is where the innovative multiplex pump assembly shows its advantage over commercially available systems where each pump speed is individually controlled and adjusted using a feedback loop form the flowmeters. With the newly developed system, the flow rate ratio of A and B is mechanically guaranteed by the positive displacement pumps. The only time the flowmeter's precision is taken into account is when the pump's plungers are adjusted to get the desired mixing ratio.

5.2 Control logic

5.2.1 Overpressure safety

The overpressure setting on the PLC for the pressure sensors is used as the primary safety device. To validate its correct operation, the overpressure value was set to 100 psig in the PLC. The pump motor speed was set to 10 Hz and plungers travel were set to 10 % and 0 % on the A and B sides respectively to increase the pressure as slowly as possible. The system was started until steady state was achieved. Then, the outlet ball valve on the A side was shut to increase the pressure in the system beyond the overpressure setting. The pressure sensor recorded the overpressure as intended and the pump stopped immediately.

The pump is not equipped with any kind of emergency braking system. This means that there is a delay between when the stop signal is sent and when the pump comes to a stop. This delay is due to the pump's inertia and will cause the pressure to keep increasing even after an

overpressure is recorded. To prevent damages to the system, the pressure increase caused by the pump's inertia was quantified. This time, all plunger pumps were set to 100% and the pump speed was set to 60 Hz to maximize the system's output flow rate. The system's output valves were abruptly shut allowing the overpressure to be recorded at 100 psig by the sensors to shut the pump's motor. The inertia increased the pressure to 115 psig before the pumps came to a complete stop. Therefore, as the rupture disks are manufactured to break at 300 psig, a large safety factor of 50 psig was set on the overpressure setting to protect the disks from breaking in the event of an emergency stop.

5.2.2 Doctor box level control

The next test performed aimed to validate the doctor box control logic presented in section 4.3.2.1 and Appendix B. To do so, water was used as not to waste too much resin in the validation phase. The lowest viscosity that the system can process while maintaining its performance and precision has not been tested. However, the low viscosity of water was not a limiting factor in this test because the goal was only to validate the doctor box control logic. The system was started in normal mode with the outlet split into both doctor boxes mock-ups, as shown in Figure 45. The goals were to validate the control logic and set the PID control feedback loop coefficients. The initial PID coefficients were estimated and adjusted through educated guesses. After four iterations, the parameters were set to P = 8, I = 0,9 and D = 0. The required sensibility and precision of the doctor box control logic are low, and simple trial and error sufficed to obtain a working system. The level sensors' output was recorded over time and results are presented in Figure 49 below for both doctor boxes.

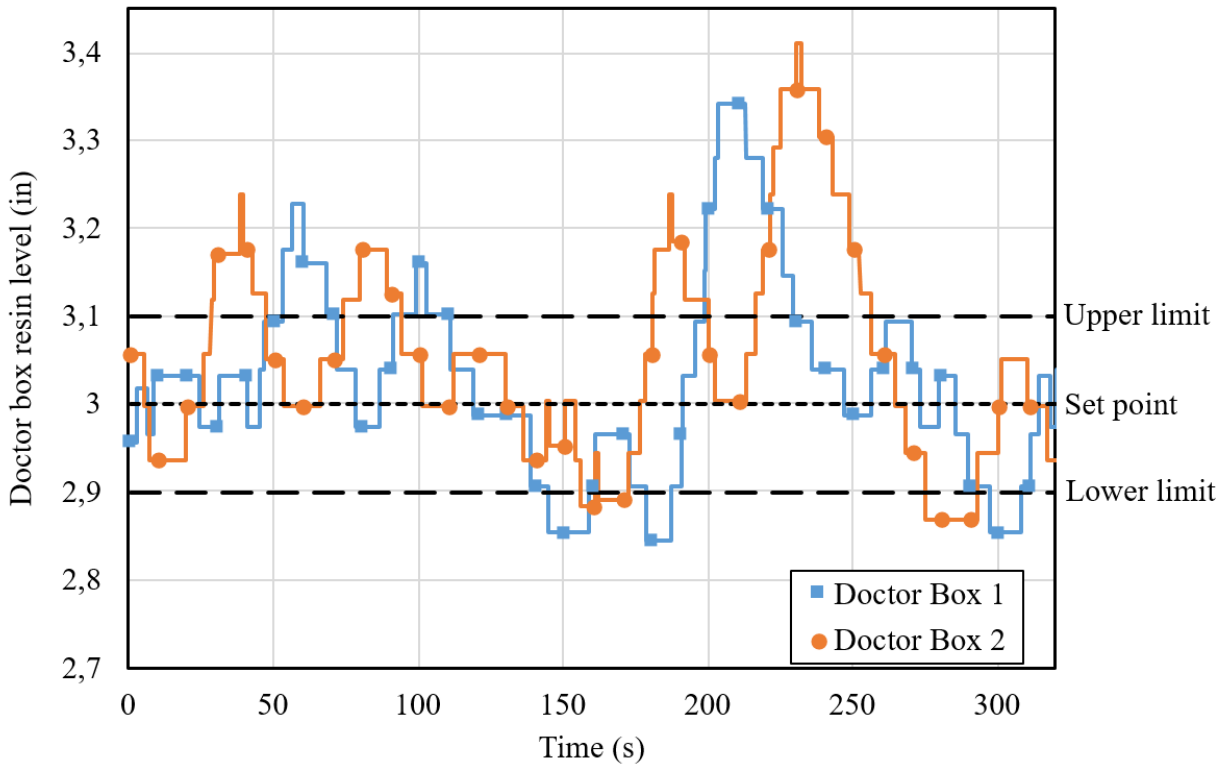

Figure 49 - Validation of doctor boxes level control logic

The level sensors' stated resolution is 0,04 in and the measuring error is ± 0,2% of its 5 meters range (which converts to an error of 0,4 in). The resolution causes the step look of the registered data presented in Figure 49. The varying step heights are caused by the smoothing of the data. Noise was present in the signal caused by minor signal amperage variations at the PLC. Luckily, the noise was of relatively low amplitude which made it easy to remove using an IF statement on the raw data in Excel. All data variations of less than 0,04 inches, the instrument's resolution, were removed by calculating the variation between data *n* and *n+1* for all *n*. Because the noise threshold was smaller than the resolution of the instrument, the data was not significantly altered by the smoothing process. Overall, the level variations of both doctor boxes seem to behave opposite to one another. This is caused by the first part of the control logic which acts on the overflow and underflow of each doctor box individually. Then, the general trend of both levels is the result of the second part of the control logic, which acts on the error from the set point of each doctor boxes depending on the status of BV-21 and BV-22. The resin level of both doctor boxes go beyond the upper and lower limits because of the system's inertia. If a valve is shut, leftover fluid in the piping at the outlet will continue dripping in the doctor box.

The control logic needs to be responsive enough to prevent underflow or overflow in each doctor box, but forgiving enough as to not continuously send on/off signals to the pump's motor and ball valve actuators. With the presented parameters and control logic, the resin level only varies by half an inch in each doctor box over time without being too sensitive either. This variation is considered negligible for the application. Obviously, the control algorithm could be improved with additional iterations, but no further modifications were included as it met the project's requirements.

5.3 Flow rate linearity

As covered in section 3.4.3, mixing ratio variations at the inlet of the static mixer will influence the homogeneity of the resin. The system's pumping technology and layout were chosen for its capability to pump high viscosity abrasive fluids while limiting flow rate pulsations. Nevertheless, plunger pumps do not generate a perfectly linear flow rate. The next test aimed at quantifying the flow rate variations produced by the system. The pump speed was set to 60 Hz with all plungers to 100 %. Based on the motor speed and gear ratio of the pump, the theoretical pulse frequency per side was calculated to be 152 strokes per minute (or 2,53 pulses per second). The system's back pressure regulators were set to approximately 100 psig and the flow rate and pressure were recorded by the PLC. Flow rate data with and without dampener for the A side is presented in Figure 50. To test the system without the dampener, a cap was used to block the connection where the equipment was installed.

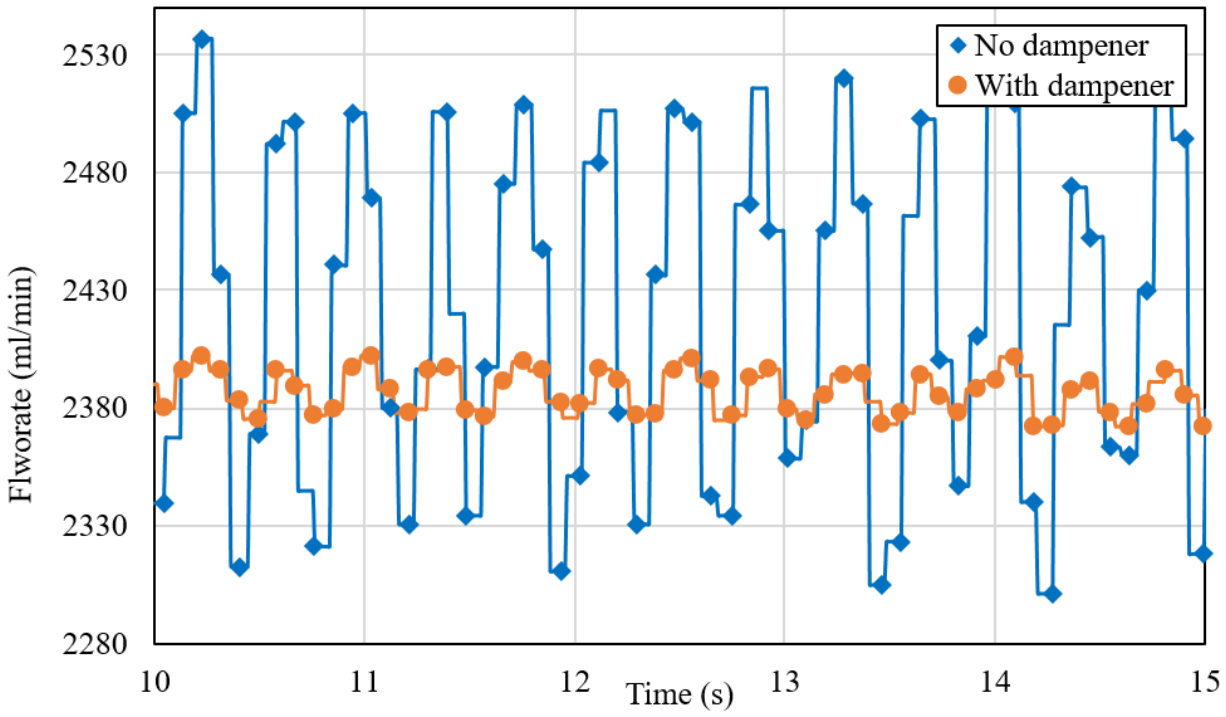

Figure 50 - Flow rate dampening of part A of the metering system at 100 psig

The theoretical pulse frequency matches the recorded flow rate variations shown in Figure 50. Data analysis is summarized in Table 24 for both parts A and B. The minimum and maximum flow rate for parts A and B with and without dampeners are presented. The variation for each case is calculated using,

$$Variation = \frac{Q_{max} - Q_{min}}{Q_{avg}} * 100 \quad (6)$$

where Q_{max}, Q_{min} anf Q_{avg} are respectively the maximum, minimum and average flowrate recorded. The damping efficiency is the reduction in variation from the recorded flowrate without and with the dampener installed. It is calculated using.

$$\eta_{damping} = \left(1 - \frac{Variation_{without\ dampener}}{Variation_{with\ dampener}}\right) * 100 \quad (7)$$

where $\eta_{damping}$ is the damping efficiency.

Table 24 - Flow rate linearity and dampening efficiency at 100 psig

		Flow rate (ml/min)			
		Minimum	**Maximum**	**Variation**	**Damping efficiency**
Part A	Without dampener	2285	2558	± 5,6 %	81 %
	With dampener	2361	2413	**± 1,1 %**	
Part B	Without dampener	110	130	± 8,7 %	90 %
	With dampener	116	118	**± 0,9 %**	

The addition of the pulsation dampeners has a significant impact on the flow rate linearity allowing the variations to be reduced by 81 % and 90 % for the A and B sides respectively. This allows the system to have an average flow rate variation of ± 1 %.

To evaluate the system's variability in terms of mixing ratio, which is the most critical process variable, the system's mixing ratio calculated from the flowmeters at nominal flow rate is presented in Figure 51. To get a volumetric mixing ratio of 20,5:1, the A and B plungers were set to 100% and 78% respectively. This project's nominal flow rate of 1511 ml/min is achieved at a pump speed of 39 Hz.

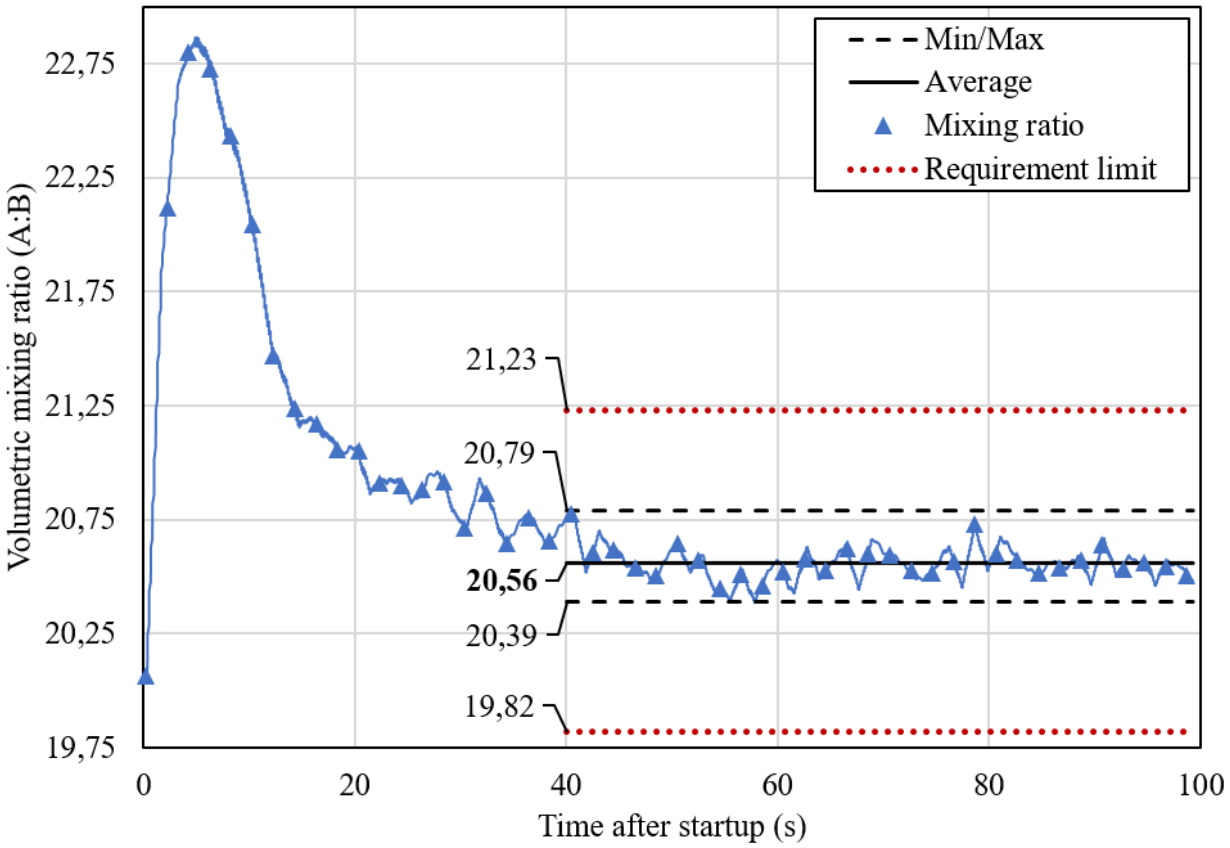

Figure 51 - Mixing ratio evolution after system start-up at nominal speed (39 Hz)

Figure 51 shows the time delay before the system reached steady state. As a conservative estimate, it was determined that steady-state conditions were achieved 40 seconds after start-up by looking at the data collected. The flow rate of part B is calculated using a moving average over several readings because of the type of flowmeter used. This probably partly explains the peak from $t = 0\ s$ to $t = 5\ s$ as the flowrate recorded for part B takes time to stabilize. During this time, the mixing ratio increases rapidly until the fluid pressure ratio stabilizes. When the system is started, the fluid pressure for each side is lower but does not increase at the same rate due to the vastly different flow rates. Luckily, because positive displacement pumps are used, the pressure of both fluids increases until their ratio reaches equilibrium. After the mixing ratio reaches a maximum, it takes some time for the mixing ratio calculation to reach equilibrium because of the moving average on part B flow rate. In reality, the positive displacement pump mechanically guarantees the accuracy of the mixing ratio. Nevertheless, after 40 seconds, the volumetric mixing ratio varies between 20,39 and 20,79 with an average of 20,56. This corresponds to a mixing ratio

precision of ± 1 %. The experimental mixing ratio is very close to the targeted 20,51. Likewise, the system's mixing ratio variations meet the requirements of 19,82 minimum and 21,23 maximum.

5.4 Cleaning

To write the cleaning procedure for the system, in-line solvent flushes were performed to evaluate the system's ease of cleaning and identify potentially harder to clean areas. The system was configured in a closed loop circuit and acetone was pumped through for five minutes per flush. After each flush, an acetone sample was collected to observe the colour and presence of resin or isocyanate. In addition, clean and dry air was blown in the system for 10 minutes in between each flush to dry the system. Three consecutive flushes were performed and the acetone samples are shown in Figure 52.

Figure 52 - Part B (top) and Part A (bottom) acetone samples colour evolution following three clean-in-place flush procedures

Based on the colour of the sample, performing three in-line acetone flushes for 5 minutes with a 10 minutes drying was sufficient to get most of the process fluids out of the system. Evidently, some process fluid is still present after the third flush, as was confirmed via FTIR analysis on the acetone sample. However, the goal of this clean-in-place flushing procedure is to get most of the resin out of the system for short leave occasions. The resin is stable enough to be left in the system for over a week if unused. Long leave occurrences of over a week would require the system to be cleaned-in-place first before manually cleaning target equipment. This equipment was chosen based on the ability of the acetone to reach every small corner for thorough cleaning.

Because of their complex geometry and orientation and position in the system, the pulsation dampeners and three-piece encapsulated ball valves were identified as the equipment that would present the most risk of containing leftover process fluid following a solvent flush. Pumps, back pressure regulators, flowmeters, rupture disks and pressure sensors all show adequate cleaning following the three clean-in-place acetone flushes.

5.5 Mix homogeneity

The last test performed on the system is the most critical and concerns the validation of its performance in terms of mix homogeneity. This time, the completed metering and mixing system was used to produce the samples and a new type of static mixer was used: a disposable polypropylene SMX mixer with a 2, 3, 6 configurations in a stainless-steel housing, as shown in Figure 53. A total of 12 mixing elements with a diameter of 12 mm were used following the manufacturer's recommendation to obtain a CoV of less than 2 %.

Figure 53 - SMX mixer used in the final system

This mixer geometry differs from the Kenics type static mixer used in Chapter 3. The SMX mixer provides the best performance of any static mixer geometry to the extent of significant pressure losses. However, as the new metering and mixing system is capable of handling relatively high pressure drops, it has been put forward as the ideal mixing technology.

To produce the mixed samples, the system was started in manual mode. A lack of resin and isocyanate did not allow the system’s performance to be validated throughout its operating range. Instead, the samples’ homogeneity was validated at a nominal flow rate and pressure. Samples were taken over time from system start-up to 60 seconds. A total of eight 60 ml samples were collected in 120 ml glass jars and five FTIR readings were performed on each sample using the

same test procedure, technique and analysis as used in section 3.3.1. The coefficient of variation result for each sample is presented in Table 25.

Table 25 - Coefficient of variation of samples mixed with the system

Sample #	Time after system start-up (s)	CoV (%)
1	5	4,25
2	15	1,84
3	30	4,66
4	60	1,23
5	5	3,97
6	15	4,92
7	30	4,97
8	60	1,85

As described earlier, the mixing ratio variations immediately after system start-up are due to an unstable pressure ratio between parts A and B. The correlation between the isocyanate level in each sample and the sample collection time after system start-up could not be observed. However, there seems to be a correlation between the coefficient of variation of each sample and mixing ratio variation curve presented in Figure 51. Except for sample #2, all sample show lower homogeneity when the slope of the mixing ratio curve is high. There is also the possibility that sample #2 was collected at the apex of the mixing ratio peak. This suggests that the rapidly changing mixing ratio in the first seconds after the system is started results in samples with high variability in terms of isocyanate concentration. In any case, the samples' coefficient of variation of isocyanate concentration is below the 5 % requirement. Furthermore, the system's coefficient of variation in steady state is 1,23 % and 1,85 % (average of 1,54 %) for samples 4 and 8 that were taken 60 seconds after system start-up. These figures are considered as the system's performance in terms of mixing homogeneity.

5.6 System performance summary

Table 26 summarizes the system's performance and capabilities and compares them to the partner's requirements covered in section 4.1.

Table 26 - System's performance, capabilities and features

	System	Partner's requirements
Performance		
Viscosity (cP)	30[1] to 9000	1050 to 5000
Pressure (psig)	up to 300	N/A
Volumetric mixing ratio (A:B)	0,8:1[2] to 320:1[3]	5:1 to 30:1
Flow rate (ml/min)[4]	390 to 2500	600 to 2000
Mixing homogeneity (CoV)[5]	1,5 %	5,0 %
Mixing ratio variation[5]	± 1,0 %	± 3,5 %
Capability and features		
Abrasive fluids capability	Yes	Yes
Mixing technology	Static	Static or dynamic
Pump technology	Multiplex Plunger	N/A
Wetted parts material	Stainless Steel, PTFE	N/A
Class 1 Div. 1 certification	Yes	Yes

[1] Limited by the geared flow meter which does not work with viscosities of less than 30 cP, [2]At 125 ml/min maximum, [3]At 2227 ml/min maximum, [4]At a volumetric mixing ratio of 20,5:1, [5] At nominal output

The developed system meets all requirements. Most significantly, the new machine is versatile by covering a wide range of mixing ratios and flow rates. In addition, it offers very precise dosing with a mixing ratio variation of only ± 1 % and highly homogeneous output with a coefficient of variation of 1,5 %. The system uses stainless steel and PTFE wetted parts throughout to offer excellent chemical compatibility. Finally, the system's electrical equipment and connections are certified to operate in Class 1 Division 1 hazardous locations.

The clean-in-place solvent flush procedure allows the system to be cleaned rapidly. In addition, its mixing performance relies on a simple and inexpensive static mixer that can be cleaned or disposed of in a timely fashion. Even with its advantages over commercially available systems, the new machine offers interesting flow rate capabilities compared to the competition. Moreover, although not validated, the new system can work with fluids of up to 9000 cP and up to 300 psig.

5.7 Commissioning

After the validation of system's performance tests performed at CTA's composites laboratory, the system was installed at the partner's facility. Training of personnel was performed and a maintenance manual with spare parts list was included. Figure 54 shows the system's resin output to doctor box one at the partner's facility.

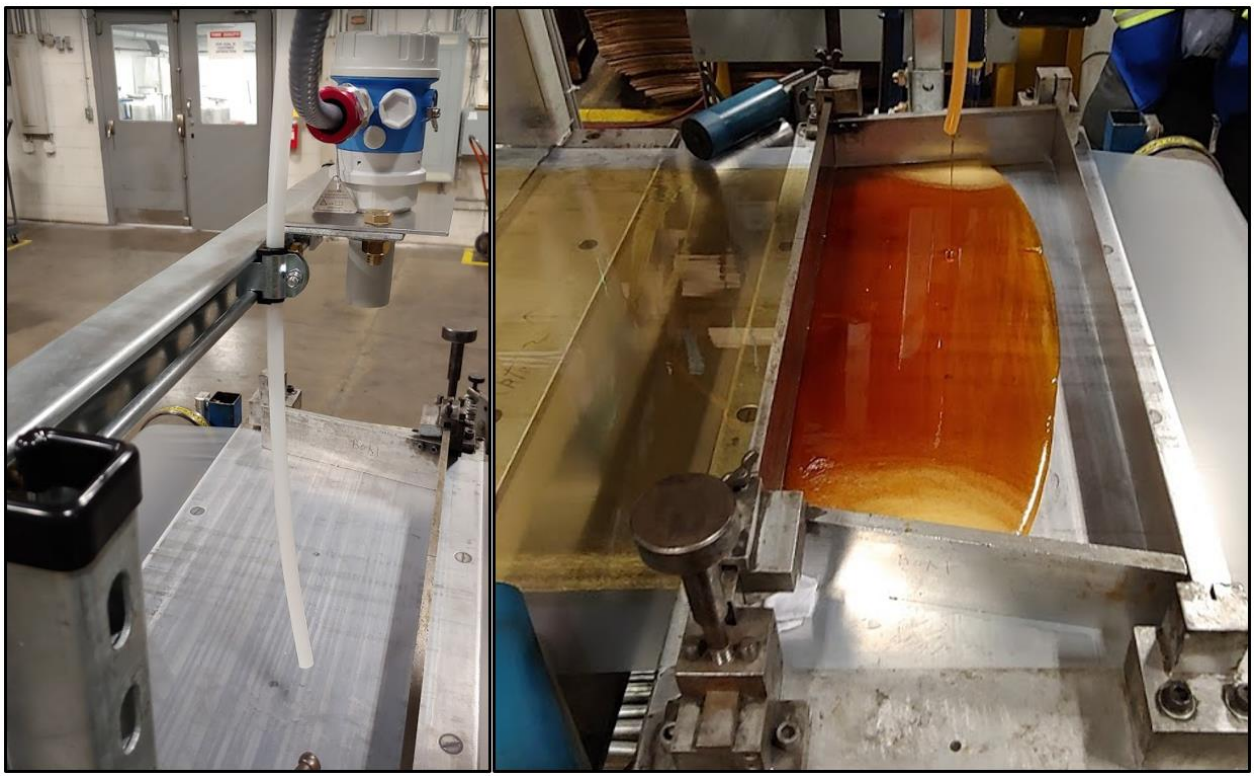

(a) (b)

Figure 54 – System resin outlet to doctor box one at the partner's facility: (a) Level sensor and system output and (b) system in operation with the prepreg line

The system's control logic in normal mode was validated along with its the integration with the SMC prepreg line. The system worked as expected and a roll of SMC prepreg material, shown in Figure 55, was manufactured using the new system.

Figure 55 - SMC prepreg material manufactured using the new in-line metering and mixing system at the partner's facility

CHAPTER 6 CONCLUSION AND RECOMMENDATIONS

Throughout the project and with the help of the composites research team at CTA and Magna Exteriors Inc., the development of a new automated two-component metering and mixing system was made possible. The project's objectives and achievement are listed below.

Chapter 3 demonstrated the performance of a static mixer to obtain a homogeneous resin sample. To achieve this objective, FTIR spectroscopy was validated as a technique to evaluate the homogeneity of a resin sample. Then, the performance of a static mixer to obtain a homogenous resin sample was demonstrated. Finally, testing was performed to qualitatively evaluate the impact of flow rate variation of mixing homogeneity.

Chapter 4 covered the development of a new automated two-component metering and mixing system for the processing of high viscosity and abrasive fluids in Class 1 Division 1 classified locations. The chapter presented the preliminary and detailed design with the complete 3D CAD model. In addition, the system is manufactured to be tested.

Finally, Chapter 5 aimed to validate the performance of the new system in terms of flow rate linearity, mixing ratio variation, overpressure safety, cleaning and mix homogeneity. The new system met all the set requirements before being installed and tested at partner's facility.

The new innovative system solves the limitation of commercially available two-component metering and mixing systems. More specifically, the new system allows processing abrasive and high viscosity fluids in Class 1 Division 1 classified locations. The system features a multiplex assembly of plunger pumps that operate together with pulsation dampeners to produce a precise and virtually pulse-free flow rate. The metering equipment is equipped with two safety devices for overpressure protection; a first software and secondary hardware protection. The system is designed to meter the two fluids, mix them with high homogeneity and dispense the output to two doctor boxes located on an SMC material manufacturing line with seamless integration.

Using various instruments and controllable equipment, the system's production is automated. More specifically, the system's production speed adjusts automatically to the speed of the SMC material manufacturing line to prevent overflow and underflow in each doctor box. Coriolis and gear flowmeters are included to continuously monitor the flow rate and the mixing ratio. The

system’s instrument readings and equipment outputs can be viewed and controlled on a touchscreen human-machine interface.

The system exclusively features stainless steel and PTFE wetted parts for excellent chemical compatibility with the process fluids and cleaning solvent. The system can be cleaned in place (CIP) using acetone flushes. For a more thorough cleaning, the system can easily be disassembled using sanitary tri-clamp piping connections.

Validation of the system’s performance allowed to confirm that the system met all design requirements. Notably, the system offers a flow rate range of 390 to 2500 ml/min and a volumetric ratio of 0,8:1 to 320:1 to process fluids with pressures up to 300 psig and viscosity up to 9000 cP. Using flowmeter data, the machine’s mixing ratio variation was confirmed to be ± 1 % at a nominal mixing ratio of 20,5:1.

The new machine relies on the performance of an SMX static mixer to mix both products together. FTIR analysis was performed with mixed resin samples to quantify the homogeneity of the product. Results show the system offers samples with a coefficient of variation of only 1,5% in steady state conditions.

In summary, the developed system offers adequate performance and versatility to allow car manufacturers to develop new SMC materials to potentially meet the upcoming high demand of the industry.

6.1 Future work and recommendations

Although the objectives of the project were met, numerous improvements and additions could be included in the system. Here are some interesting upgrades to increase the system’s performance or ease of operation:

1. Include an automated cleaning sequence to flush the A side of the system from leftover resin using a pig system [108]. This method uses compressed gas to push a tightly fitted foam plug through the pipes to expel and scrape the pipe walls. Such cleaning method is efficiently used at the industrial partner’s facility for their paint system and was proposed to be included in this project’s metering and mixing system. However, to simplify the complexity of the innovative system, this solution was left aside. This feature would improve the ease of maintenance of the system.

2. Automating the dampening pressure of the pulsation dampeners by using the fluid pressure readings from the pressure sensors. Because the dampening depends on the process fluid to dampening bladder pressure ratio, having an adjustable system compared to a pre-charged and static solution could improve the flow rate linearity of the system.
3. Evaluating the wear rate of the system's critical components with abrasive fluids. Although the system was used with resin containing abrasive additives and fillers in the validation phase, a limited amount of approximately 500 L of resin was processed. Ideally, optical microscopy of components at risks like check valve seats and plunger packing could be performed to quantify the wear rate.
4. Upgrading the system to offer the ability to mix the dry additives and fillers in-line as a third component. This would limit the work required to manually mix part A with its additive and fillers before feeding the mixed resin to the two-component metering and mixing system.
5. Adding in-line degassing capabilities to improve the quality of the composite parts by reducing porosity. A gas permeable membrane with vacuum chamber could potentially be used to achieve this feature.
6. Optimizing the PID control feedback loop parameters for the doctor boxes. The impact of doctor box resin level variations on SMC prepreg sheet weight has not been quantified. Due to hydrostatic pressure, more resin in the doctor boxes will likely increase the resin film thickness slightly and reduce the consistency of the material.
7. Adding tank level monitoring to signal the operator when the tanks need to be refilled.
8. Automating the various manual valves to prevent the system to be started by accident when the outlet valves are not open. This could prevent risks of overpressure.

If this project was to be done again, significant time would be spent in the component and technology identification phase. The system's performance depends almost exclusively on the equipment choice and this system was developed and optimized for this project's specific fluids and applications. Therefore, with another resin system, for example, some technologies could potentially not be optimal or simply not used.

BIBLIOGRAPHY

[1] "Progress towards Canada's greenhouse gas emissions reduction target," *Government of Canada*, 20-Jul-2012. [Online]. Available: https://www.canada.ca/en/environment-climate-change/services/environmental-indicators/progress-towards-canada-greenhouse-gas-emissions-reduction-target.html. [Accessed: 17-Apr-2018].

[2] "Canada's 2016 greenhouse gas emissions reference case," *aem*, 09-Dec-2016. [Online]. Available: https://www.canada.ca/en/environment-climate-change/services/climate-change/publications/2016-greenhouse-gas-emissions-case.html. [Accessed: 17-Apr-2018].

[3] P. W. and G. S. C. Government of Canada, "Canada Gazette – Regulations Amending the Passenger Automobile and Light Truck Greenhouse Gas Emission Regulations," 08-Oct-2014. [Online]. Available: http://www.gazette.gc.ca/rp-pr/p2/2014/2014-10-08/html/sor-dors207-eng.html. [Accessed: 04-Sep-2018].

[4] J. Lauzon and D. Poirier, "Analyse de cycle de vie (ACV) de pièces de train, autobus et autocar en matériaux composites." May-2017.

[5] E. Witten, T. Kraus, and M. Kühnel, "Composites Market Report 2015," Sep. 2015.

[6] T. G. Gutowski, *Advanced Composites Manufacturing*, Wiley-Interscience. 1997.

[7] D. White, "SMC resin and primer advances prevent paint pops." [Online]. Available: https://www.compositesworld.com/columns/smc-resin-and-primer-advances-prevent-paint-pops. [Accessed: 17-Apr-2018].

[8] H. Caliendo, "Magna develops prototype carbon fiber composite subframe." [Online]. Available: https://www.compositesworld.com/news/magna-develops-prototype-carbon-fiber-composite-subframe. [Accessed: 17-Apr-2018].

[9] "The transforming automotive market: Is the time right for carbon fiber?" Future Materials Group (FMG), Feb-2016.

[10] Global Market Insights, Inc., "Automotive Composites Market to exceed $24bn by 2024," *Global Market Insights*, 15-Jan-2018. [Online]. Available: https://www.gminsights.com/pressrelease/automotive-composites-market. [Accessed: 20-Sep-2018].

[11] "carsalesbase.com - Automotive Industry analysis, opinions and data," *carsalesbase.com*. [Online]. Available: http://carsalesbase.com/. [Accessed: 12-Sep-2018].

[12] H. Suong, *Principles of the manufacturing of composite materials*, DEStech Publications, Inc. Lancaster, PA, 2018.

[13] "Nuplex - Hot Moulding." [Online]. Available: http://www.nuplex.com/composites/processes/hot-moulding-processes. [Accessed: 19-Sep-2018].

[14] "Evaluation Guide for Selecting the Best FRP Composite Process for Your Project." Molded Fiber Glass Companies.

[15] S. Boylan, L. M. Abrams, and J. M. Castro, “Predicting molding forces during sheet molding compounds (SMC) compression molding. II: Effect of SMC composition,” *Polym. Compos.*, vol. 24, no. 6, pp. 731–747, Dec. 2003.

[16] Molded Fiber Glass Companies, “Compression Molding with SMC | Composite Parts,” *Molded Fiber Glass Companies*, 2018. [Online]. Available: https://www.moldedfiberglass.com/processes/processes/closed-molding-processes/compression-molding-process. [Accessed: 20-Sep-2018].

[17] BASF, “Additives for Thermoset Composites.” [Online]. Available: https://www.dispersions-pigments.basf.com/portal/load/fid830461/Thermoset%20Composites.pdf. [Accessed: 21-Sep-2018].

[18] “Bulk moulding compound launched for auto market,” *Reinf. Plast.*, vol. 47, no. 8, p. 21, Sep. 2003.

[19] Quadrant, “GMT,” *Quadrant*. [Online]. Available: https://www.quadrantplastics.com/en/products/composite-material/gmt.html. [Accessed: 20-Sep-2018].

[20] Staff, “Fabrication methods.” [Online]. Available: https://www.compositesworld.com/articles/fabrication-methods. [Accessed: 17-Sep-2018].

[21] M. Baskaran, I. O. de Mendibil, M. Sarrionandia, J. Aurrekoetxea, J. Acosta, and D. Chico, “MANUFACTURING COST COMPARISON OF RTM, HP-RTM AND CRTM FOR AN AUTOMOTIVE ROOF,” p. 8, 2014.

[22] “Demystifying the RTM Process,” *RTM Composites*. [Online]. Available: https://www.rtmcomposites.com/blog/demystifying-the-rtm-process. [Accessed: 20-Sep-2018].

[23] “Corvette Sales Volume by Year - Production Numbers Since 1953,” *CorvSport.com*, 14-Mar-2017. .

[24] “Fiberglass to Carbon Fiber: Corvette’s Lightweight Legacy,” *media.gm.com*, 16-Aug-2012. [Online]. Available: https://media.gm.com/content/media/us/en/gm/news.detail.html/content/Pages/news/us/en/2012/Aug/0816_corvette.html. [Accessed: 11-Sep-2018].

[25] “Record sales for BMW Group worldwide during 2017 while it boosts the Premium car market in Mexico, Latin America and the Caribbean.” [Online]. Available: https://www.press.bmwgroup.com/latin-america-caribbean/article/detail/T0278223EN/record-sales-for-bmw-group-worldwide-during-2017-while-it-boosts-the-premium-car-market-in-mexico-latin-america-and-the-caribbean?language=en. [Accessed: 13-Sep-2018].

[26] A. Wüllner, “Increasing use of carbon fibre in automotive,” *JEC Compos. Mag.*, no. 98, pp. 30–31, Jul. 2015.

[27] “THE ELECTRIC CAR ACCORDING TO BMW.” [Online]. Available: https://www.pneurama.com/en/rivista_articolo.php/THE-ELECTRIC-CAR-ACCORDING-TO-BMW?ID=2632. [Accessed: 12-Sep-2018].

[28] M. Goia, A. Santini, and F. Pulina, “Sheet moudling compression of prepreg sheets for a composite subframe,” *JEC Mag.*, no. 119, pp. 39–41, Mar. 2018.

[29] “JEC Magazine,” no. 123, p. 82, Sep-2018.

[30] “Composites: On good form,” *Automotive Manufacturing Solutions*, 17-Nov-2014. .

[31] S. Jaswal and B. Gaur, “New trends in vinyl ester resins,” *Rev. Chem. Eng.*, vol. 30, no. 6, pp. 567–581, 2014.

[32] W. Liu, W. Jiao, F. Yang, R. Wang, L. Li, and W. Jiao, “Study on rheological behavior of vinyl ester resin during thickening,” *J. Vinyl Addit. Technol.*, vol. 24, no. 3, pp. 239–247, Aug. 2018.

[33] C. A. I. Mazali and M. I. Felisberti, “Vinyl ester resin modified with silicone-based additives. I. Mechanical properties,” *J. Appl. Polym. Sci.*, vol. 99, no. 5, pp. 2279–2287, Mar. 2006.

[34] Y. Zhang, L. Dai, Y. Wang, F. Li, and Z. Jin, “Study on Anti-tracking Properties of Unsaturated Polyester Resin SMC,” in *2006 IEEE 8th International Conference on Properties applications of Dielectric Materials*, 2006, pp. 861–864.

[35] SP Systems, “The Advantages of Epoxy Resin versus Polyester in Marine Composite Structures.” .

[36] “BMW Official Website | Sports Cars | Convertibles | BMW Canada.” [Online]. Available: https://www.bmw.ca/en/home.html. [Accessed: 14-Sep-2018].

[37] “Huntsman reveals epoxy role in BMW i3 passenger cell.” [Online]. Available: https://www.compositesworld.com/news/huntsman-reveals-epoxy-role-in-bmw-i3-passenger-cell. [Accessed: 14-Sep-2018].

[38] P. Malnati, “SMC: Old dog, new tricks.” [Online]. Available: https://www.compositesworld.com/articles/smc-old-dog-new-tricks. [Accessed: 18-Sep-2018].

[39] Ford, “December 2017 Sales,” Sales Report.

[40] H. Greimel, “Magna delivers carbon fiber subframe prototype to Ford,” *Automotive News*. [Online]. Available: http://canada.autonews.com/article/20180421/CANADA01/304219993/magna-delivers-carbon-fibre-subframe-prototype-to-ford. [Accessed: 18-Sep-2018].

[41] B. Kaffashi and F. M. Honarvar, “The effect of nanoclay and MWNT on fire-retardency and mechanical properties of unsaturated polyester resins,” *J. Appl. Polym. Sci.*, vol. 124, no. 2, pp. 1154–1159, Apr. 2012.

[42] A. B. Inceoglu and U. Yilmazer, “Synthesis and mechanical properties of unsaturated polyester based nanocomposites,” *Polym. Eng. Sci.*, vol. 43, no. 3, pp. 661–669, Mar. 2003.

[43] P. Jain, V. Choudhary, and I. Varma, “Flame retarding epoxies with phosphorus,” *J MACROMOL SCI—POLYMER Rev.*, vol. C42(2), pp. 139–183, Feb. 2007.

[44] M. S. Harber and J. J. Young, “Carbon Black: Theory and Uses in Thermoset Composite Applications,” p. 8.

[45] C. Hopmann, M. Theunissen, and S. Haase, “Analysis of the process influences on injection molded thermosets filled with hollow glass bubbles,” *J. Polym. Eng.*, vol. 38, no. 7, pp. 695–701, 2018.

[46] J. D. Satterthwaite, A. Maisuria, K. Vogel, and D. C. Watts, “Effect of resin-composite filler particle size and shape on shrinkage-stress,” *Dent. Mater.*, vol. 28, no. 6, pp. 609–614, Jun. 2012.

[47] D. Perrin, C. Guillermain, A. Bergeret, J.-M. Lopez-Cuesta, and G. Tersac, “SMC composites waste management as reinforcing fillers in polypropylene by combination of mechanical and chemical recycling processes,” *J. Mater. Sci.*, vol. 41, no. 12, pp. 3593–3602, Jun. 2006.

[48] J. T. Shen, F. Van Rijn, Y. T. Pei, and J. T. M. De Hosson, “On the abrasiveness and reinforcement of fillers in PTFE/epoxy composites,” *Polym. Compos.*, vol. 39, no. 3, pp. 698–707, Mar. 2018.

[49] Y. Jahani and M. Ehsani, “The effects of epoxy resin nano particles on shrinkage behavior and thermal stability of talc-filled polypropylene,” *Polym. Bull.*, vol. 63, no. 5, p. 743, Aug. 2009.

[50] W. Ferdous, A. Manalo, T. Aravinthan, and G. Van Erp, “Properties of epoxy polymer concrete matrix: Effect of resin-to-filler ratio and determination of optimal mix for composite railway sleepers,” *Constr. Build. Mater.*, vol. 124, pp. 287–300, Oct. 2016.

[51] R. Srinivasan, C. Almonacil, S. Narayan, P. Desai, and A. S. Abhiraman, “Mechanism, Kinetics and Potential Morphological Consequences of Solid-State Polymerization,” *Macromolecules*, vol. 31, no. 20, pp. 6813–6821, Oct. 1998.

[52] A. Kukukova, J. Aubin, and S. M. Kresta, “A new definition of mixing and segregation: Three dimensions of a key process variable,” *Chem. Eng. Res. Des.*, vol. 87, no. 4, pp. 633–647, Apr. 2009.

[53] W. J. Sichina, “Characterization of Epoxy Resins Using DSC,” *Therm. Anal.*, p. 4.

[54] D. Rauline, J.-M. Le Blévec, J. Bousquet, and P. A. Tanguy, “A Comparative Assessment of the Performance of the Kenics and SMX Static Mixers,” *Chem. Eng. Res. Des.*, vol. 78, no. 3, pp. 389–396, Apr. 2000.

[55] A. Bakker, R. D. LaRoche, and E. M. Marshall, “Laminar Flow Static Mixers with Helical Elements,” p. 11.

[56] J. Schoonenboom and R. B. Johnson, “How to Construct a Mixed Methods Research Design,” *Kolner Z. Soziol. Sozialpsychologie*, vol. 69, no. Suppl 2, pp. 107–131, 2017.

[57] “Determining the Mixing Efficiency of a Static Mixer using Coefficient of Variation (CoV) Analysis.” Storm Mixer.

[58] J. B. Krolczyk, “THE EFFECT OF MIXING TIME ON THE HOMOGENEITY OF MULTI-COMPONENT GRANULAR SYSTEMS,” Opole University of Technology, Opole, Poland, Dec. 2015.

[59] C. F. I. A. Government of Canada, “Developing Mixer Performance Testing Procedures,” 04-Jun-2013. [Online]. Available: http://www.inspection.gc.ca/animals/feeds/inspection-

program/developing-mixer-performance-testing-procedures/eng/1370381600539/1370381604148. [Accessed: 08-May-2018].

[60] M. Naseska, "FOURIER TRANSFORM INFRARED SPECTROSCOPY," *Fourier Transform Infrared Spectrosc.*, p. 12.

[61] M. G. González, J. C. Cabanelas, and J. Baselga, "Applications of FTIR on Epoxy Resins – Identification, Monitoring the Curing Process, Phase Separation and Water Uptake," *Mater. Sci.*, p. 25, Apr. 2012.

[62] M. A. Omar, K. R. Nara, A. Obieglo, N. Belk, and R. Schalausky, "Analysis of non-load bearing, 2 component epoxy-adhesive to the hemmingprocess variations; Thermo-Gravimetric, Differential Scanning Calorimetry,and Fourier Transform Infrared Spectroscopy FT-IR analyses," *Prog. Org. Coat.*, vol. 65, pp. 104–108, 2009.

[63] B. H. Stuart, *Infrared Spectroscopy : Fundamentals and Applications*. Hoboken, UNITED KINGDOM: John Wiley & Sons, Incorporated, 2004.

[64] S. Kang *et al.*, "Characterization of Compositional Heterogeneity in Chemically Amplified Photoresist Polymer Thin Films with Infrared Spectroscopy," *Macromolecules*, vol. 40, no. 5, pp. 1497–1503, Mar. 2007.

[65] "AIST:Spectral Database for Organic Compounds,SDBS." [Online]. Available: https://sdbs.db.aist.go.jp/sdbs/cgi-bin/cre_index.cgi. [Accessed: 09-Oct-2018].

[66] B. R. Bogner, "Sheet molding compounds having improved viscosity," US5159044A, 27-Oct-1992.

[67] J. R. M. d'Almeida and S. N. Monteiro, "The effect of the resin/hardener ratio on the compressive behavior of an epoxy system," *Polym. Test.*, vol. 15, pp. 329–339, Jan. 1996.

[68] W. Tu *et al.*, "Unveiling the Dependence of Glass Transitions on Mixing Thermodynamics in Miscible Systems," *Scientific Reports*, 17-Feb-2015.

[69] K. Alemaskin, I. Manas-Zloczower, and M. Kaufman, "Entropic Analysis of Color Homogeneity," *Society of Plastics Engineers*, no. 45, pp. 1031–1038, 2005.

[70] S. ltd, "Stamixco ltd." [Online]. Available: http://www.stamixco.com/. [Accessed: 02-May-2018].

[71] "How do Static Mixers Fit in the Polymer Industry?," *Komax Systems Inc*, 08-Jun-2015. [Online]. Available: https://www.komax.com/how-do-static-mixers-fit-in-the-polymer-industry/. [Accessed: 10-Oct-2018].

[72] O. S. Galaktionov, P. D. Anderson, G. W. M. Peters, and H. E. H. Meijer, "Analysis and Optimization of Kenics Static Mixers," *Int. Polym. Process.*, vol. 18, no. 2, pp. 138–150, May 2003.

[73] H. E. H. Meijer, M. K. Singh, and P. D. Anderson, "On the performance of static mixers: A quantitative comparison," *Prog. Polym. Sci.*, vol. 37, pp. 1333–1349, Oct. 2012.

[74] M. K. Singh, P. D. Anderson, and H. E. H. Meijer, "Understanding and Optimizing the SMX Static Mixer," *Macromol. Rapid Commun.*, vol. 30, no. 4–5, pp. 362–376, Feb. 2009.

[75] F. J. Muzzio, P. D. Swanson, and J. M. Ottino, "The statistics of stretching and stirring in chaotic flows," *Phys. Fluids Fluid Dyn.*, vol. 3, no. 5, pp. 822–834, May 1991.

[76] Stamixco, “Stamixco_2K-Resin Plastic Disposable & Metal Static Mixer Technical Bulletin.pdf.” 17-Aug-2011.

[77] M. Regner, K. Östergren, and C. Trägårdh, “Influence of Viscosity Ratio on the Mixing Process in a Static Mixer: Numerical Study,” *Ind. Eng. Chem. Res.*, vol. 47, no. 9, pp. 3030–3036, May 2008.

[78] H. Lee, M. Huh, J. Yoon, D. Lee, S. Kim, and S. Kang, “Fabrication of carbon fiber SMC composites with vinyl ester resin and effect of carbon fiber content on mechanical properties,” vol. 22, p. 4, 2017.

[79] Huntsman, “Adhesives, Coatings and Elastomers Isocyanate Product Line 2010.” 2010.

[80] B. Wu, “Computational Fluid Dynamics Study of Large-Scale Mixing Systems with Side-Entering Impellers,” *Eng. Appl. Comput. Fluid Mech.*, vol. 6, no. 1, pp. 123–133, Jan. 2012.

[81] Silverson, “Inline Mixer | High Shear In-Line Mixers.” [Online]. Available: http://www.silverson.com/us/products/in-line-mixers/. [Accessed: 05-Oct-2018].

[82] “Static-dynamic Mixing System.” [Online]. Available: https://www.dopag.ca/products/2k-metering-systems/mixing-systems/static-dynamic-mixing-system/. [Accessed: 09-Jan-2018].

[83] “Mixing heads - Tartler GmbH.” [Online]. Available: https://www.tartler.com/en/mixingheads.html. [Accessed: 13-Jan-2019].

[84] “High-Pressure Impingement Metering Equipment.” [Online]. Available: https://polyurethane.americanchemistry.com/High-Pressure-Impingement-Metering-Equipment/. [Accessed: 12-Oct-2018].

[85] da F. Cláudio António Pereira, “Mixing Studies with Impinging Jets - PIV/PLIF Experiments and CFD Simulation,” Universidade do Porto, 2012.

[86] C. L. Tucker and N. P. Suh, “Mixing for reaction injection molding. I. Impingement mixing of liquids,” *Polym. Eng. Sci.*, vol. 20, pp. 875–886, Sep. 1980.

[87] “Cannon USA | FPL SR Mixing Head Offer,” *Cannon USA | PU machinery, Composites Equipment,Thermforming*. [Online]. Available: http://www.cannonusa.com/mix-head-offer. [Accessed: 10-Oct-2018].

[88] R. Dubé, “Développement d’un système d’injection pour la fabrication des composites,” Thesis, École Polytechnique de Montréal, 2009.

[89] A. Mohammadi, P. J. Moghaddas, and A. Ariamanesh, “Residence Time and Concentration Distribution in a Kenics Static Mixer,” *Chem. Eng. Commun.*, vol. 202, no. 2, pp. 144–150, Feb. 2015.

[90] E. B. Nauman, D. Kothari, and K. D. P. Nigam, “Static Mixers to Promote Axial Mixing,” *Chem. Eng. Res. Des.*, vol. 80, no. 6, pp. 681–685, Sep. 2002.

[91] “BLACOH Fluid Control Literature.” [Online]. Available: https://www.blacoh.com/literature.aspx. [Accessed: 11-Oct-2018].

[92] J. A. Bossert, *Hazardous Locations - Guide for the Design, Testing, Construction, and Installation of Equipment in Explosive Atmospheres*, 3rd ed. Toronto, Ontario: CSA International, 2001.

[93] J. J. Coronado, “Effect of Abrasive Size on Wear,” *Abrasion Resist. Mater.*, p. 20.

[94] R. H. Frith and W. Scott, “Wear in external gear pumps: A simplified model,” *Wear*, vol. 172, no. 2, pp. 121–126, Mar. 1994.

[95] “General Purpose Units,” *Cannon Polyurethane & Reactive Polymers Technologies*. [Online]. Available: http://www.afros.it/en/prodotti/LP-Dosing-Unit/general-pourpose.html#. [Accessed: 19-Apr-2018].

[96] R. F. Miller, “Hardness vs. Wear,” *Superior Consumables*. [Online]. Available: http://www.superiorconsumables.com/hardness-vs-wear.asp. [Accessed: 07-Jan-2019].

[97] ASTM, Ed., “E168-16 Standard Practices for General Techniques of Infrared Quantitative Analysis.” ASTM, 2016.

[98] “ASTM E1252-98 (Reapproved 2013)Standard Practice for General Techniques for Obtaining Infrared Spectra for Qualitative Analysis.” ASTM, 2013.

[99] “2016 Statistics | OICA.” [Online]. Available: http://www.oica.net/category/production-statistics/2016-statistics/. [Accessed: 06-Sep-2018].

[100] Z. Zeng, R. Kang, and Y. Chen, “Using PoF models to predict system reliability considering failure collaboration,” *Chin. J. Aeronaut.*, vol. 29, no. 5, pp. 1294–1301, Oct. 2016.

[101] “Brewers Hardware 1" Tri Clover Compatible Economy Ball Valve.” [Online]. Available: https://www.brewershardware.com/1-tri-clover-compatible-economy-ball-valve-flat-handle-design.html?category_id=314. [Accessed: 11-Jan-2019].

[102] “Sanitary Ball Valve,” *Rodger Industries Inc.* [Online]. Available: http://www.rodgerindustries.com/commercial/products/product-view?productId=1028&categoryId=424. [Accessed: 11-Jan-2019].

[103] “CSA Control Drawing XA01322P-B Cerabar PMC21, PMP21, PMP23 4...20mA (IS).” Endress+Hauser.

[104] “Amazon.com: Online Shopping for Electronics, Apparel, Computers, Books, DVDs & more.” [Online]. Available: https://www.amazon.com/. [Accessed: 11-Jan-2019].

[105] “PicClick UK • Search eBay Faster,” *PicClick UK*. [Online]. Available: https://picclick.co.uk/. [Accessed: 11-Jan-2019].

[106] “Resistance Coefficient Method – K Method,” *Nuclear Power*. [Online]. Available: https://www.nuclear-power.net/nuclear-engineering/fluid-dynamics/minor-head-loss-local-losses/resistance-coefficient-method-k-method-excess-head/. [Accessed: 12-Jan-2019].

[107] “Darcy-Weisbach Pressure and Major Head Loss Equation.” [Online]. Available: https://www.engineeringtoolbox.com/darcy-weisbach-equation-d_646.html. [Accessed: 12-Jan-2019].

[108] “T.D. Williamson - Pipeline Cleaning Pigs.” [Online]. Available: http://www.tdwilliamson.com/solutions/pipeline-pigging/pipeline-pigs/cleaning-pigs. [Accessed: 14-Jan-2019].

APPENDIX A – CHEMICAL COMPATIBILITY

Table 27 - Chemical compatibility of various chemicals of interest with metals, plastics and elastomers

Chemical	Metals					Plastics and elastomers												
	Aluminum	Carbon Steel	Cast Iron	304 Stainless Steel	**316 Stainless Steel**	Acetal	Buna	EPDM	Fluor elastomer	Hastelloy C	TPE	Nitrile (TS)	Nitrile (TPE)	Nylon	Polypropylene	**PTFE**	UHMWPE	Urethane
Acetone	B	A	A	A	**A**	B	D	A	D	A	C	D	D	B	D	**A**	A	D
Amines	B	D	D	A	**A**	D	D	C	D	B	D	D	D	D	B	**A**	A	D
Peroxide	A	B	D	B	**A**	D	D	D	A	A	D	B	C	D	B	**A**	A	C
Isocyanates	-	-	A	A	**A**	A	-	-	B	A	B	B	C	-	A	**A**	-	B
Vinyl Acetate	B	B	C	B	**B**	-	D	B	A	A	-	D	D	-	D	**A**	D	D
Styrene	A	A	B	A	**A**	A	D	D	B	D	D	D	D	B	D	**A**	A	D

Legend:
A: Excellent, B: Good, C: Fair to Poor, D: Not recommended, - No Data

APPENDIX B – DOCTOR BOX LEVEL CONTROL LOGIC

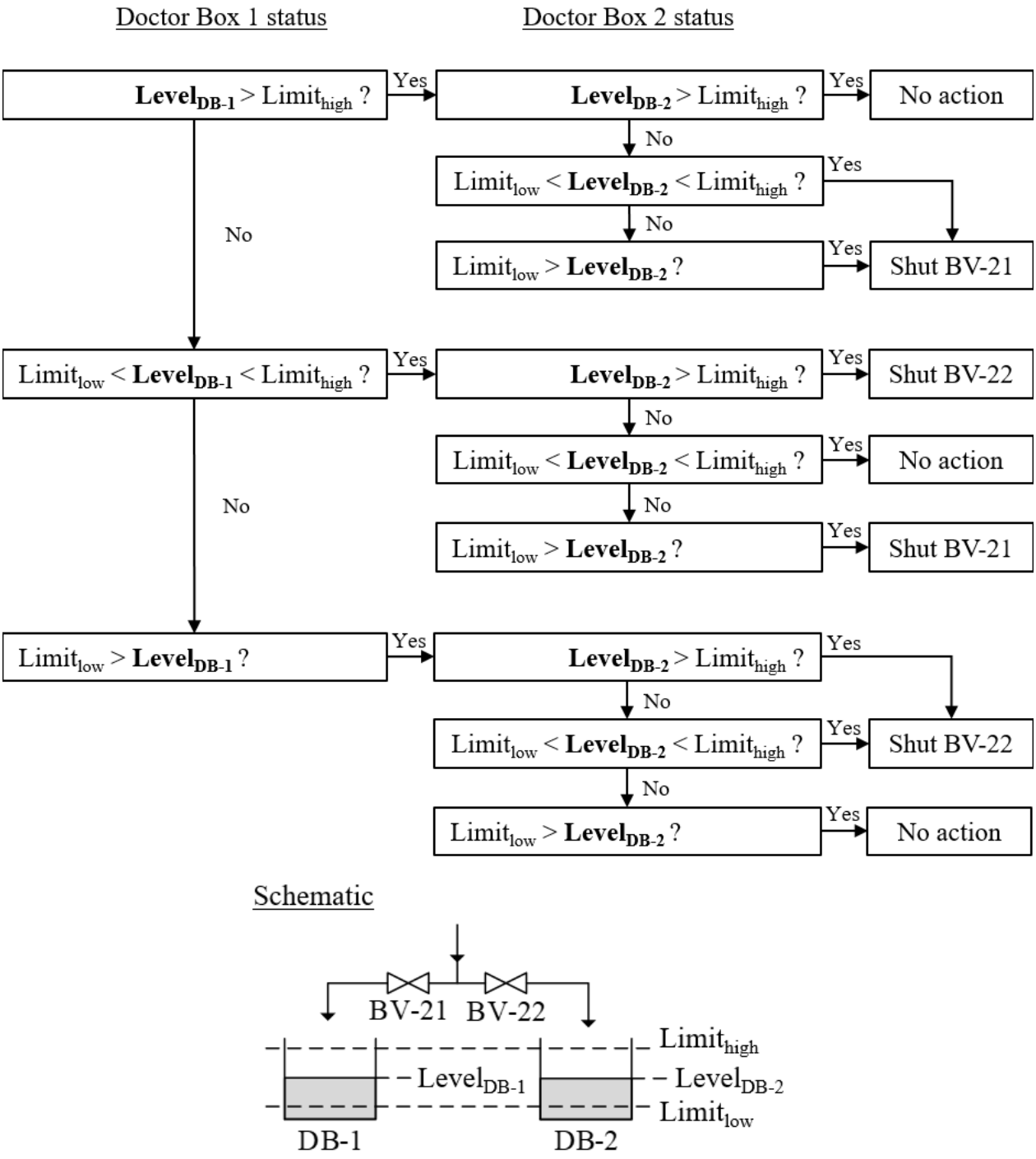

Figure 56 - Doctor box individual control logic

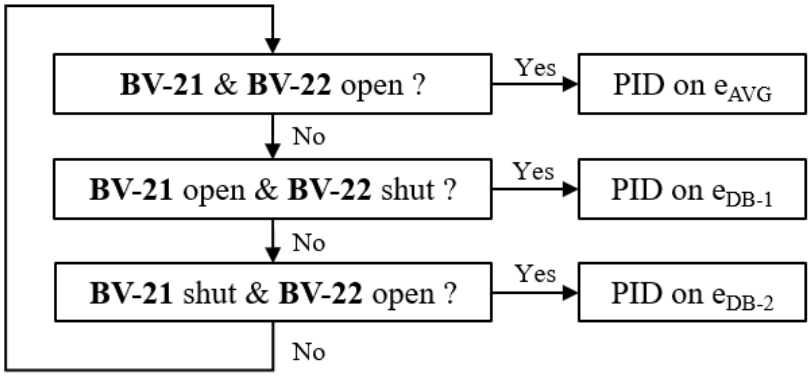

Legend:
e_{AVG} = Average of the combined error of both doctor boxes
e_{DB-1} = Error of doctor box 1
e_{DB-2} = Error of doctor box 2

Figure 57 - PID cases for metering system output control